九州大学学術情報リポジトリ Kyushu University Institutional Repository

Tribological Properties of Hydrogels with Hemispherical Surface Dimples

竹藤,春菜

https://hdl.handle.net/2324/7363592

出版情報:Kyushu University, 2024, 博士(理学), 課程博士

バージョン: 権利関係:

Tribological Properties of Hydrogels with Hemispherical Surface Dimples

(表面に半球状くぼみ形状をもつハイドロゲルのトライボロジー特性)

Haruna TAKEFUJI

Graduate School of Science

Department of Chemistry

Laboratory of Physical Chemistry of Soft Matters

January 2025

Contents

General Introduction	1
Chapter 1 Normal contact and adhesion of Poly (vinyl alcohol) gel against the glass su	bstrates with
different hydrophobicity	6
1-1 Introduction	6
1-2 Materials and Methods	10
1-2-1 Materials	10
1-2-2 Droplet Replication	10
1-2-3 Hydrogel Preparation	11
1-2-4 Substrate Preparation	14
1-2-5 In situ Observation	15
1-2-6 Compression Test	16
1-2-7 Adhesion Test	17
1-3 Results and Discussion	18
1-3-1 Normal contact between the glass substrate and the PVA gel	18
1-3-2 Work of adhesion of the PVA gel	25
1-4 Conclusion	27
Chapter 2 Friction behavior of PVA gels with hemispherical surface dimples on their	surfaces 29
2-1 Introduction	29
2-2 Materials and Methods	32
2-2-1 Materials	32
2-2-2 Hydrogel Preparation	33
2-2-3 Friction Measurement	33
2-2-4 In situ observation	35
2-3 Results and Discussion	35
2-4 Conclusion	55
Chapter 3 Effect of elasticity of hydrogel on the surface property	59
3-1 Introduction	59
3-2 Materials and Methods	60
3-2-1 Materials	
	60
3-2-2 Preparation of Poly(vinyl alcohol) gels with different elasticities	
	60

3-2-5 Friction measurement	62
3-2-6 Adhesion test	62
3-3 Results and Discussion	62
3-3-1 Friction behavior	62
3-3-2 Adhesion property	65
3-4 Conclusions	66
Chapter 4 Wear Evaluation of Poly(vinyl alcohol) Hydrogel by UV Spectrometry	and Total
Organic Carbon Measurement of Lubricant	68
4-1 Introduction	68
4-2 Materials and Methods	70
4-2-1 Materials	70
4-2-2 Hydrogel preparation	70
4-2-3 Sliding test	71
4-2-4 Wear evaluation	72
4-3 Results and Discussion	76
4-3-1 UV spectra and TOC	76
4-3-2 Wear of PVA gels	77
4-3-2-1 Gel vs. rough glass	77
4-3-2-2 Gel vs. flat hydrophobic glass	84
4-3-2-3 Gel-on-gel	87
4-4 Conclusion	93
Conclusions	95
References	99
A cknowledgement	107

General Introduction

Hydrogel is a substance in which the three-dimensional network structure of polymers is swollen with water. Softness, high water content, permeability, and stimuli responsiveness are the representative characteristics for the hydrogel. Our biological soft tissues also contain a large amount of water and are soft tissue, and it can be said that hydrogel is the substance closest to the biological tissue among artificial compounds. Therefore, hydrogel is a promising substance as a biological model and as a biomaterial. Above all, research on applying gel as artificial cartilage is being actively conducted, and it is very important to understand the tribological properties such as friction and wear of gel for application.

Many studies on friction of cross-linked polymer have been carried out. Schallamach and Leonov et al. explained the concept of polymer friction against smooth surfaces like glasses, now known as "adhesive friction" ^{1–4}. Persson et al. also reported that the sliding friction of rubber against rough and hard surfaces was caused by the internal friction of rubber ^{5,6}.

Most of the studies on soft matter friction used rubber as described above, and especially there were few reports on the friction of hydrogels until the 1990s. Hydrogel is a substance similar to rubber in that it is soft, has a crosslinked structure of polymer, and exhibits viscoelastic properties, but it is different from rubber in that it contains a large amount of water. Especially bio-soft tissues such as articular cartilage contain approximately 70-80 wt% water, and synthetic gels contain as much as 99.9 wt% water. Such water cannot be easily trickled or squeezed like a sponge and interacts strongly with the polymer network to maintain a hydrated state. Due to its high-water content, the internal friction of the gel is extremely small compared to rubber. Therefore, it is not possible to understand the friction of gel exactly by applying the theory of friction of rubber to gel.

Amontons and Coulomb summarized the basic friction properties between two dry solid surfaces as follows.

First law: Friction force is proportional to the normal load.

Second law: Friction force does not depend on the apparent contact area.

Third law: Dynamic friction does not depend on sliding velocity.

The friction force of the solid material F is easily formulated using Amontons-Coulomb law, in the following formula,

$$F = \mu W \tag{1}$$

where μ is the friction coefficient and W is the normal load applied to the material. This equation can be described for both static and dynamic friction. Since μ is a value unique to each solid, the friction

force depends only on the load and the surface properties of the solid.

However, it is known that soft matter such as rubber and gel does not follow this law and exhibits complicated behavior⁷. The friction properties of gel include the following⁸; friction force depends on the sliding velocity and contact area between the gel and the substrate, and the friction coefficient is small up to about 1/100 compared to that of solids. These are considered to be due to the unique properties of gels such as flexibility and high-water content that solids like wood or metals do not have.

Incidentally, articular cartilages especially in the hip or knee joints, shows low friction for decades, even though it weighs several tens of kilograms. Due to the low surface friction of articular cartilage, we can smoothly get in motion without any physical resistance in any action of our daily life, such as walking, sitting down, reaching out, etc. However, it has not been clearly understood why the cartilages show low friction under different pressure or moving velocities yet⁷.

It is known that the surface geometry of the friction surface has a great effect on the friction of living tissues and gels. For example, it has been reported that the dynamic friction coefficient of articular cartilage increases as the roughness of the counter surface increases^{9–11}. On the other hand, it is known that the surface of articular cartilage has fine irregularities on the micro-metre order¹², but its role remains unclear.

Currently, the population is aging, and many elderly people are hindered their daily lives because of the pain caused by the wear of cartilage due to aging. Since cartilage is a tissue that is difficult to self-repair, more than 100,000 times of artificial joint replacement surgeries have been performed in a year, only in Japan. The artificial joints used there are manufactured using ceramics, ultra-high molecular weight polyethylene (UHMPE), and so on, but there is an issue that these friction coefficients are about 10 times higher than those of living joints. In some cases, inflammation of surrounding tissues and loosening due to wear particles generated by high friction, which limits the useful life and requires replacement¹³. Compared to this, gel shows low friction and has properties such as high water content or permeability, it has attracted attention as a new artificial cartilage and has been studied by many researchers^{9,13–22}. However, many studies focused on the chemical composition of gels or lubricants, and few focused on the surface geometry of gels.

As mentioned above, the surface shape is known to change the surface properties of the substance. In nature, gecko's finger²³, shark skin, and sucker structures of octopus or starfish are well-known examples. Although the elastic modulus is different from that of gel, it has been reported that friction is reduced by imparting a concave structure to the metal surface^{24,25}. If the friction of a gel with a

surface shape can be understood, it will lead to elucidating the role of the surface structure of cartilages and the friction mechanism of joints using the gel as a model substance. In addition, if it becomes possible to control the friction characteristics by changing only the surface shape without changing the chemical composition of the gel or the surrounding environment, etc., further high functionality can be expected without impairing the original mechanical properties of the gel, and it is also expected to lead to application to biomaterials such as artificial cartilage.

To understand the role of the surface structure of the gel, ideally, a simple method is needed to impart many pattern structures to the gel surface at one time over a wide area. In addition, if the shape is a square or cylindrical pillar, the effect of the edge significantly might appear under sliding motion in the friction measurement, so it is difficult to evaluate only the effect of the pattern shape. Therefore, a spherical pattern structure is considered to be desirable as a starting point.

In addition, although wear of gel is studied, there are few reports on that. Material wear is an important evaluation item as it can impair durability and original performance. Regarding artificial joints, as mentioned above, the generation of wear particles causes inflammation of surrounding tissues and osteolysis, which limits the useful life. For wear evaluation of artificial joints made of metal or ceramic that are currently used, ISO 14242-1 and ISO 14242-2 stipulate strict international standards. Gels are expected to be applied to various fields as biomaterials in the future, and it is disadvantageous for application in that accurate wear evaluation of gels has not been established. Therefore, it would be very meaningful if there was a method that could be evaluated simply and quantitatively.

Also, the relationship between wear and friction of gel has not been clarified at present, and it is not clear whether gels showing low friction show low wear at the same time, but it is very interesting to investigate.

Herein, Poly(vinyl alcohol) gels with hemispherical surface dimples were prepared and their friction, adhesion and wear properties were investigated in this study and aimed to make the friction and wear of the hydrogel surface lower by imparting the dimple pattern structure while maintaining its bulk properties, such as the elastic modulus, water content, permeability and so on. Considering the application of gel, the lower friction and wear may lead to a longer lifetime to use and energy saving, so it is advantageous to have a slippery surface. We selected Poly (vinyl alcohol) (PVA) gel as the target gel because it has high mechanical strength and can withstand friction and wear tests and it is suitable for examining the effect of hemispherical dimples on hydrogel surfaces on sliding friction and wear. In addition, PVA gel has a biocompatible nature^{26,27,28}, so it may be applicable in biomedical fields like artificial cartilage if the surface properties can be controlled by surface structure.

Among the factors that influences on the surface properties of the gels, the surface shape, the elasticity of the gel and the surface wettability of the counter substrate are presented as examples and we studied their effects systematically in this study. We state about them in Chapter 1 to Chapter 4 respectively as shown below.

In chapter 1, we report on the normal contact and the adhesion strength of the gel and the glass substrate with different wettability. First, poly(vinyl alcohol) gel with hemispherical surface dimples was prepared by applying the method for imparting the pattern structure on the surface of polydimethylsiloxane silicone rubber to the gel^{29,30}. Moreover, three kinds of glass substrates with different contact angle to water were prepared by varying the surface treatment of the glass substrate surface in this study. The contact state between the gel and the glass substrate was evaluated when the normal load was applied to the gel using the strain-controlled rheometer by *in situ* observation³¹. In addition, the adhesion test that raise the glass substrate, that contacts the gel, at a constant rate was performed and the adhesive force that works between the gel and the glass was estimated.

In chapter 2, we report on the friction of the gel against the glass substrates with different wettability. In the previous study, it is shown that the sliding velocity dependence of the friction of the gel varies with the surface wettability³². However, almost all the gels used in the previous studies had flat surfaces^{31–33} and few studies on the friction of hydrogel with textured surface were reported¹⁰. Particularly in this chapter, we focused on the gel with hemispherical surface dimples and researched how that surface structure affects the friction of the gels and whether it affects the friction property similarly when the surface wettability is changed.

In chapter 3, we report on the effect of the elasticity of the gel on the friction of the gel with hemispherical surface dimples. For example, the articular cartilage in our bodies is a tissue which is in the hydrogel state, and its elastic modulus is high enough in the order of MPa³⁴ while showing quite low surface friction. It should be demanded hydrogels with high elastic moduli when the hydrogels are applicated as biomaterials in the future. Therefore, three kinds of gels with different elasticity were prepared by changing the concentration of the solution before gelation or adding the dry-anneal^{16,34} treatment after the gelation to investigate the effect of elasticity. Then, the adhesion test and the friction test were conducted in the same way stated in chapter 1 and chapter 2.

In chapter 4, we report on the quantitative wear evaluation of the gel. The microscopic observation was mainly used as a wear evaluation method of the gel so far, therefore the evaluation method was remained at the qualitative one^{35–37}. In this chapter, in addition to the microscopic observation of the gel surface after the sliding test, we focused on the lubricant and performed the quantitative wear

evaluation by detecting the wear particles of the gel that are contained in the lubricant using the UV spectrometry and the total organic carbon measurement.

Chapter 1 Normal contact and adhesion of Poly (vinyl alcohol) gel against the glass substrates with different hydrophobicity

1-1 Introduction

Hydrogel is a substance that is the polymeric three-dimensional network structure swollen with water and its softness or high-water content are characteristic. It is the substance that resembles to the living soft tissues at the most among the artificial materials. Since it is swollen with water, it is expected to be applied in the wet environment, for example, in water.

In nature, there are many organisms that control their contact property by their surface structure. For instance, octopus and starfish contact firmly against any face even in water thanks to their sucker structure like cupule and the nature does not be lost at only one time of contact and they can repeatedly contact and detach. It is predicted to be advantageous for many applications that gels can also control their contact and detachment freely in water.

When controlling the surface properties of gels by the surface structure, it narrows the possibilities for gels to applicate as materials if its properties are only valid for a certain counter face. If the significance of the surface structure can be shown for every counter surface, the worth of the gel having pattern structure on its surface as a material is considered to increase. It is interesting and useful that the surface properties of the gel could be easily changed depending on the purpose of use by the surface structure, such as showing strong and quick contact, or peeling off with a weak force even if it is pasted once.

In the previous study, the gels with hexagonal facets fashioned after the surface structure of clingfish were prepared and their adhesive property was investigated³⁸. It is shown that these gels could contact the glass substrate quickly and firmly compared with the gel with flat surface, though the gel/glass contact area was decreased, and reversibly adhere. This strong adhesive property is considered to be attributed to the increase in the contact pressure due to the small contact area and the promotion of fast water drainage from the interface due to the existence of interconnecting grooves.

It is important for understanding other surface properties like friction or wear too to research on the contact and adhesive properties of gels. Herein, we investigate the contact and adhesive properties of poly(vinyl alcohol) gels against the glass substrates.

Since we conduct the tests under water in this study at first, the difference of the surface wettability of the glass substrates would make the difference in the easiness of the water drainage at the gel/glass interface and influence on the adhesive strength of the gels and the substrate. In case the hydrophilic substrate is used, water is more favor to contact the substrate compared with the gel, it is expected that it is difficult to finish the complete drainage between the gel and the substrate, so the contact of them is inhibited. While on the contrary, in case the hydrophobic substrate is used, the gel is more favor to contact the substrate compared with water, then it is predicted that the water drains quickly at the interface and the gel contacts the glass substrate firmly.

Though W_{adh} of the gels may varies with the change of the wettability of the substrate, we especially investigated how does the surface dimple on the gel influence on the W_{adh} of the gels. As the surface design, the reduction in contact area between the gel and the substrate will occur, for that, the decrease in work of adhesion on aby substrates is predicted. In particular, the effect may be clear for the hydrophobic substrate that it is considered to the gel make firm contact.

Here, we consider the energy change by the contact and the detachment of two substances with clean surfaces based on the concept of adhesive work. As seen in Fig. 1-1, by separating the interface where the substance A and B are in contact with each other, new surfaces of the substance A and B are generated. Assuming γ_A , γ_B , and γ_{AB} as surface energy of the substance A, B, and interfacial energy of A/B contact interface, respectively, the adhesive work W_{AB} is expressed by the following equation Eq. 1-1.

$$W_{\rm AB} = \gamma_{\rm A} + \gamma_{\rm B} - \gamma_{\rm AB} \tag{Eq. 1-1}$$

This Eq. 1-1 is called Dupré's equation.

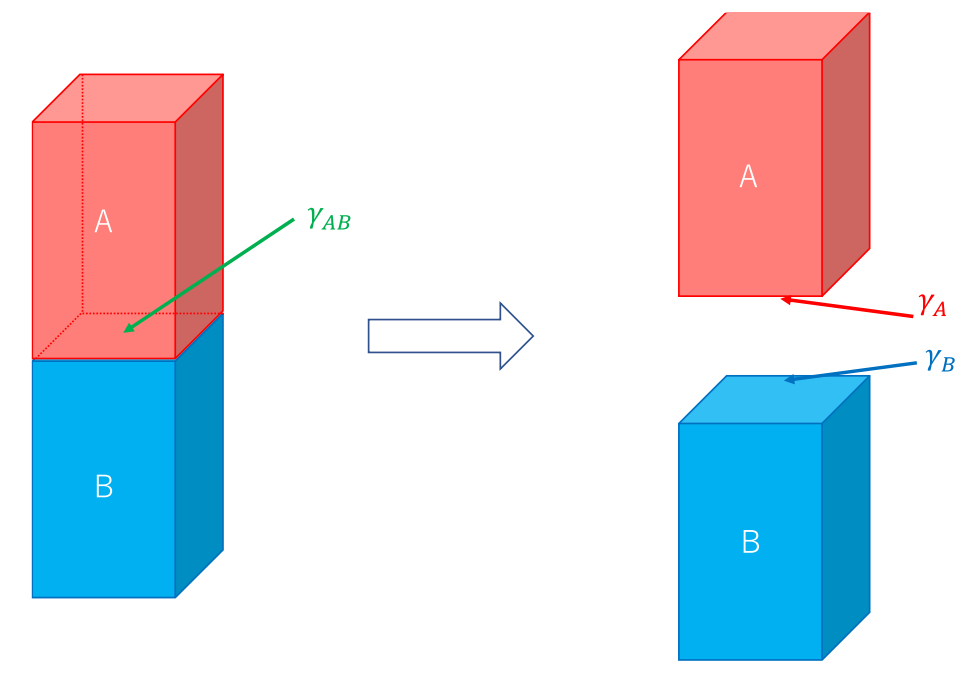


Fig. 1-1 Schematic illustration of contact of two materials and their interfacial free energy.

If the surface tension (or surface free energy) of two solid substances and the interfacial tension (or interfacial free energy) at the time of contact are known, the adhesive work can be obtained by using Eq. 1-1. However, there is currently no direct way to calculate their values. As a method of computing the surface free energy of a solid, there is a method of measuring the contact angle of a droplet having a known surface tension on the solid surface and estimating it from a theoretical formula related to adhesive work.

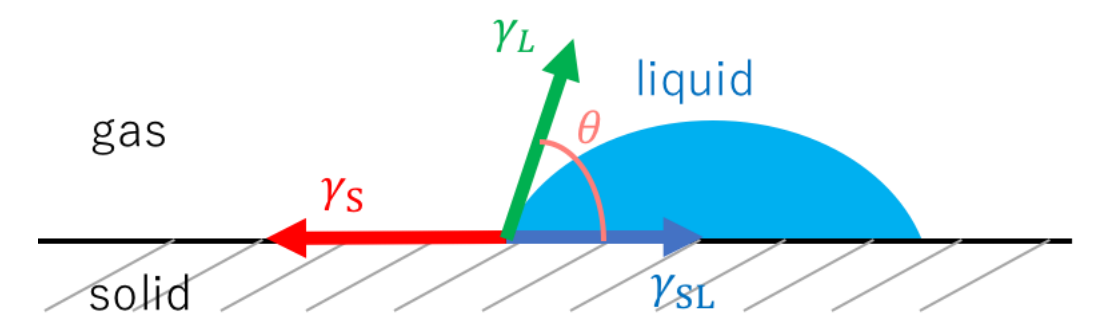


Fig. 1-2 Schematic illustration of a droplet on a solid surface.

Let γ_S be the surface tension of the solid, γ_L be the surface tension of the liquid, γ_{SL} be the interfacial tension of the solid-liquid interface, and θ be the contact angle. When the droplets are in

an equilibrium state on the solid surface, the interfacial tensions are balanced as Eq. 1-2.

$$\gamma_{\rm S} = \gamma_{\rm L} \cos \theta + \gamma_{\rm SL} \tag{Eq. 1-2}$$

This Eq. 1-2 is called as Young's equation. Combining Eq. 1-1 and Eq. 1-2, Eq. 1-3 is derived.

$$W_{\rm SL} = \gamma_{\rm L}(1 + \cos \theta) \tag{Eq. 1-3}$$

This Eq. 1-3 is called as Young- Dupré's equation. From the equation shows that the adhesive work at the solid/liquid interface can be obtained by measuring the contact angle of the droplet with known surface tension. However, there is no method to obtain the adhesive work between two solid substances, some methods, such as Fowkes method, are proposed to calculate surface free energy of solid substances^{39–41}.

Regarding on the normal contact of the glass substrate and the hydrogel with surface dimples, the following two effects are expected. (1) The contact area between the hydrogel and the substrate is reduced due to the dimples on the surface. (2) Water in dimples can sustain the normal load²¹, and local contact pressure of the flat part does not increase compared with the hydrogel with a flat surface. If the dimples on the gels form complete contact with the glass substrate and are not deformed with gels macroscopic deformation, water in the dimples is considered to be able to sustain the normal load due to its incompressibility. The expected effect (1) is consistent with the previous study³⁸. However, if effect (2) is true, the work of adhesion of hydrogels with surface dimples should be lowered compared with that of the hydrogel with a flat surface, unlike the previous study. Besides, it is predicted that the surface dimple structure makes it difficult to drain the water in dimples differently from the grooves, so strong adhesion is hindered, but it is unclear how surface dimples influence the gel/glass contact or adhesion properties.

In this chapter, poly(vinyl alcohol) gel was selected as a gel that has high mechanical properties to withstand some tribological tests. We prepared a gel with a flat surface and gels with hemispherical surface dimples. Herein, we present a method for imparting dimple patterns on hydrogel surfaces applying the technique used for PDMS^{29,30}. Then, we evaluate the normal contact between the gels with flat or dimpled surfaces and the glass substrate when the normal load is applied to the gel. In addition, the adhesion test is performed to investigate the work of adhesion between them and examined the effects of surface dimples on PVA gels.

1-2 Materials and Methods

1-2-1 Materials

Poly(vinyl alcohol) (PVA) (degree of polymerization: 2000; degree of saponification: >98.5 mol%) was purchased from Nacalai Tesque, Inc. Dimethyl sulfoxide (DMSO), hexamethyldisilazane (HMDS), and *1H*, *1H*, *2H*, *2H*-perfluorodecyltrichlorosilane (FDTS) were purchased from Wako Pure Chemical Industries, Ltd. Polydimethylsiloxane (PDMS) (SILPOT 184) was purchased from Dow Corning Toray Co. All chemicals were used without further purification.

1-2-2 Droplet Replication

To impart the hemispherical surface dimples on the PVA gel, PDMS template were prepared by replicating the condensed droplets on a HMDS-treated hydrophobic glass surface^{29,30}. To obtain hemispherical water droplets, float glasses were modified with HMDS. To clean the glass surface, the glass was soaked in a solution of 10 wt% NaOH in ethanol for 2 hours and then 10 wt% HCl aqueous solution for at least 1 day. For further cleaning, vacuum ultraviolet (UV) light with wavelength of 172 nm was irradiated to the glass surface for 3 minutes using an Excimer irradiation unit (UER 20-172, USHIO Inc.). The cleaned float glass pieces were exposed to HMDS vapor under 20 kPa for 16 hours in a desiccator.

The contact angle to water θ of the glass substrate and hydrogels were measured with a Drop Master 300 (Kyowa Interface Science Co., Ltd) in air at room temperature. The volume of the water droplet (2 μ l) was maintained constant for all the measurement in order to prevent changes in the droplet due to the gravity effect. Each data was the average over 36 points; 4 samples were used and 9 places of each sample were measured. The θ of the HMDS-coated glass was $71.8\pm1.5^{\circ}$.

Water evaporated from a water bath heated to 70°C was condensed on an HMDS-treated hydrophobic glass kept at room temperature (~25°C), resulting in numerous droplets on the surface. The size of the water droplets could be changed by varying the time of exposure of the glass to the vapor from water bath, the exposure time was ranged from 20 to 600 seconds in this work. Then, a degassed mixture of cross-linkable liquid silicone, polydimethylsiloxane (PDMS, SILPOT 184, Dow Corning Toray Co.) was poured to the glass surface with droplets and cured at 70°C for 2 hours. When the crosslinked PDMS was peeled off from the HMDS-treated glass, concave depressions, a negative image of condensed water droplets, appeared on its surface. To achieve positive replication of droplets, liquid PDMS was poured onto the negative replicated PDMS template and crosslinked. These templates were used to make gels with surface dimples as molds for the hydrogel preparation process (Fig. 1-3).

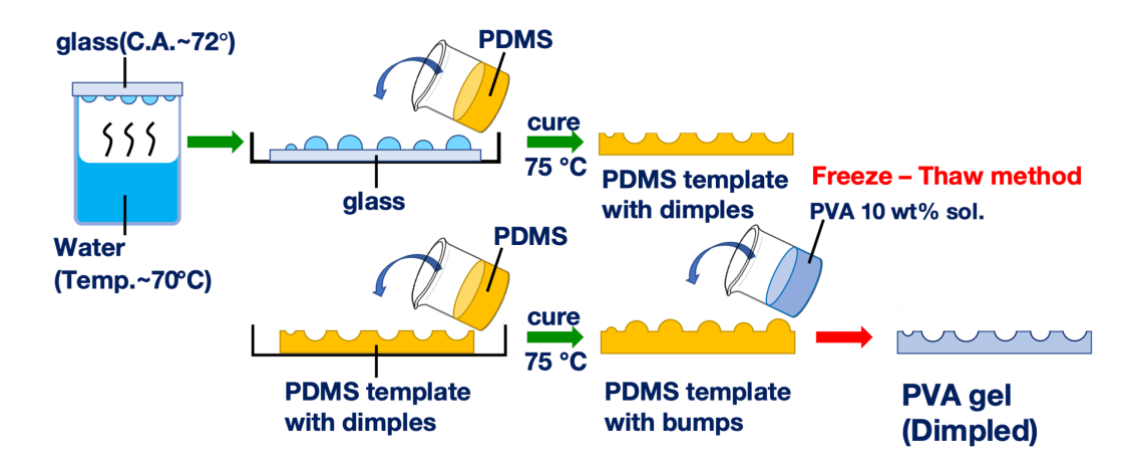


Fig. 1-3 Schematic of the preparation of PDMS templates by droplet replication method and PVA gel with surface dimples.

1-2-3 Hydrogel Preparation

Physically crosslinked PVA hydrogels were prepared from 10 wt% PVA solution of mixture solvent (DMSO: H₂O = 3:1, w/w) by quenching. Polymer solutions were prepared by heating a mixture of PVA and the solvent for 2 hours at 100°C. Then, the degassed PVA solution was poured into a homemade reaction cell consisting of two glass plates separated with a 3.0-mm-thick silicone rubber spacer to form a hydrogel sheet with 100 mm square. To impart dimples on the hydrogel surface, one of the glass plate surfaces of the reaction cell was covered by a PDMS template with surface hemispherical bumps. The solution was quenched at -40°C for 16 hours. The hydrogel sheets were then allowed to warm to room temperature and subsequently immersed in a large amount of deionized water for at least one week to extract DMSO and replace the internal liquid with water⁴². Using a mixed solvent lowers the solvent's melting point, which prevents the solvent from freezing and growing of ice crystals in the gelation process, resulting in a homogeneous network structure or an ability to obtain a smooth surface. In addition, while water and DMSO are good solvents for PVA, they are poor solvents when used in a mixed solvent⁴³. As a result, PVA gel with high mechanical properties that can withstand friction tests such as this study is obtained. The water content of the gels was approximately 86% regardless of the surface structure. As a control sample, a flat surface gel was also prepared on a flat PDMS template. The thickness of the gel sample was measured using the calliper with a minimum scale of 50 µm, and it was confirmed that there was no difference in thickness of 0.05 mm in a 100 mm square.

Herein, PVA hydrogel with a flat surface is referred to as "Flat", and that with surface dimples is referred to as "Dimpled X" (X = 90, 190, 470 and 820), where X indicates the mean diameter in μ m

of surface dimples on each hydrogel (Table 1-1).

Table 1-1 Sample names and mean pattern size on each sample's surface. The "Ratio of flat region" is the ratio of the flat surface area to the whole surface area on hydrogels with surface dimple patterns.

Exp. Time [s]	Sample	Diameter [μm]	Depth [μm]	Ratio of flat region[-]
20	Dimpled 90	93±16	21±9	0.580
60	Dimpled 190	190±40	79±21	0.574
180	Dimpled 470	470±90	220±50	0.479
600	Dimpled 820	820±80	390±50	0.502

1-2-3-1 Surface morphology of hydrogels

The surface morphology of hydrogel samples was observed using a geometry measurement laser microscope (KS-1100, Keyence Corp.). In this observation, the diameter and depth of each dimple shape on the surface of Dimpled series were evaluated. The X–Y range was set to $1000 \times 1000 \ \mu m$ for Dimpled 90 and Dimpled 190, $3000 \times 3000 \ \mu m$ for Dimpled 470, and $5000 \times 5000 \ \mu m$ for Dimpled 820. The mean values of the diameter and depth were averaged over 30 dimples for each sample.

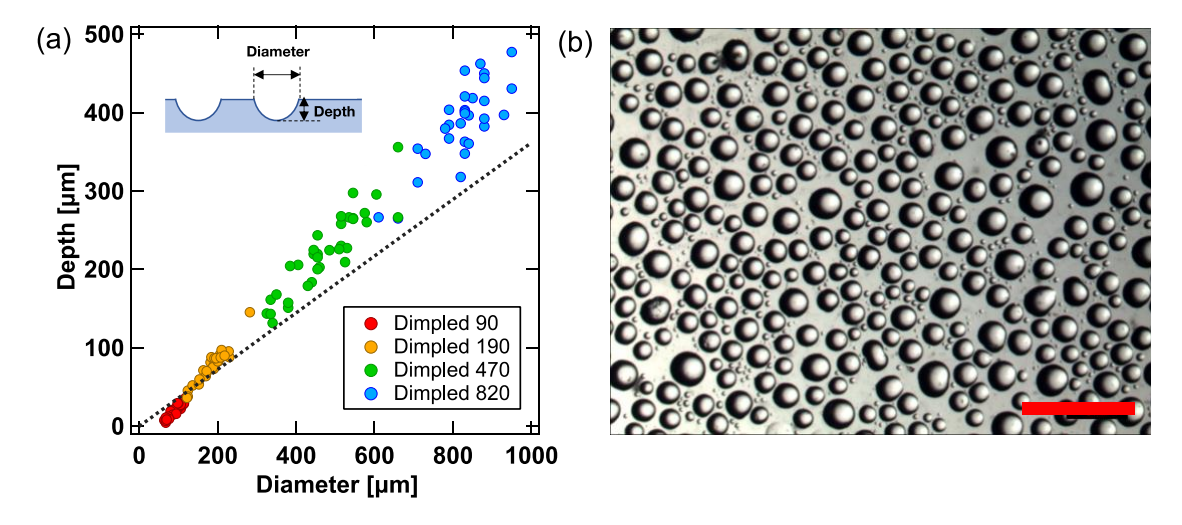


Fig. 1-4 Surface morphology of gels with surface dimples. (a) Depth and diameter of hemispherical dimples on gels surface. The dashed line is the ideal line derived from the contact angle to water of the glass, 72°, for droplet replication. (b) Typical surface image observed by the optical microscope (Dimpled 470). Scale bar: 2 mm.

The hydrogel surface was also observed using an optical microscope (SZX-12, OLYMPUS). This method could observe a wider area compared with the observation by a laser microscope. The obtained two-dimensional image was analyzed using an image processing software, ImageJ⁴⁴, to calculate the Ratio of flat region, which is defined as the ratio of the flat surface area ($A_{\rm flat}$) to the whole surface area ($A_{\rm whole} = A_{\rm flat} + A_{\rm dimple}$) on the surface of Dimpled series. That is, Ratio of flat region is $A_{\rm flat}/A_{\rm whole}$. In case of the Flat, the Ratio of flat region was defined as 1.

The surface morphology of gels with surface dimples is shown in Fig. 1-4 and Table 1-1. Distributed surface hemispherical dimples were obtained, which varied in size depending on the exposure time. The diameter and depth of the dimples have a linear relationship, indicating that the shape of the dimples is similar regardless of the exposure time for all four samples.

1-2-3-2 Elasticity of hydrogels

The Young's modulus E of the gel was measured using a commercially available strain-controlled rheometer (ARES, TA Instruments Ltd.). A disc-shaped sample of smooth surface, 15.70 mm in diameter and 2.70 mm in thickness, was compressed with a velocity of 0.0167 mm/s (= 1 mm/min). In this measurement, silicone oil was dropped to the gel to prevent it from drying and to allow it to deform freely in the compression process. From the strain and normal stress, Young's modulus was calculated for the strain of 10% to 20%. A typical strain-stress curve is presented in Fig. 1-5. This compression test was performed 6 times for each sample, and Young's modulus is the average of the results for all the tests. The E of PVA gel was 94.0 ± 1.4 kPa.

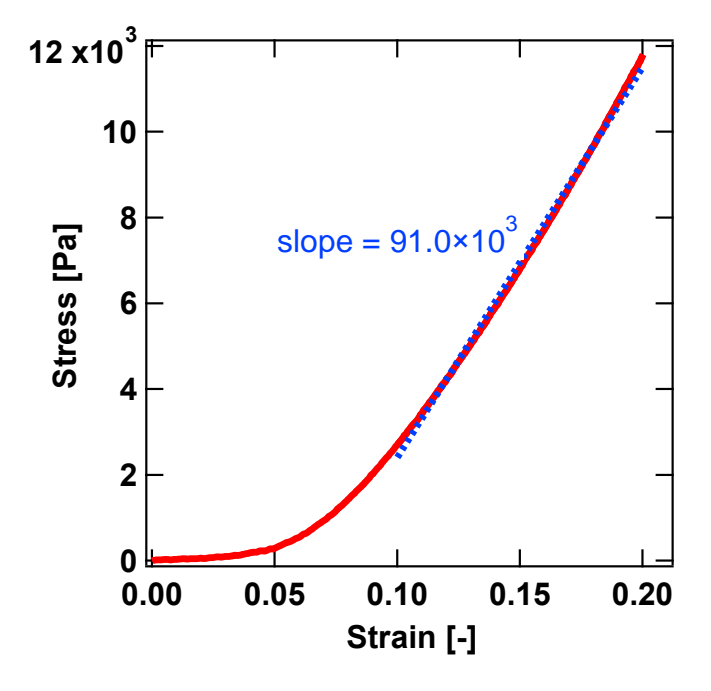


Fig. 1-5 Typical Strain-Stress curve of the PVA gel with a flat surface.

1-2-4 Substrate Preparation

To investigate the influence of the wettability of the counter substrate on the surface property of the gel, three kinds of the glass substrates were prepared. The contact angle to water of the substrate was changed by treatment with silane-coupling agent, FDTS and HMDS. Cover glasses (micro cover glass, C050701, Matsunami Glass Ind. Ltd) were soaked in 10 wt% HCl aqueous solution for 3 days to remove some special coating agent from the surface and washed with water. Then, vacuum UV light with a wavelength of 172 nm was irradiated to the glass surface for extra surface cleaning. The cleaned glasses were exposed to FDTS or HMDS vapor in a vacuum desiccator at room temperature and the pressure of 20 kPa for 8 hours for silane-coupling in a vacuum desiccator at room temperature. The contact angle to water θ of the FDTS-coated glass substrate was $110 \pm 1^{\circ}$, and that of the HMDS-coated glass substrate was $71.8 \pm 1.5^{\circ}$.

The chemical structures of the silane-coupling agents, FDTS and HMDS, and the photograph of the water droplet on the glasses after the surface modification are presented in Fig. 1-6.

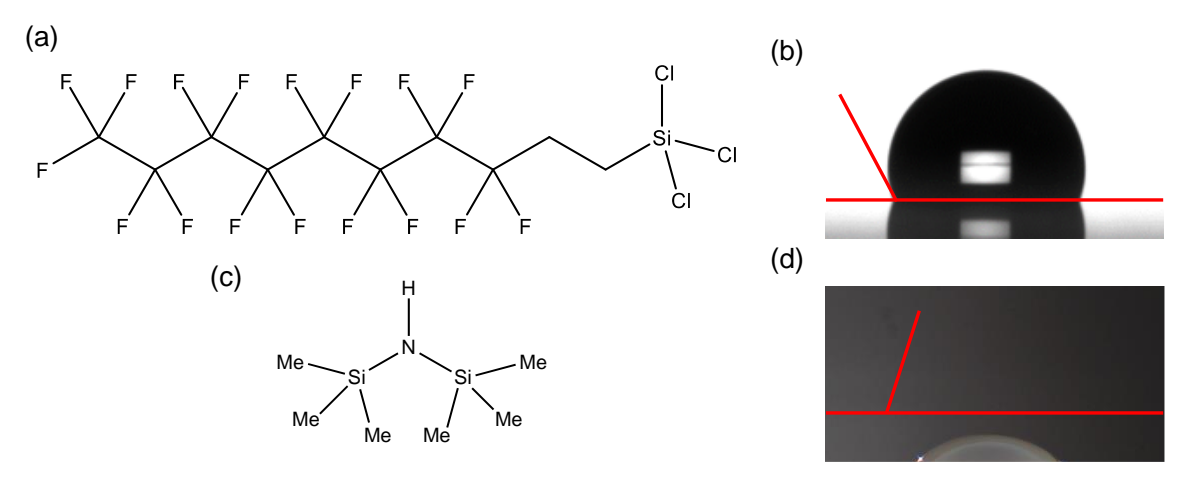


Fig. 1-6 Chemical structure of silane-coupling agent and the photograph of the water droplets on the surface modified glass substrate. (a) Chemical structure of FDTS, (b) the photograph of the water droplet on the FDTS-treated glass surface, (c) chemical structure of HMDS, and (d) the photograph of the water droplet on the HMDS-treated glass surface.

In addition, the glass cleaned by soaking in HCl aqueous solution over three days was used as a hydrophilic substrate. The same amount of water droplets (2 μ L) were placed on this substrate, however, the contact angle was quite low and the water spread so thinly, making it difficult to accurately evaluate the contact angle by taking a water droplet photograph and analysing the image. Therefore, in this study, the contact angle of the substrate cleaned by HCl solution was set to <10° for convenience.

1-2-5 *In situ* Observation

The contact of the hydrogel and the glass surface was observed during sliding friction using a homemade system based on the principle of critical refraction³¹, as shown in Fig. 1-7. Owing to the higher refractive index of the glass than that of the gel, the light from the gel side refracts at angles less than the critical refraction angle $\theta_{\rm gel}{}^{\rm c}$ determined by the relation $\sin\theta_{\rm gel}{}^{\rm c} = n_{\rm gel}/n_{\rm glass}$. On the other hand, when there is a water layer at the hydrogel/glass-substrate interface, the critical refraction angle $\theta_{\rm water}{}^{\rm c}$ is determined by $\sin\theta_{\rm water}{}^{\rm c} = n_{\rm water}/n_{\rm glass}$. Here, $n_{\rm glass}$, $n_{\rm gel}$, and $n_{\rm water}$ are the refractive indices of the glass, gel, and water, respectively.

Because of the slightly larger refractive index of hydrogel than that of water, the critical refraction angle is in the relation of $\theta_{gel}{}^c > \theta_{water}{}^c$, when one observes from an angle θ between these two critical angles, that is, $\theta_{water}{}^c < \theta < \theta_{gel}{}^c$, a bright image of the gel is observed when it is in contact with the substrate (Fig. 1-7a). However, a dark image was observed when a water layer was present at the interface (Fig. 1-7b).

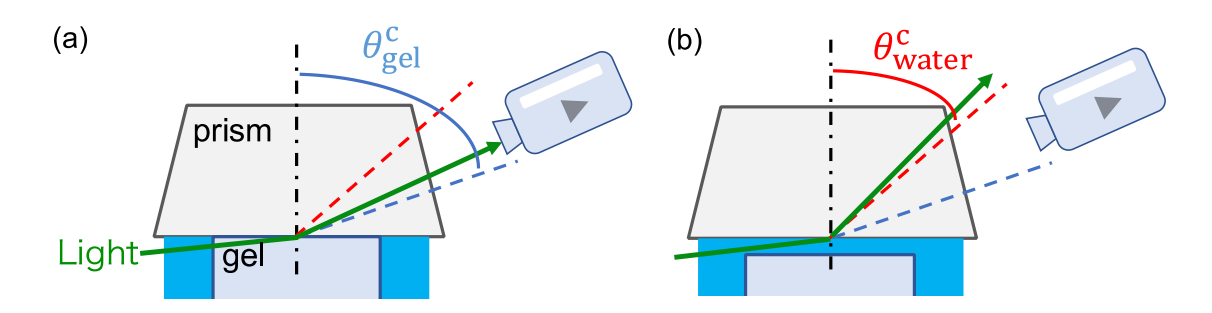


Fig. 1-7 Schematic of the *in situ* observation. The dashed lines represent the critical angle of the gel (blue) and water (red). The camera was located between the critical angle of the gel and that of water. The image of the gel could be observed only when the gel was *in contact* with the substrate (a) and the image could not be observed when the gel was *not in contact* with the substrate (b). This figure was drawn by modifying from Fig. 1 of Yamamoto et al., *Soft Matter*, 2014³¹.

In this study, the trapezoidal prism and a digital video camera (Handycam FDR-AX100, Sony. Co. Ltd) were used. The distance between the sample and the camera is about 1.2 m for the digital video camera for observing the entire sample. The camera was located at the angle θ_r that satisfies the condition $\theta_{\text{water}}^c < \theta_r < \theta_{\text{gel}}^c$. The friction interface was irradiated with white LED light to obtain clear images. The zoom function of the cameras was used to get close images. The focus and exposure were manually adjusted. When the camera is located at a short distance, the difference of the observable depth range in front and back side is larger due to the difference in observation angle. It is desirable to observe the gel as far away from the sample as possible, to evaluate the contact of gel/glass

on the entire surface of samples. Therefore, when using the digital video camera, the contact of the entire gel sample can be evaluated, however, only relatively large dimples can be captured due to the low magnification. The contact state between the hydrogel and the glass substrate was observed *in situ* under loading. By capturing an image in the video, the contact state was evaluated at some sliding velocity. We could determine the contact position because the contact part could be observed as a bright image and the non-contact part as a dark image. The disc-shaped sample was observed as an ellipse shape in the raw images due to the observation at about 60° from the vertical axis to the sample normal surface. The aspect ratio of the images was corrected so that the hydrogel could be observed as a precise circle from ellipse, and image binarization was performed with the contact part as 1 and the non-contact part as 0 to calculate the contact area.

1-2-6 Compression Test

The compression test was performed using the rheometer and the gel/glass contact images were acquired. Disc-shaped samples with 15.70 mm in diameter and 2.70 mm in thickness were used. The sample was fixed to the stage with a cyanoacrylate instant adhesive agent (Toa Gosei Co., Ltd) and the test was performed in water. The normal strain was applied to the PVA gel at a constant strain rate of 10 µm/s until the prescribed normal load was reached, fixed for about 2 seconds to record the normal strain and the gel/glass contact image, and then normal strain was applied to the next prescribed normal load, repeatedly. This test takes about 120 seconds, and although stress relaxation is expected to occur, it is very small and can be negligible, especially for comparing Flat and Dimpled. The characteristic time of stress relaxation due to the flow of water in the gel was calculated to be on the order of a^2/D_c according to the work by Hui et al⁴⁵, and based on this calculation, it was on the order of 10³-10⁴ s. In this calculation, the radius of the indenter compressing the gel, a, in the reference paper, was set to 1.35 mm, which is half the thickness of the gel as a characteristic length, in this paper, and D_c is the cooperative diffusion coefficient, which was calculated as $D_c = k_B T / 6\pi \eta \xi_h$, and was in the order of 10^{-10} to 10^{-11} m/s². k_B , T, η , ξ_h , are the Boltzmann constant, temperature, viscosity, and hydrodynamic shielding length respectively. Since the temperature is 25 °C and the solvent is water, $k_BT =$ 4.11×10^{-21} Nm, $\eta = 0.894 \times 10^{-3}$ Ns/m². ξ_h was assumed to be the order of 10^{-9} to 10^{-8} m. The calculated time $(10^3 - 10^4 \text{ s})$ is longer than our measurement time scale $(10^2 - 10^3 \text{ s})$, and the stress relaxation due to solvent flow during the measurement is considered to be negligible.

The contact area was evaluated using the above-mentioned *in situ* observation method and analyzed by ImageJ. The normal force dependence of the normal strain and contact area was investigated. Also, the contact pressure was calculated (denoted as Cal. Contact Pressure in Fig. 1-14), assuming only the contact part sustains the normal load. Cal. Contact Pressure is defined as (normal force / contact area), where contact area is the value obtained by the image analysis, and the dimple area shown in a dark

in the image was treated as a non-contact area.

1-2-7 Adhesion Test

To measure the adhesion between the gel and the glass substrate, a rheometer (ARES, TA Instruments Ltd.) was used. The schematic of the measurement system is displayed in Fig. 1-8 Schematic of the adhesion test setup.

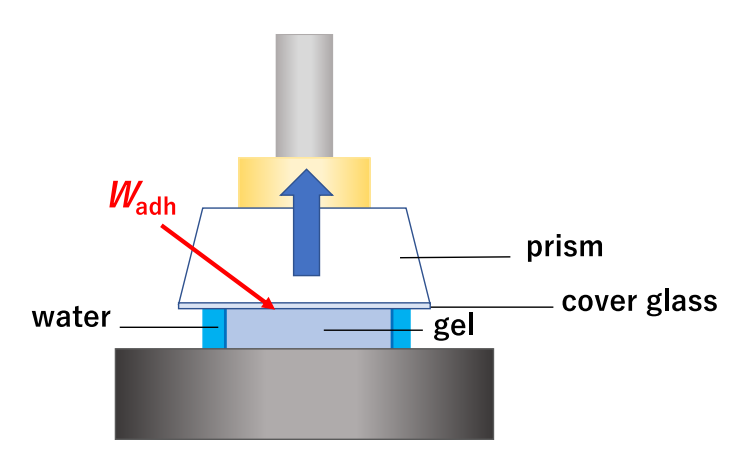


Fig. 1-8 Schematic of the adhesion test setup.

PVA gel, cut into the disc-shape of 15.30 mm in diameter and 2.70 mm in thickness, was fixed on the stage with a cyanoacrylate instant adhesive agent (Toa Gosei Co., Ltd). For *in situ* observation, a trapezoidal prism with the glass substrate on the bottom surface was fixed to the upper jig. Note that, a drop of silicone oil that has the same refractive index as the glass was lodged between the prism and the glass substrate so that the prism and the glass substrate can be treated as one medium and the light not be reflected at the interface to observe the gel/glass contact image.

The normal load was applied to the gel until it reaches the normal stress σ =11 kPa as the primary pressure, after 10 minutes of pre-loading, the adhesion test was started. In the test, the jig with the glass substrate was pulled up at a constant velocity of 0.167 mm/s for 3.5 seconds from the state where the gel and the substrate were in contact (Fig. 1-9a). The displacement and the normal force data at the time were acquired at the rate of 100 points/s.

Displacement-normal force curve was drawn using the obtained data, and the area where the normal force is smaller than 0 gf is defined as the work of adhesion, W_{adh} , and calculated (Fig. 1-9b). The tests were conducted in water and in air.

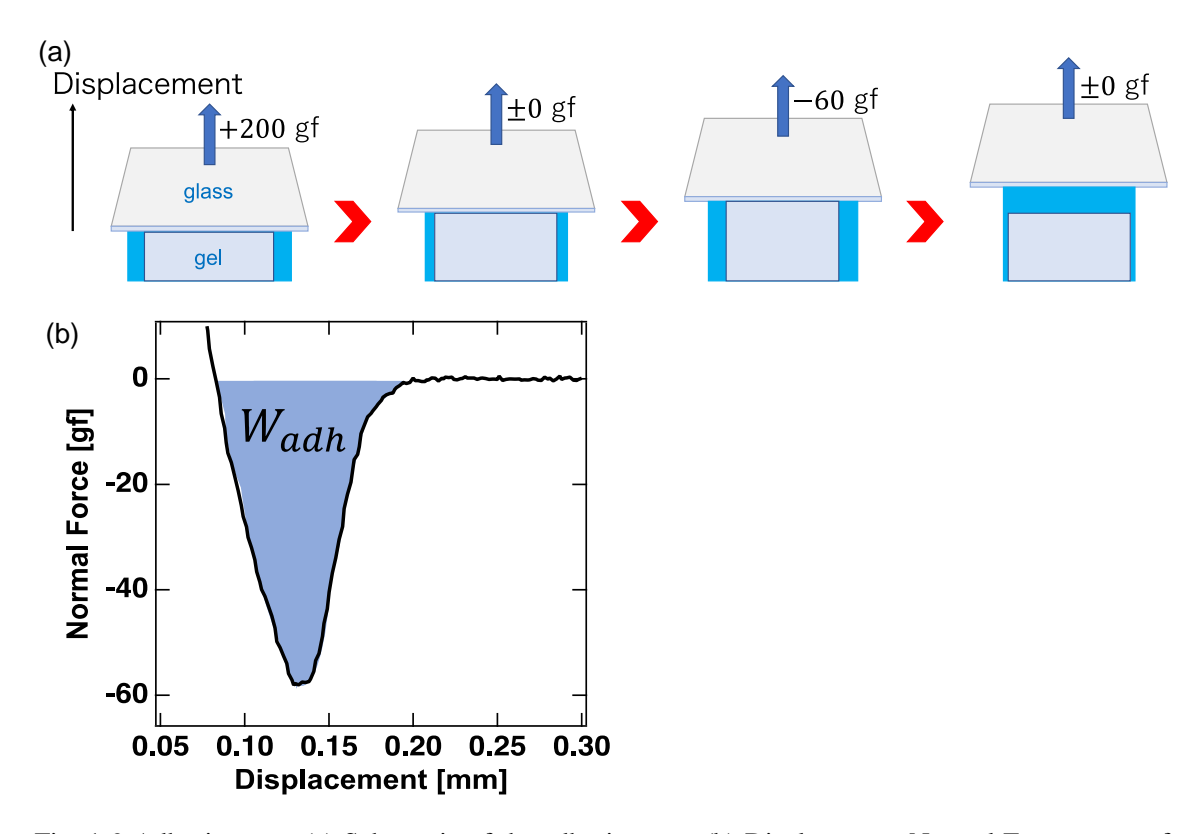


Fig. 1-9 Adhesion test. (a) Schematic of the adhesion test. (b) Displacement-Normal Force curve of the adhesion test. The shaded area was defined as the $W_{\rm adh}$ in this study.

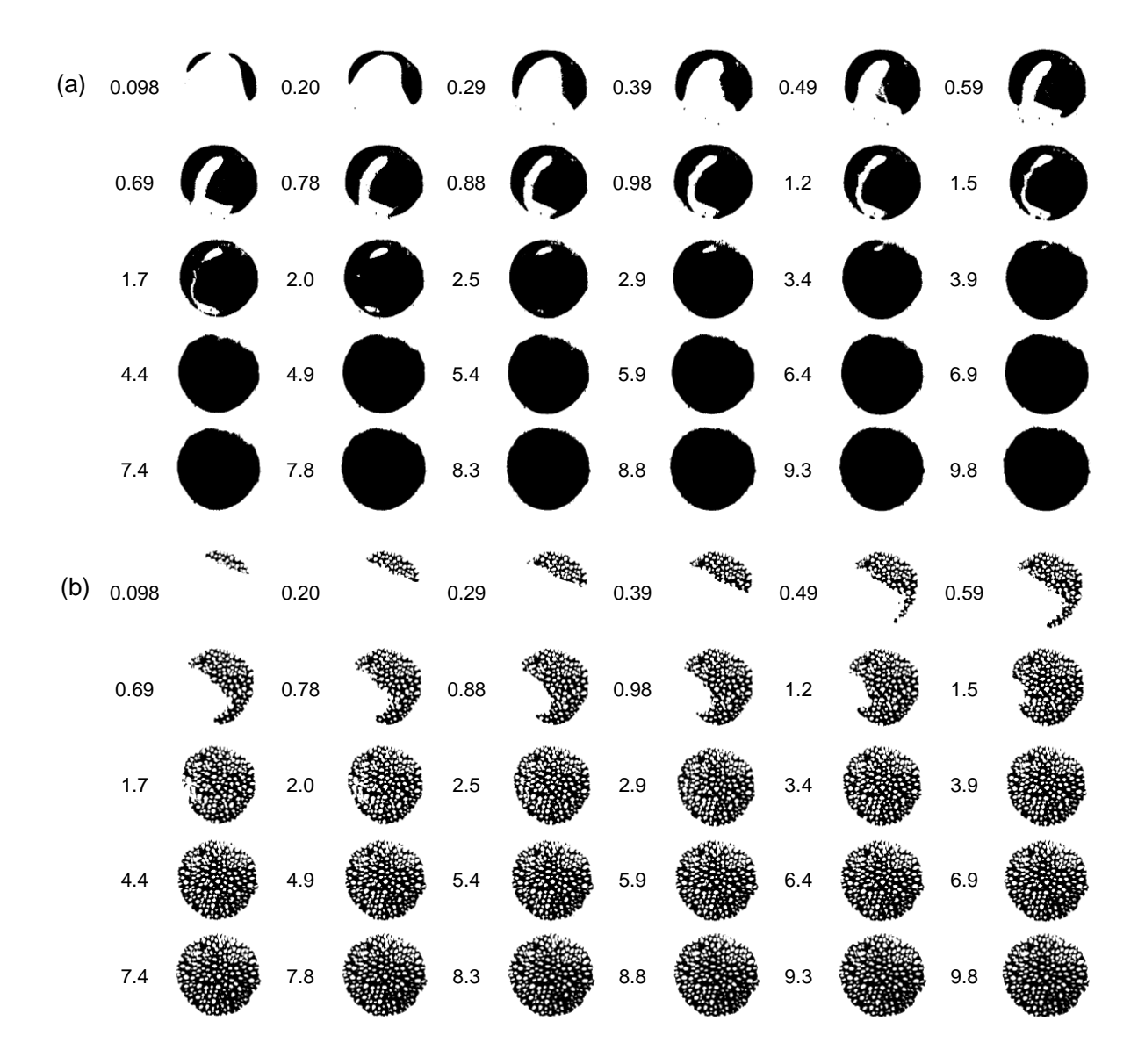
1-3 Results and Discussion

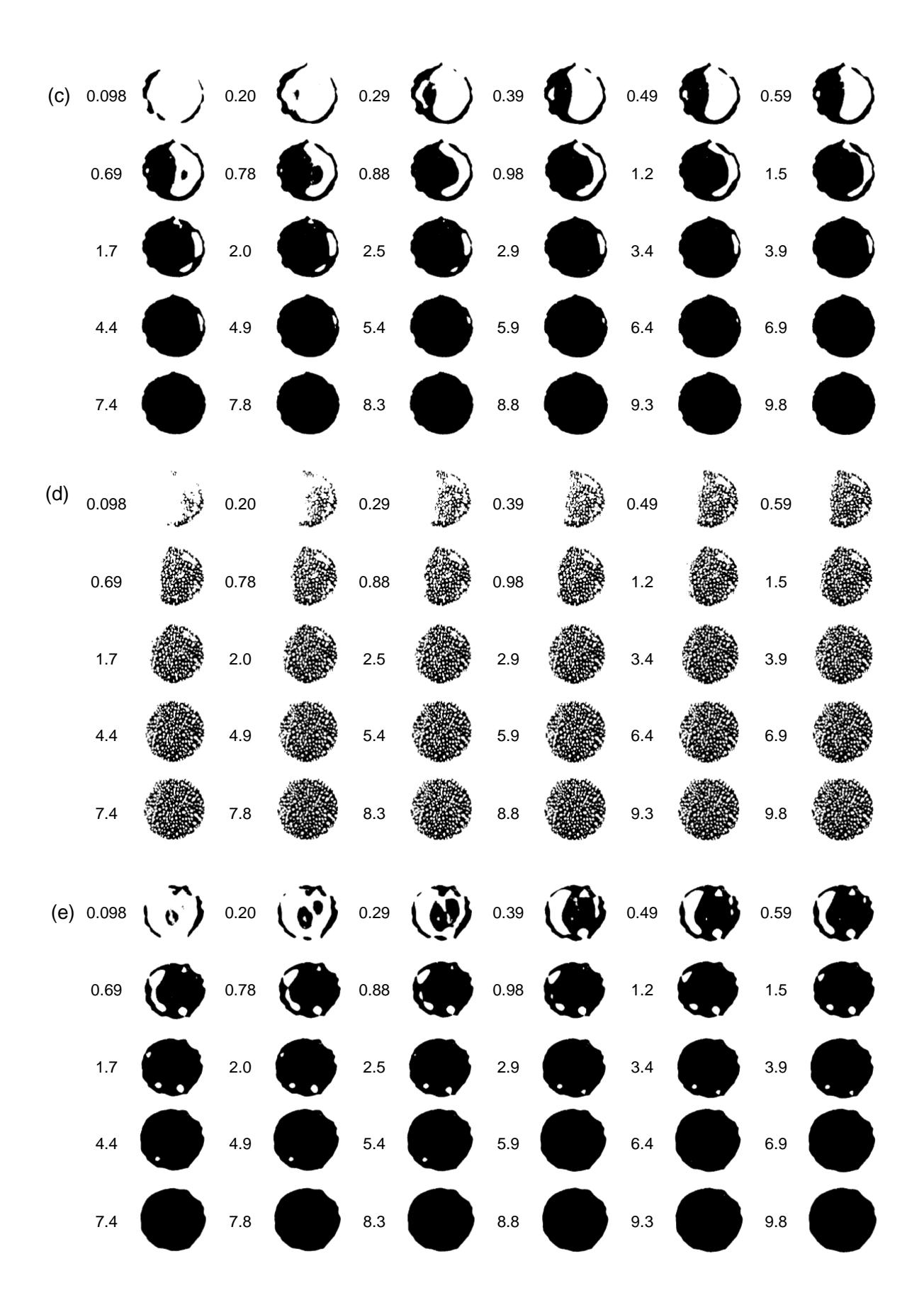
1-3-1 Normal contact between the glass substrate and the PVA gel

Results of compression tests in which gels were compressed against the glass substrates with three kinds of wettability are discussed. Because of the limitation of the observation magnification, the dimple size was too small to be observed by the digital video camera for Dimpled series, except for Dimpled 820, image analysis could be performed for only Dimpled 820, the gel with the largest mean diameter or depth of dimples, so the comparison of Flat and Dimpled 820 is shown here.

First, the relation of the normal force applied to the gel and the contact area between the gel and the substrate calculated by the image analysis is presented in Fig. 1-11, and the contact images are shown in Fig. 1-10. In the image analysis, only the area where looked in white is treated as the contact area, and the area where looked in black colour and water exist is treated as the non-contact area. The "contact area" was calculated by observing the interface between the gel and the counter glass substrate in water, and the "whole area" is the actual area of the top surface of the gel calculated from

the diameter measured by calliper, in Fig. 1-11.





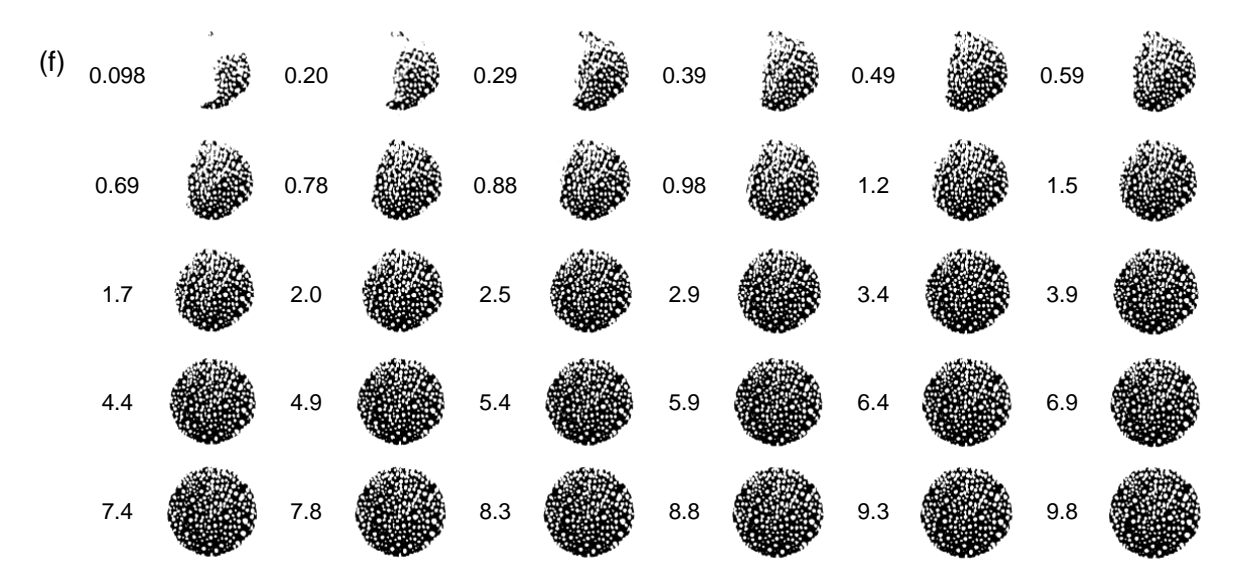


Fig. 1-10 Contact image of the gel/glass interface in compression tests. The contact angle to water of the glass substrate was (a, b) $\sim 110^{\circ}$, (c, d) $\sim 70^{\circ}$, and (e, f) $< 10^{\circ}$. The images (a, c, e) are the binarized contact images of Flat gel and the images (b, d, f) are that of Dimpled 820 gel.

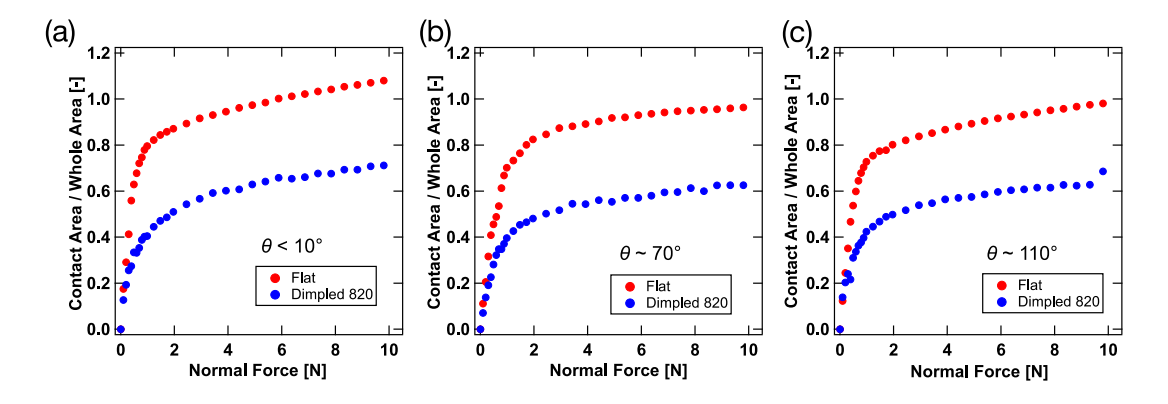


Fig. 1-11 Relation of normal force and contact area. The contact angle of the substrate is (a) $< 10^{\circ}$, (b) $\sim 70^{\circ}$ and (c) $\sim 110^{\circ}$.

From Fig. 1-11, the shape of dimples on Dimpled surface was maintained in the process of compression against three kinds of the glass substrates, and it was obvious from the design of the surface shape, the contact area of Dimpled 820 was smaller than that of Flat due to the dimples, indicating the reduction in contact area for all of the substrates, which is the effect (1) shown in the introduction section.

Next, the relation of the normal force and the normal strain applied to the gels are presented in Fig. 1-12.

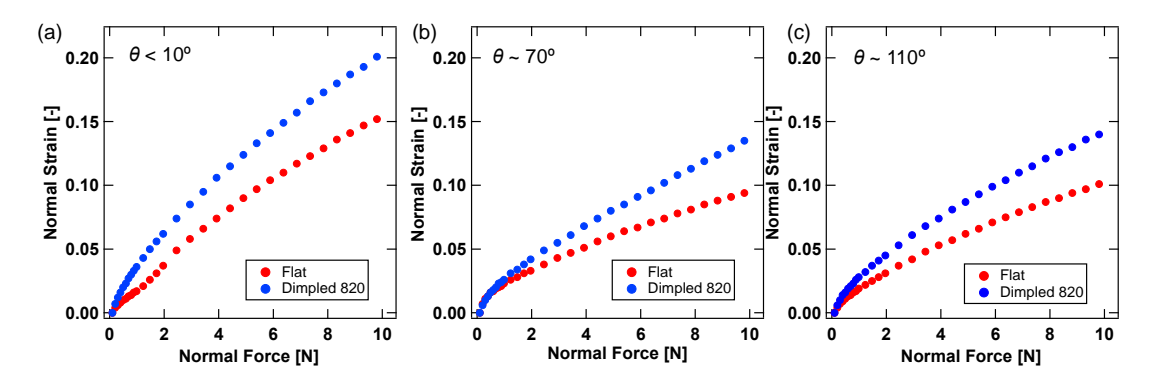


Fig. 1-12 Relation between normal strain and normal force. The contact angle of the substrate is (a) $< 10^{\circ}$, (b) $\sim 70^{\circ}$ and (c) $\sim 110^{\circ}$.

The relationship between the normal force and strain applied to the gel sample is shown in Fig. 1-12. The normal strain required to reach the same load was higher for Dimpled gel than for Flat gel on any substrates, regardless of the wettability, indicating that the water trapped in the dimples makes a less or negligible contribution in sustaining the normal load. If the water in dimples is sustaining the load, the relationship between the normal strain and the contact pressure for Flat and Dimpled 820 calculated from the contact area should not coincide in Fig. 1-14 (strain vs contact pressure). This is because the contact pressure is calculated by dividing the normal load by the observed contact area, so if the load is sustained by water at the same strain, the contact pressure of Dimpled will be higher than that of Flat in the calculation.

From the results shown in Fig. 1-11 and Fig. 1-12, we state the difference in the normal contact depending on the surface wettability of the glass substrates.

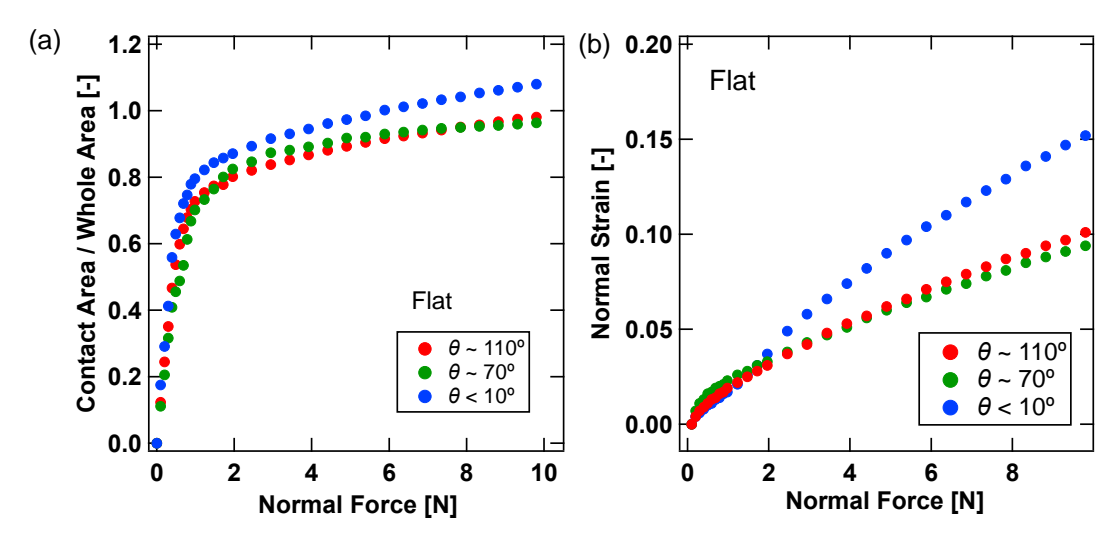


Fig. 1-13 Comparison of the relation between the normal force applied to the Flat gel and (a) the ratio of contact area, (b) the normal strain, on three kinds of glass substrates with differnt wettability.

Among three kinds of substrates with different hydrophobicity, the ratio of the contact area or the normal strain were almost the same for the substrates with the contact angle of $\theta \sim 70^{\circ}$ and $\theta \sim 110^{\circ}$, however those values for the substrates with the contact angle of $\theta < 10^{\circ}$ were higher compared with other substrates, as shown in Fig. 1-13. This result shows that the surface of the gel slid to the planar direction and be well extended against the substrate with $\theta < 10^{\circ}$ under compression. On the other hand, it is reasonable to consider that the deformation to the planar direction was limited when the normal load was applied to the gel and the gel was compressed against the substrates with $\theta \sim 70^{\circ}$ and $\theta \sim 110^{\circ}$. For this, water trapped in surface dimples was confined and the force for the compression direction was applied to the water, so it is predicted that the water in dimples is likely to sustain the normal load than the substrate with $\theta < 10^{\circ}$. Also, it is expected that the adhesion strength between the gel and the substrate with $\theta < 10^{\circ}$ is lower compared with other substrates, we discuss this in the later section 1-3-2.

The pressure applied to the contact area was calculated by dividing the load applied to the gel by the actual contact area between the gel and the glass substrate obtained in Fig. 1-11 and expressed as Cal. Contact Pressure in Fig. 1-14.

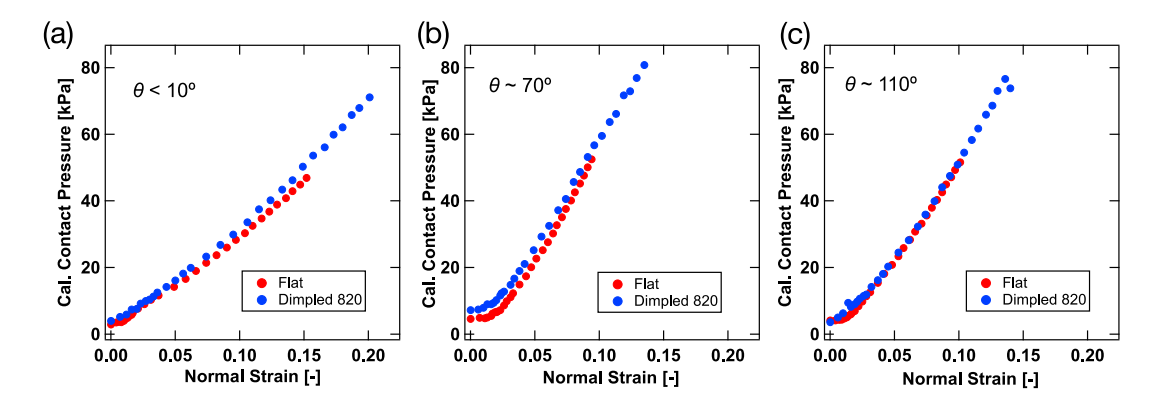


Fig. 1-14 Relation of normal strain and contact pressure. The contact angle of the substrate is (a) $< 10^{\circ}$, (b) $\sim 70^{\circ}$ and (c) $\sim 110^{\circ}$.

In real, the relationship between the normal strain and the calculated contact pressure for both Flat and Dimpled 820 (Fig. 1-14) is almost the same on any substrates, which confirms that the water in the dimples does not sustain the load.

We consider that whether the water in the dimples sustains the normal load depends on whether the gel is in contact with the substrate slides and elongates in the planar direction or not. When the gel contacts the substrate and the gel deforms smoothly in the planar direction with compression, we believe that the contacting part of the gel will sustain the normal load dominantly. This is because as

long as the gel deforms in the planar direction upon compression, the dimples will also deform, and water in dimples will not be compressed. As a result of the image analysis, the contact part of the gel/substrate was elongated in the planar direction, and the deformation was similar to the case where the gel was assumed to deform into a flat plate with constant volume (Diameter: 15.30 mm to 15.64 mm).

Based on the above results and the relationship between normal load and strain, the pressure at the contact part of Dimpled is higher than that of Flat under the same normal load. Also, the effect (2) was disproved, indicating that water trapped in the dimples did not sustain the normal load. This means that the pressure at the contact part of Dimpled 820 was higher than that of Flat in friction measurement under the same nominal normal load (corresponds to normal pressure of $\sigma = 11$ kPa).

To sum up, the normal strain of Dimpled 820 was larger than Flat and water in the surface dimples could not sustain the normal load under the same loading condition. Therefore, it can be said that σ_{local} , the pressure applied to the local flat part on the Dimpled gel surface where contacts to the glass substrate, is higher than σ_{Flat} , the pressure applied to the contact part on the Flat gel surface ($\sigma_{local} > \sigma_{Flat}$).

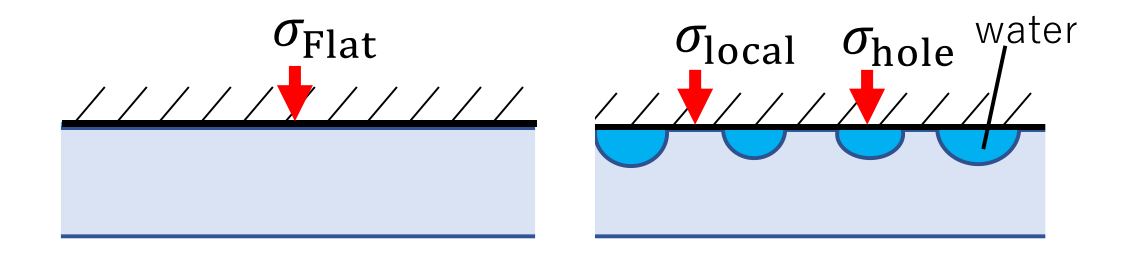


Fig. 1-15 Schematic of the contact of the glass substrate and Flat gel or Dimpled gel.

In the friction measurement discussed in Chapter 2, the loading time was 10 minutes, but the relationship between the contact and the strain was similar. From Persson's work⁴⁶, the relationship between the thickness of the water layer h between two parallel plates of radius R under the normal pressure σ and squeezing time t is expressed as $t = 3\eta R^2 / 4\sigma h^2$. According to this equation for a squeezing time, assuming that the contact is formed at the distance of 100 nm, it takes about 370 seconds, so the loading time for the friction measurement was set to 600 seconds. Considering the squeezing time, the results shown in Fig. 1-11, Fig. 1-12 and Fig. 1-14 are less reliable for the low load region, but for the relatively high load region, both the time and the load are enough to squeeze, and it can be assumed that we are observing the contact between the gel and the glass after the squeezing is completed. This time dependence is also considered to be a small difference for

comparing Flat and Dimpled.

1-3-2 Work of adhesion of the PVA gel

In this chapter, the adhesion test was conducted in water and in air. We should consider the contact of three bodies, that is the gel, water, and the glass substrate for the test in water and two bodies, that is the gel and the glass substrate for the test in air. Commonly, the work of adhesion is stated by Dupré's equation, Eq. 1-1. Factors that affect the $W_{\rm adh}$ (or adhesion force) of the gel include (i) the ease of contact between the gel and the substrate and (ii) the adhesion strength between the gel and the substrate. The factor (i) is whether water is easily drained from the interface, and is determined by the contact angle of the substrate with water. Further, factor (ii) is determined by the interfacial energy between the gel and the substrate. The test in water is affected by both factors, but the test in air is affected only by factor (ii). The adhesion of the gel is discussed in more detail using the surface energy below.

Generally, the surface (interface) energy γ acting between two different substances A and B is described by the following formula.

$$\gamma_{AB} = \gamma_A + \gamma_B - 2(\gamma_A \cdot \gamma_B)^{\frac{1}{2}} = (\sqrt{\gamma_A} - \sqrt{\gamma_B})^2$$
 (Eq. 1-4)

From Eq. 1-4, when $\gamma_A = \gamma_B$, the interface energy takes the minimum value with $\gamma_{AB} = 0$, so it can be said that the contact is most stable when the surface energies of the two substances are the same. Applying this argument to the system in this study, substances A and B are PVA gels and glass substrates. The contact angle of PVA gel is about 60° , and among the glass substrates used in this study, the surface energy is the closest to the substrate with contact angle $\theta \sim 70^\circ$, so it is theoretically predicted that it is possible to make it relatively strong contact. Note that, we can also make similar discussion using the spreading coefficient determined by the interfacial energy. In addition, the previous studies showed that the slip length depends on the surface hydrophobicity in micro/nanometre scale fluid channel by some experiments or MD simulations^{47–49}. Therefore, without having to consider the interfacial energy of gels, there is a possibility that the rate of water drainage at the interface is varied depending on the wettability of the substrate surface and this influences the easiness to the contact of the gel and the substrate, however, it is unclear at present that there can be seen the effect similar with the previous studies in this macroscopic system. Fig. 1-16 shows the relationship between the adhesion force W_{adh} measured in water and in air and the substrate contact angle.

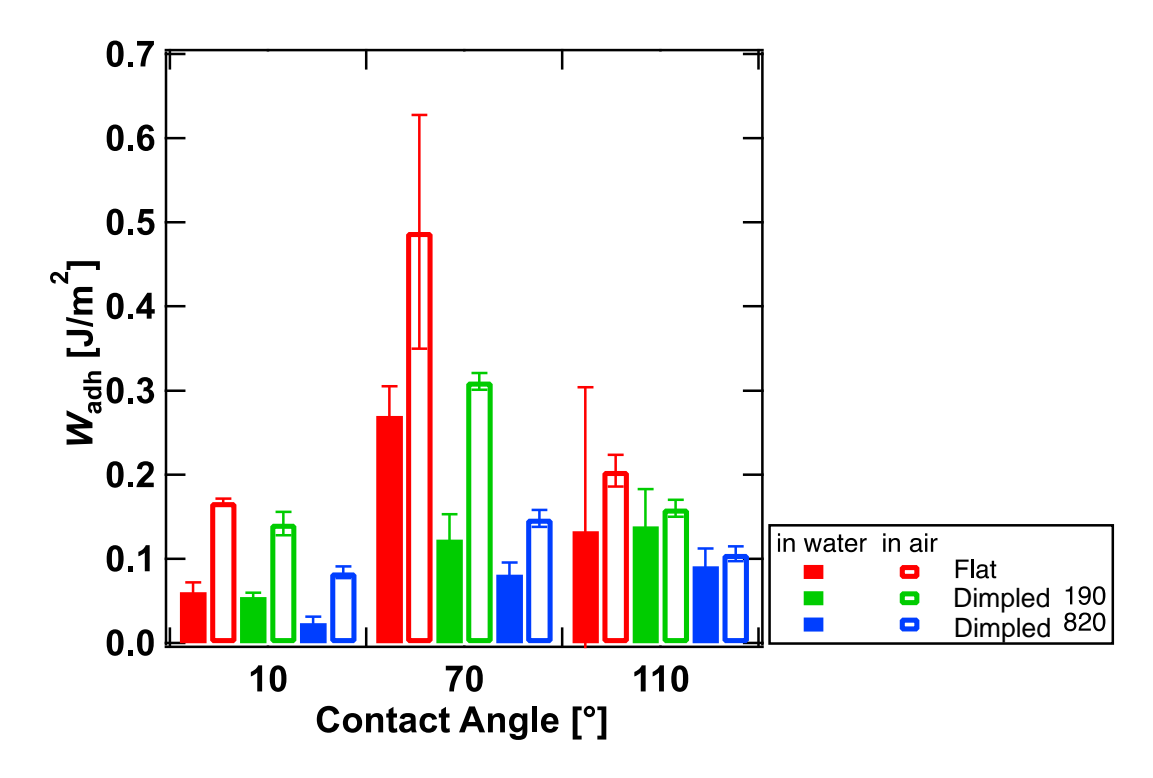


Fig. 1-16 Relation of Contact Angle of the glass substrate and Work of Adhesion.

First, when we focused on the wettability of the substrates, W_{adh} against the substrate with $\theta \sim 70^{\circ}$ showed the largest value. In addition, the values measured in air were larger than the values measured in water.

We consider the factor (i) and (ii) that may have influences on $W_{\rm adh}$ stated earlier. Regarding the factor (i), it is expected that water drainage is the easiest for the most hydrophobic substrate with $\theta \sim 110^{\circ}$ and is the most difficult for the most hydrophilic substrate with $\theta < 10^{\circ}$. For the factor (ii), it is predicted that the contact between the gel and the glass substrate is the most stable for the substrate with $\theta \sim 70^{\circ}$, and the stability of the substrates with $\theta \sim 110^{\circ}$ or $\theta < 10^{\circ}$ are inferior to that with $\theta \sim 70^{\circ}$.

The tests, conducted in air, did not need to drain water, so the gel and the glass substrate should contact firmly, and the results that the $W_{\rm adh}$ measured in air were higher compared with the $W_{\rm adh}$ measured in water are reasonable. Also, because only the contact stability is reflected in the $W_{\rm adh}$ for the tests performed in air, the result that the $W_{\rm adh}$ had the highest value against the substrate with $\theta \sim 70^{\circ}$ can be said that it is consistent with the initial theoretical prediction.

Next, when we focused on the effect of surface dimples, the relation, $W_{\text{adh, Dimpled}} < W_{\text{adh, Flat}}$

came into existence for the tests conducted both in water and in air against any substrates. This might be attributed to the reduction in the contact area between the gel and the glass substrate due to the surface dimple structure of Dimpled and the promotion of the detachment because water trapped in dimples was provided to the interface. In addition, comparing for Dimpled 190 and Dimpled 820, both gels have similar surface dimples, the relation, $W_{\rm adh,\ Dimpled\ 820} < W_{\rm adh,\ Dimpled\ 190}$ was confirmed. It is considered that this is because the larger the volume of the dimple, the larger the amount of water that can be trapped, and the easier it is to provide water through the interface.

1-4 Conclusion

We prepared PVA gels with hemispherical surface dimples, then investigated the normal contact and adhesive properties against glass substrates with different wettability.

The droplet replication technique, which was developed to change the surface geometry of PDMS^{29,30}, was applied to the hydrogel template to impart the dimples on the surface of the hydrogel. The diameter or depth of dimples was distributed but all the dimples were almost similar shapes.

The normal contact of gels to three kinds of the glass substrate was evaluated by *in situ* observation³¹ when the normal load was applied to the gel using the rheometer. Effect (1), as predicted from the surface design, was confirmed: the reduction in contact area due to the surface dimples was observed. The dimple shape on the surface was remained intact under compression and the contact area was reduced by approximately 50% compared to the hydrogel with a flat surface. Regarding effect (2), we initially predicted that the contact pressure of the contact part of Dimpled does not increase because trapped water in dimples would sustains the normal load. However, it was clear that this prediction was not accurate. The water in dimples contributed minimally load support compared to the other flat contact region, resulting in a higher local contact pressure for the Dimpled gel than for the Flat gel.

In addition, the adhesion test of the gels against the glass substrates was performed. As a result, the work of adhesion of the gel against the substrate with the contact angle of $\theta \sim 70^{\circ}$, which shows intermediate wettability among the substrates used in this test, was the largest. The surface energy of this substrate was the most similar to that of the PVA gel, so the reason for the largest work of adhesion on this substrate was that the interfacial energy got most stable by the contact. Dimpled gels, in comparison to Flat gel, tended to show smaller work of adhesion on any substrates, this may be attributed to the reduction in the contact area for Dimpled gel compared with the Flat gel up to about 50% and also the promotion of the detachment by being provided water, trapped in the surface dimples, to the interface due to the surface deformation. In addition, though the local contact pressure of

Dimpled gel was higher than Flat gel, there were no pathways to drain the water on the Dimpled gel surface. Therefore it was considered that the strong adhesion between the gel and the glass was hindered.

To summarize, the reduction in gel/glass contact area, increase in the local contact pressure, and the smaller work of adhesion were confirmed for Dimpled gel compared with Flat gel, in this chapter. While higher contact pressure would generally lead the higher friction, the reduced contact area and the small work of adhesion suggest the lower friction of Dimpled gel. Therefore, this surface design would be suitable to make the sliding friction of hydrogels lower. The friction behavior of Dimpled gel is discussed in detail in Chapter 2.

Chapter 2 Friction behavior of PVA gels with hemispherical surface dimples on their surfaces

2-1 Introduction

Articular joints show quite low sliding friction and can move smoothly without feeling any physical resistance. Living cartilages on the sliding surface of bones are soft tissues containing a large amount of water and are in the form of a hydrogel. A hydrogel is a substance in which a three-dimensional network polymer structure is swollen with water. Hydrogels have unique features, such as permeability and stimuli responsiveness. Hydrogels and living tissues are similar in that they are soft and contain a large amount of water. Therefore, hydrogels can be used as a cell culture scaffold and biomaterial in biomedical fields ^{50,51}. They are also suitable for bio-models of soft tissues.

In this study, our purpose was to reduce the sliding friction of the hydrogel surface while maintaining its bulk properties, such as the elastic modulus, water content, and permeability. In practical applications, reducing friction can lead to a longer service life and energy saving, making a slippery surface advantageous.

Several studies have already explored methods to lower the friction of hydrogels. For instance, preparing the hydrogels using electrolyte monomers or polymers are available ^{33,52}. Preparing the gels with polymer brush structure on the gel surface is also useful ^{17,53}. These methods can reduce the surface friction of gels by lowering the polymer concentration in gels or polymer density on the gel surface due to high swelling and maintaining a hydrated lubrication layer on the surface. However, a disadvantage is that these methods often results in poor mechanical strength of gels or its surface. In addition, the friction strongly depends on the charge of the counter surface, ionic strength of lubricant and the charge density of the hydrogel surface for the electrolyte gel, so it is difficult to use as a universal method to reduce friction under all conditions. On the other hand, adding linear polymers like hyaluronic acid (HA) or surfactant to the lubricant ^{54,55} and incorporating phospholipids to gels ^{56,57} are helpful to reduce the surface friction. However, these methods cannot reduce the friction of gel itself, but they can be combined with other methods to reduce the friction of gel itself.

Observations of the cartilage surface, which is predicted to be responsible for the low friction between joints, has revealed micrometer-order dimples¹², but the role of such structures is still unclear. The frictional behavior of articular cartilage has been extensively studied using models such as the biphasic lubrication theory⁵⁸ and poroelastic models^{59–62}. The biphasic lubrication model explains the superior friction mechanism of articular cartilage, which shows quite low friction. In this model, cartilage is

considered to be composed of two phases: a solid phase and a liquid phase. The former is made of polymers such as collagen and proteoglycan, and the latter is the interstitial water. The friction is considered to occur mainly in the solid phase at the sliding interface, but even in areas where the solid phases are in contact, the liquid phase supports the applied load, lowering the contact pressure in the solid phase and providing lubrication. Hydrogels are substances in which the three-dimensional network structure of polymers is swollen with water and are biphasic substances like cartilage, so the friction mechanism is expeted to resemble the articular cartilage. Additionally, recent studies highlight the role of synovial fluid components, such as hyaluronic acid and lubricin, in boundary lubrication mechanisms^{63,64}. However, the model which takes into consideration the surface structure of cartilage has not been proposed. These models take into account the bulk structure of the substance, but not the surface geometry of the substance; therefore, the effect of the surface geometry is considered to appear as an additive effect to these models.

It is generally known that surface geometry affects its surface properties. For instance, geckos have fine seta on their hands, and the spatula structure at the tip of the seta creates efficient adhesive strength²³. Also, in artificial objects, grooves carved on the surface of car tires promote water drainage, hindering lubrication and forming quick contact with the ground.

The moduli of hydrogels and metals are significantly different, but the dimple structures on metal surfaces are good examples of cases where sliding friction is changed by surface shape. When a metal surface is textured to obtain dimple shapes, friction is reduced compared to that on a flat surface^{24,25,65–68}. It was reported that the surface dimples of metals have roles as a lubricant reservoir or trap for wear particles and promote lubrication. However, there are few reports on sliding friction of hydrogels with dimple shapes, but several reports on the friction of hydrogels with modified surface geometry. For example, it has been found that hydrogels with macroscopic roughness on the surface have more stable contact and increased friction than flat hydrogels, due to the faster squeezing between the gel and the glass substrate resulting from the higher contact pressure owing to the surface roughness¹⁰. Also, the effects of surface roughness on the sliding friction of hydrogels are limited to relatively low loading conditions and are affected by Young's moduli, roughness size, and/or distribution⁶⁹. Thus, surface geometry has been indicated to be a key factor for the friction of not only solid materials but also hydrogels.

Therefore, we expected friction reduction by imparting hemispherical dimples on the smooth flat surface of hydrogels. This research, which changes the surface geometry, is different from similar past research in that it achieves low friction for the gel itself without changing its bulk properties such as mechanical strength. Furthermore, if it is possible to reduce friction by varying the gel surface

geometry it is expected that this will be possible to coexist with the friction reduction methods used in these previous studies. In addition, further research on the friction mechanism of hydrogels, which mimic cartilages and have dimples on their surface, will lead to clarifying the friction mechanism of joints.

In this chapter, we examined the effect of hemispherical dimples on hydrogel surfaces on sliding friction. Poly (vinyl alcohol) (PVA) hydrogel was selected as the target hydrogel. PVA hydrogel has high mechanical strength and can withstand friction tests. The measurement and observation system we used in this study was the same as the previous studies 31,33. However, we prepared PVA hydrogel, which is neutral and shows adsorptive properties to the glass, so the chemical species which compose the hydrogel were different from those studies. Also, the hydrogel used in the previous studies had a flat surface, but we prepared PVA gels with dimples on their surfaces and investigated the effects of surface geometry on friction property. The swelling degree of the gel may differ between the surface and the bulk, but PVA gel shrinks to about 90% in thickness in the process of solvent displacement, that is, the size change occurs, but the dimple shape imparted on the surface is likely to be maintained. Therefore, it is suitable for investigating the effect of surface geometry.

The "adsorption model" is one of the models to explain the friction of PVA gel, and we considered the effect of surface geometry based on this model. In this model, the friction is expressed by the sum of the elastic resistance, which arises between the hydrogel and the substrate, and the viscous resistance by lubricant (water in this study) at the interface.

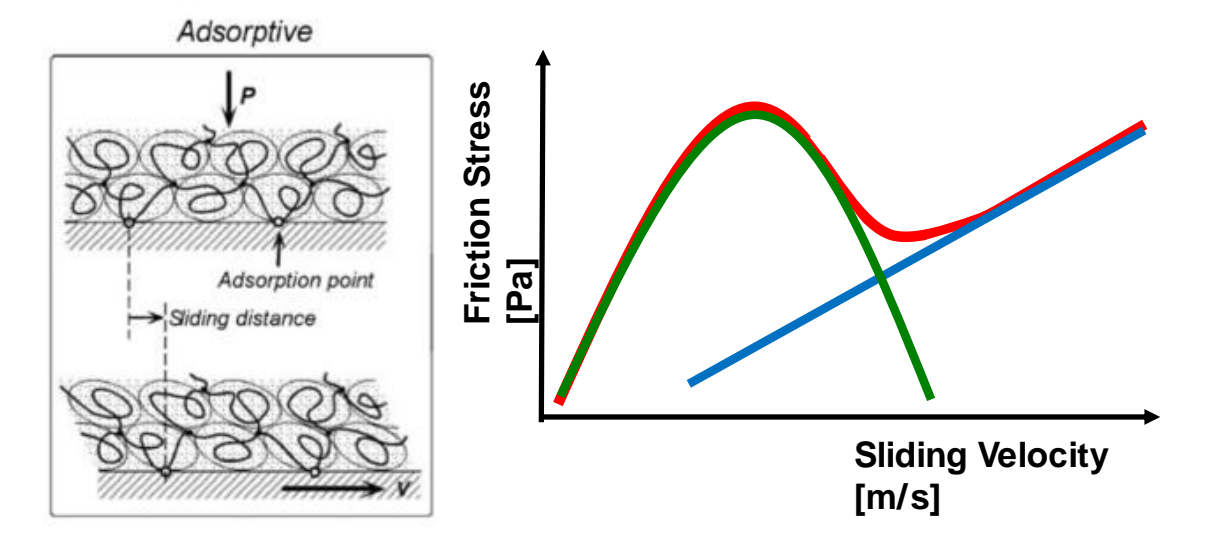


Fig. 2-1 Schematic explanation of adsorption model. The left image is quoted from the reference⁷.

Elastic resistance is induced when polymers adsorbed to the substrate are extended, and resistance has

a maximum at a certain velocity. Viscous resistance obeys Newton's law of viscosity and has a great contribution, particularly at a high-velocity region because it increases linearly with velocity.

The following four effects are expected by imparting hemispherical dimples on the hydrogel surface:

- (1) The contact area between the hydrogel and the substrate is reduced due to the dimples on the surface.
- (2) Water trapped in the dimples is supplied to the interface, which serves as a lubricant.
- (3) Since water in dimples behaves like a thick water layer, a uniformly thin lubricating layer cannot be formed at the interface. Water in dimples do not contribute significantly to friction as a viscous resistance, even at high-velocity, lubrication regions.
- (4) Water in dimples cannot sustain the normal load and the local contact pressure of the flat part of Dimpled surface is higher compared with that of Flat gel. This makes flat contact part of the gel surface firm contact.

Considering these effects in light of the adsorption model, the contribution of elastic resistance decreases from (1) and (2), and the contribution of viscous resistance decreases from (3). Also, from the effect (4), the elastic resistance gets larger and the interface is difficult to transfer to the lubrication state. However, it has been already reported that the normal pressure (σ) dependence of friction stress (τ) for PVA gel is small⁷, that is, $\tau \sim \sigma^{\alpha}$ for $0 < \alpha < 1$. This means that the reduction in contact area actually leads the increase in the contact pressure, but it is expected to decrease the friction stress by imparting the dimple structure on the hydrogel surface.

To investigate these effects, the dynamics of contact at the gel/glass interface was observed using an *in situ* observation system studied before^{31,33}. Especially a high-speed camera, not only a home digital video camera which used in the previous studies, would be helpful for us to confirm the lubrication in the high-velocity regions, the expected effect (2).

In this chapter, we prepared PVA gels with hemispherical dimples on the surface, aiming to reduce the sliding friction of PVA gels. The velocity dependence of friction was measured using a flat glass as a counter substrate. The effect of surface dimples on the friction of the hydrogel and its interface dynamics is presented. The friction behavior of hydrogel with surface dimples is discussed considering the contact state of the hydrogel/glass substrate during sliding friction.

2-2 Materials and Methods

2-2-1 Materials

All the chemicals for the hydrogel and the substrate preparation are the same with what we have already shown in Chapter 1, Section 1-2-1.

2-2-2 Hydrogel Preparation

Physically crosslinked PVA hydrogels with hemispherical surface dimples were prepared using the same method mentioned in Chapter 1, Section 1-2-3. PVA gel was prepared by the same conditions regarding concentration, temperature, reaction time and PDMS template for imparting the surface dimples on the gel surface, and the surface morphology of the gel was the same with that shown in Table 1-1 and Fig. 1-4. Also, the modulus of the gel was 94.0 ± 1.4 kPa, and the equilibrium water content was about 86 wt%.

2-2-3 Friction Measurement

Friction was measured using the rheometer operated in a constant compressive strain mode. Disc-shaped hydrogels, which were cut into 15.30 mm in diameter, were glued on the stage of the rheometer using a cyanoacrylate instant adhesive agent. The thickness of hydrogels was 2.70 mm. The any of three kinds of counter substrate, FDTS-coated cover glass, HMDS-coated cover glass, or the cover glass treated by HCl aqueous solution was glued onto the upper jig of the rheometer. Fig. 2-2 shows a schematic of the measurement system.

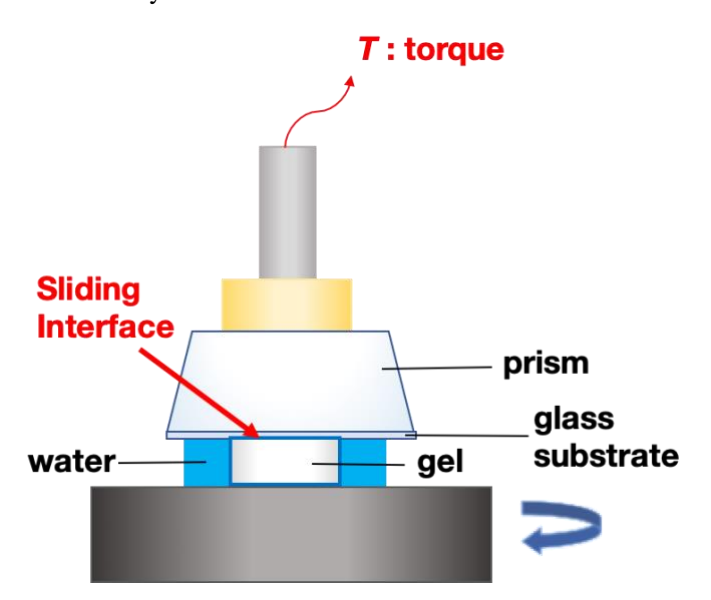


Fig. 2-2 The schematic illustration of the system for the friction measurement. The disc-shaped hydrogel was glued on the stage, and the counter glass substrate was attached to the upper jig with the prism for the *in situ* observation. This figure was drawn by modifying from Fig. 2 of Yamamoto et al., *Soft Matter*, 2014³¹.

The normal pressure σ was set as an experimental parameter. Before the friction measurement, the normal strain was applied until the normal stress reached a prescribed value ($\sigma = 11$ kPa) with a

constant normal strain rate (10 μ m/s). After 10 minutes of preloading, friction was measured in the steady rate sweep test (SRST) mode. During the 10 minutes of preloading, the normal strain hardly changed and was about 0.2% of the sample thickness. From the Persson's work⁴⁶, the relationship between the thickness of the water layer h between two parallel plates of radius R under the normal pressure σ and time t is expressed as $t = 3\eta R^2 / 4\sigma h^2$. According to this equation for a squeezing time, assuming that the contact is formed at the distance of 100 nm, it takes about 370 seconds, so the loading time was set to 600 seconds. An angular displacement was applied to the lower plate at a constant angular velocity ω . The angular velocity ω was increased stepwise from 1.3×10^{-2} to 1.3×10^{1} rad/s without separating the two rotating surfaces. For each ω , the measurement lasted for 40 seconds, and the average torque T in the last 20 seconds was adopted.

To calculate the friction force F, we denoted the friction force per unit area as τ . The total friction force F obtained from the whole surface area of the gel is expressed by Eq. 2-1,

$$F = \int_0^R \tau \cdot 2\pi r \, dr = \pi \tau R^2 \tag{Eq. 2-1}$$

where R (=7.65 mm) is the radius of the gel sample^{33,52}. Then, the total friction torque T is calculated in Eq. 2-2, similarly.

$$T = \int_0^R \tau \cdot r \cdot 2\pi r \, dr = \frac{2}{3}\pi \tau R^3$$
 (Eq. 2-2)

From Eq. 2-1 and Eq. 2-2, the friction force F can be calculated as Eq. 2-3.

$$F = \frac{3T}{2R} \tag{Eq. 2-3}$$

The average friction stress τ generated at the interface is defined as the friction force per nominal area of the gel sample, $\tau = F/\pi R^2$. The sliding velocity varies along the radial direction in parallel plate geometry, the velocity changes with the distance from the rotational center, r, following the formula $v = \omega r$, so the velocity range should be from 0 (at the rotational center) to ωR (at the perimeter). We hereafter adopted the sliding velocity v at the perimeter of disc-shaped samples, $v = \omega R$, when indicating the sliding velocity.

After the 1st run, the normal strain was released, and the gel sample was separated from the substrate. Thereafter, the normal strain was applied again for 10 minutes, and the 2nd run of measurement was performed. In a similar way, the 3rd to 5th runs were performed. Friction behavior for the 1st run tends to have poor reproducibility compared to the 2nd to 5th run. Therefore, friction stress for the 2nd to 5th run were averaged and the standard deviations were adopted as the error bars. The measurement of the rotational sliding friction has some advantages; (1) the lubrication is not easily affected by the

edge shape of the gel sample, and (2) the water present at the normal contact of gel/glass interface tends to determine the friction³¹, it is suitable for evaluating the influence of the surface dimples.

2-2-4 In situ observation

In situ observation of the gel/glass interface under sliding³¹ was also performed in the same way as mentioned in Chapter 1, section 1-2-5. The principle and the system were the same, but a high-speed camera (FASTCAM Mini AX100, Photron. Co. Ltd) was also used to capture the sliding interface where the gel slid at a high velocity. This camera was located about 0.3 m for the high-speed camera for capturing with higher magnification. When the camera is located at a short distance, the difference of the observable depth range in front and back side is larger due to the difference in observation angle. Therefore, high magnification observation with the high-speed camera cannot be used to estimate the contact area.

2-3 Results and Discussion

The results of the friction tests in which gels slid against the glass substrates with different wettability are presented in Fig. 2-3.

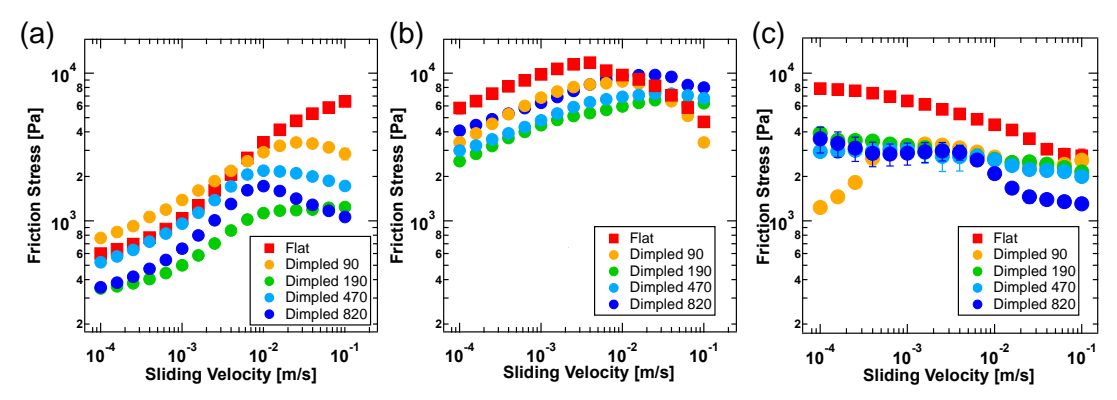


Fig. 2-3 Results of the friction test. The contact angles to water, θ of each glass substrate were (a) < 10° , (b) ~ 70° , and (c) ~ 110° .

Regardless of the surface dimple structure, friction behavior varied with the wettability of the substrates.

The fact that the friction behavior changes depending on the wettability of the substrate is consistent with the results of previous studies³². This is explained in connection with the adsorption model. The

adsorption model is expressed by the sum of the elastic resistance of the polymer adsorbed at the interface and the viscous resistance derived from the water layer existing between the gel and the substrate, and the magnitude of their contribution is expected to change depending on the wettability of the substrate. The friction behavior of Flat gel is explained in the previous study³² as below.

On the most hydrophilic substrate with a contact angle of $\theta < 10^{\circ}$, water has a higher affinity for the substrate than gel, so the contact between water and substrate is more stable than the contact between gel and substrate. Therefore, it is considered that the contribution of elastic resistance is small, and the contribution of viscous resistance is large. For this reason, it is considered that the friction is low in the low velocity range which tends to be affected by the elastic resistance, and the friction increases as the viscous resistance increase with the velocity.

As shown in the section of adhesion test, the substrate with a $\theta \sim 70^{\circ}$ is the substrate in which the gel and the substrate are in relatively stable contact. Therefore, it is expected that the contribution of elastic resistance will be large. Also, since it is predicted that the lubricating area is small, the contribution of viscous resistance by the water layer between the gel and the substrate is small. Elastic resistance increases with the velocity but changes to decrease at a certain velocity, and viscous resistance does not increase even if the velocity increases. Therefore, it is considered that the velocity dependence of friction drew an upwardly convex curve.

It has been pointed out in the previous study³², the friction behavior on the substrate of $\theta \sim 110^{\circ}$ cannot be explained by the adsorption model anymore. Since the substrate is the most hydrophobic among the substrates used in this study and the substrate contacts the gel more stable than water, it is stable even with ununiform contact, and the surrounding water is lodged between the gel and the substrate like a coin shape to make the wetting and dewetting domain. When shear was applied during the rotational friction test, the water lodged between the interfaces caused forced wetting, and the water spread on the interface to shift to lubrication, so it is conceived that the friction decreased as the sliding velocity increased.

In this study, the friction behavior of Dimpled gel was also changed depend on the wettability of the counter substrate and Dimpled series tended to show lower friction compared with Flat. Hereafter, we consider the effects of surface dimples for each substrate.

First, we consider the friction behavior of Dimpled gel against the substrate with the contact angle to water $\theta \sim 110^{\circ}$.

Fig. 2-4 shows the velocity dependence of the friction stress of the gel. The friction stress of Flat, a

flat-surface gel demolded from flat PDMS, decreased with increasing velocity, which is consistent with the tendency reported in previous studies³². Dimpled series showed lower friction stress over the entire velocity range than Flat. In the velocity region of 10^{-4} to 10^{-3} m/s, the friction stress was about half of that of Flat, independent of the surface dimple size. In the higher-velocity region, above 10^{-2} m/s, the friction stress reduced with an increase in the dimple size. Dimpled 90 demonstrated lower friction than the other Dimpled series in the low-velocity region ($< 10^{-3}$ m/s).

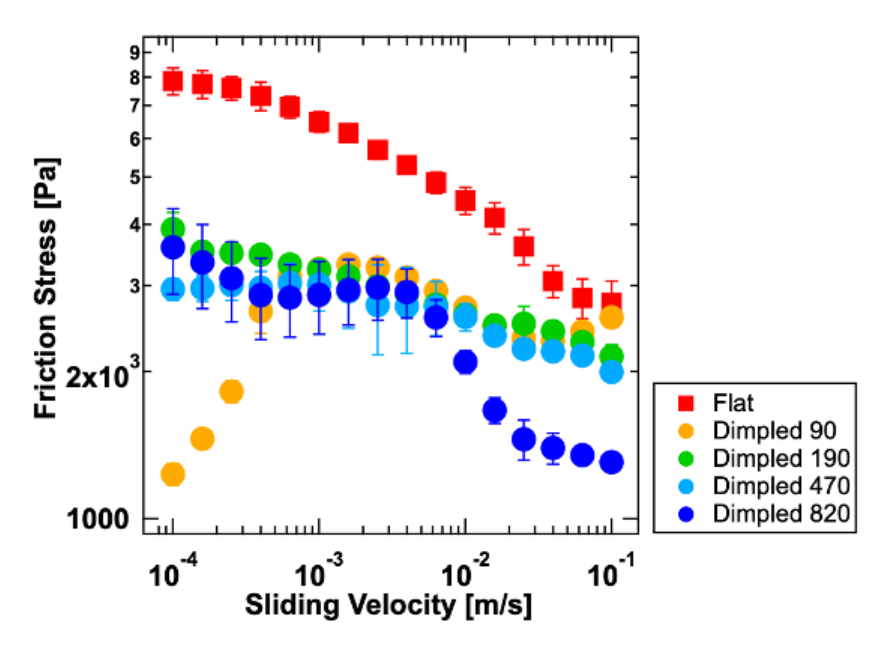


Fig. 2-4 Sliding velocity dependency of friction stress in gels with different surface geometries. The contact angle of the counter substrate was $\theta \sim 110^{\circ}$. Dimpled series showed lower friction than Flat over a wide range of sliding velocities.

The low friction for Dimpled series could be attributed to their reduced contact area to the counter substrate (effect (1)). The reduction in contact area could also lead to an increase in the contact pressure, but it was reported that the normal pressure dependence of friction stress for PVA gels was small⁷, and we have experimentally confirmed the dependence too, and the results are shown in Fig. 2-5 for Flat gel.

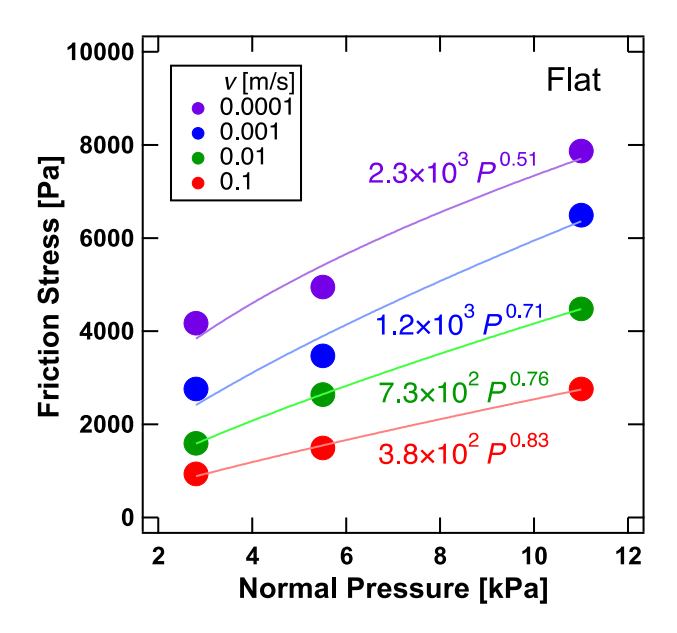


Fig. 2-5 Representative examples of normal pressure dependence of friction stress for Flat samples. The friction stress, τ , was expressed using the normal pressure, σ , in the formula $\tau = k\sigma^{\alpha}$. The constant k and exponent α were determined from the load dependence of friction stress at different sliding velocities.

As shown in Fig. 2-5, the exponent was less than 1 (0.5 < α < 0.8), so the friction reduction effect would be larger when the gel/glass contact area was decreased. Therefore, to confirm the effect (1), we normalized the friction stress by dividing it with the Ratio of flat region shown in Table 1-1 in Chapter 1, and the result is shown in Fig. 2-6. This normalization was simply calculated from the perspective of the surface design of hydrogels, and the normalized friction stress can be considered as the friction force per contact area, assuming that all dimples are not in contact, and all flat parts are in contact.

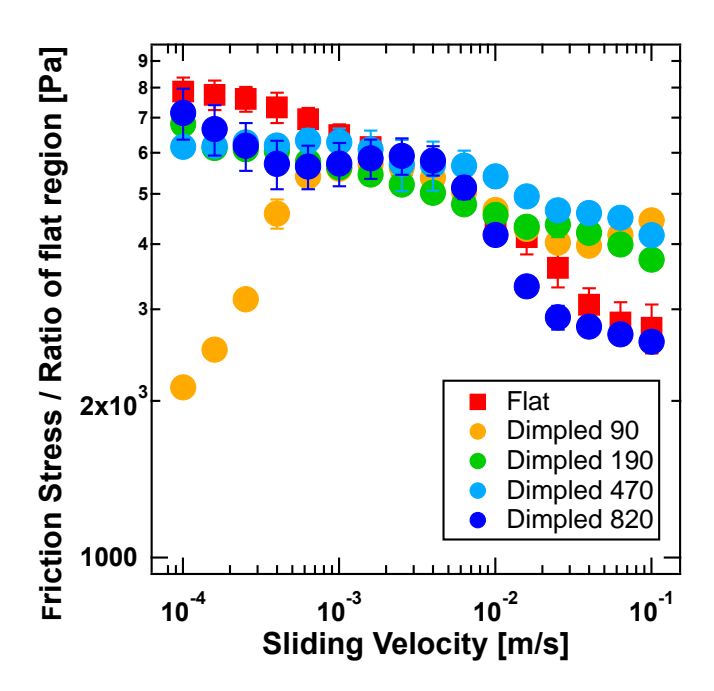


Fig. 2-6 Sliding velocity dependency of friction stress divided by the Ratio of flat region (shown in Table 1-1). The contact angle of the counter substrate was $\theta \sim 110^{\circ}$. In the region with 10^{-4} to 10^{-2} m/s, the normalized values of Dimpled series were almost the same as that of Flat.

Following the previous work⁷⁰, considering that the gel and substrate make partial macroscopic contact, the friction stress τ is expressed by the sum of the elastic resistance $\tau_{\rm ela}$ from the contact part and the viscous resistance $\tau_{\rm vis}$, from the non-contact, lubrication part,

$$\tau = \tau_{\text{ela}}\phi + \tau_{\text{vis}}(1 - \phi) \tag{Eq. 2-4}$$

where ϕ is the macroscopic contact area ratio. Here, we assume that ϕ corresponds to the Ratio of flat region.

Considering Newton's law of viscosity, the friction stress derived from the viscous resistance $\tau_{\rm vis}$ can be estimated. Regarding the minimum dimple on the Dimpled surface, we assumed that the dimple as the disc-like circular dimple with 10 μ m in depth for simplicity though the mean depth of the minimum dimple shown in Table 1-1 is about 20 μ m and the dimple is hemispherical shape. The viscous resistance is roughly $\tau_{\rm vis} = \eta \, v/h \sim 8.9 \, \text{Pa}$, where η is the viscosity of water (0.89 mPa s at 25°C), v is the sliding velocity at the perimeter (0.1 m/s) and h is the depth of the dimple (10 μ m). At the sliding velocity $v = 1 \times 10^{-1} \, \text{m/s}$, the friction stress τ was on the order of $10^3 \, \text{Pa}$, and the contribution of the viscous resistance $\tau_{\rm vis} \sim 8.9 \, \text{Pa}$ is quite small. In lower sliding velocity region, $\tau_{\rm vis}$ is even smaller. Therefore, the contribution of the viscous resistance is negligible, and the elastic resistance is dominant to determine the total friction stress τ . Also, the normalization of the friction

stress by the Ratio of flat region (Fig. 2-6) is appropriate in that the viscous resistance can be ignored.

In the region with velocities below 10^{-2} m/s, Flat and Dimpled series were almost identical, except for Dimpled 90. This would indicate that the friction reduction of Dimpled series at a low-velocity region is mainly due to reduced contact area.

Currently we do not have a clear explanation for the very low friction of Dimpled 90 at low velocity region. The sum of the perimeter lengths of surface dimples were 2.41, 1.17, 0.843, and 0.237 m for Dimpled 90, 190, 470, and 820, respectively. The perimeter, which is the origin of water invasion that serves as a lubricant, was the largest for Dimpled 90. Therefore, the low friction stress of Dimpled 90 at a low-velocity region (Fig. 2-4 and Fig. 2-6) can be attributed to the micro-lubrication. Another possible explanation is related to the initial contact process. When the gel is compressed during loading, its surface undergoes lateral expansion, causing it to slide slightly along the counter body. Since Dimpled 90 has the shortest pattern spacing, the relative displacement during this initial contact is the largest among the samples. This may lead to the flat regions being wetted by water from the dimples, which could contribute to the observed lower friction at low velocities.

The results of the friction reduction for all sizes of Dimpled in a wide range of sliding velocities including low velocity (10⁻⁴ m/s) indicate that even small dimples did not become completely flat under the normal pressure (11 kPa) and reduced the contact area. Therefore, the friction reduction effect due to the reduction of contact area (effect (1)) is considered to have occurred for all the Dimpled series.

In the high-velocity region, above 10^{-2} m/s, the normalized friction stress of the Dimpled series was larger than that of Flat, except for Dimpled 820. This result suggests that the friction force of Flat is reduced by lubrication, and if macroscopic lubrication is taken into consideration to determine the friction force per contact area, the Ratio of flat region of Flat should not be calculated as unity. That is, friction stress normalized by the Ratio of flat region for Flat is underestimated.

Therefore, we observed the sliding friction interface and calculated the Torque fraction φ , which is reduced by detaching from the glass substrate, as shown in Eq. 2-5. A part of the observation images is shown in Fig. 2-7. It was observed that the perimeter of the Flat partially separated from the substrate and was lubricated. In addition, water lubrication from dimples by effect (2) was expected to be observed in Dimpled 470 and Dimpled 820, but all the flat region was in contact, indicating that no observable thick lubrication layer was formed.

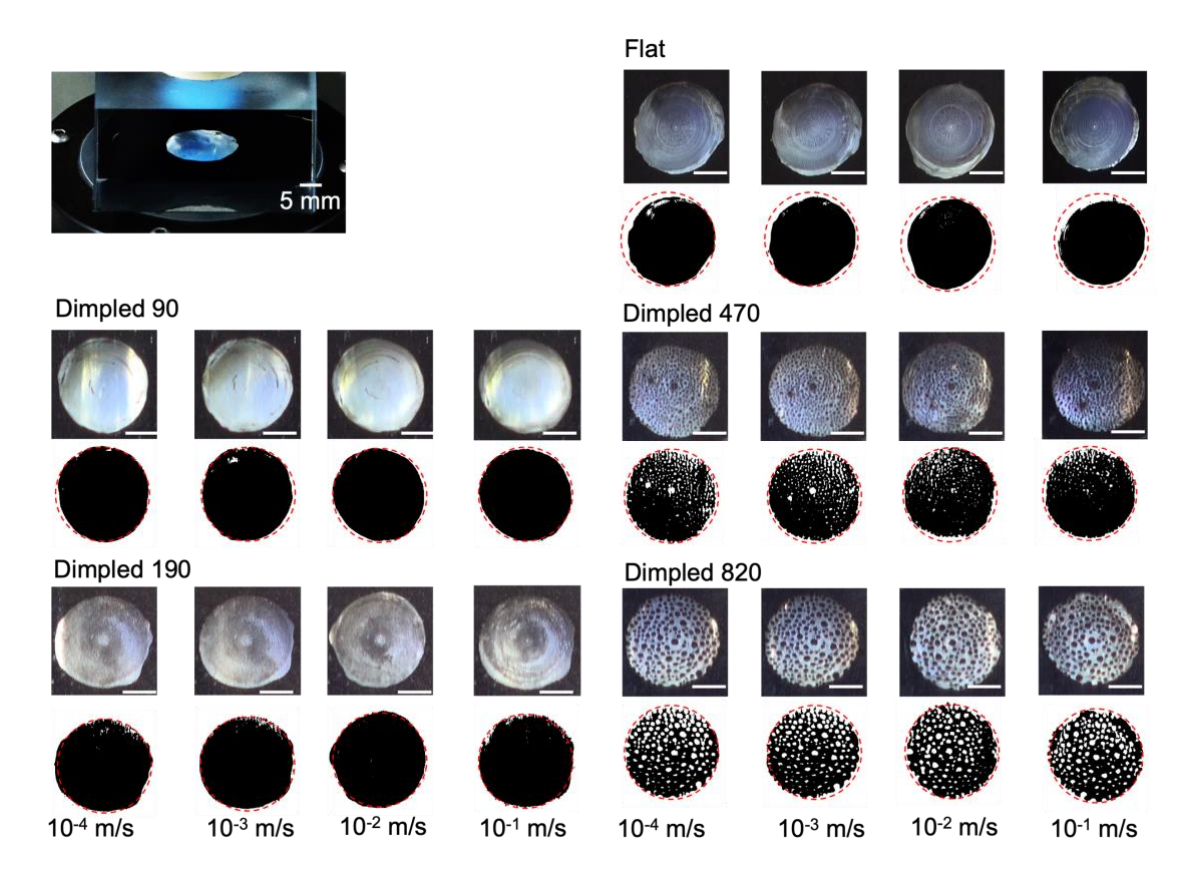


Fig. 2-7 Contact images of the hydrogel with various surface concavities. The contact angle of the counter substrate was $\theta \sim 110^{\circ}$. The surface pattern could be recognized for hydrogels only Dimpled 470 and Dimpled 820 due to the limitations of the resolution. The colored images in the upper row were converted to the binary images in the lower row. Scale bar: 5 mm. The dashed line represents the perimeter of the gel.

The density of the dimples in each image shown in Fig. 2-7 was almost the same in the upper and the lower half, but the binary images in the lower row showed a lower density than the colored images in the upper row. This might be because applying the same threshold to a single image in the image binarization process, some dimples could not be recognized well as dimple due to the in-plane brightness non-uniformity of the gel. Therefore, it is probable that the dimple density at the bottom of the gel was reduced in the binary image.

The Torque fraction φ was calculated as follows, considering the contact position because the value of the torque originating from near the rotating centre of the hydrogel is smaller than that from near the perimeter.

$$\varphi = \frac{T_{\text{contact}}}{T_{\text{theory}}}$$
 (Eq. 2-5)

$$T_{\text{contact}} = \int_{0}^{2\pi} \int_{0}^{R} \tau \cdot r \cdot \delta_{r\alpha} \cdot r \, dr d\theta$$

$$\begin{cases} \delta_{r\alpha} = 1 & \text{(in contact)} \\ \delta_{r\alpha} = 0 & \text{(not in contact)} \end{cases}$$
(Eq. 2-6)

In Eq. 2-5, $T_{\rm theory}$ is the theoretical value of torque in the case where the hydrogel completely contacts with the glass substrate, and $T_{\rm contact}$ is the value calculated from Eq. 2-6, where τ is the friction force per unit area, shown in Eq. 2-1 and Eq. 2-2, using the picture under sliding. In Eq. 2-6, (r,α) is the spherical coordinate in the picture, and the rotational center is the origin of the spherical coordinate. Furthermore, $\delta_{r\alpha}$ is 1 when the hydrogel is in contact with the substrate at the coordinate (r,α) , and $\delta_{r\alpha}$ is 0 when it is not in contact. Due to the resolution limitations of the optical system used herein, the surface geometry could only be observed for Dimpled 470 and 820.

As shown in Fig. 2-8, the Ratio of flat region of Flat was set to unity in Fig. 2-6, but the φ of Flat measured from images of the contact at the friction interface was less than unity. Moreover, the φ of Flat was almost constant with velocity and slightly decreased at 10^{-1} m/s. On the other hand, for the Dimpled series, φ was approximately 0.6, almost the same value as the Ratio of flat region, and was nearly constant with sliding velocity.

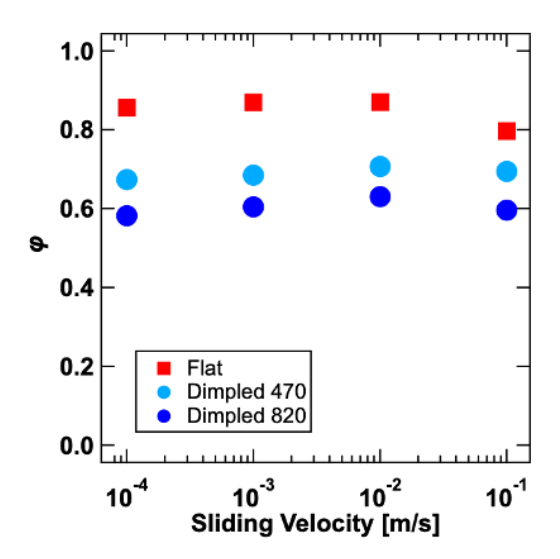


Fig. 2-8 Sliding velocity dependency of Torque fraction, φ , taking in account to considering the distance between the contact position and the rotation center. The contact angle of the counter substrate was $\theta \sim 110^{\circ}$. For hydrogels, Dimpled 90 and Dimpled 190, the surface patterns could not be observed because of the resolution limitations of the optical system.

Here, we consider the friction stress of gels by two factors; the elastic resistance at the contact part and the viscous resistance of the lubricants as shown in Eq. 2-4. Fig. 2-9 shows the result that Dimpled 820 and Dimpled 470 have smaller τ/φ compared with Flat, using the Torque fraction φ considering the observable lubricating region and dimples.

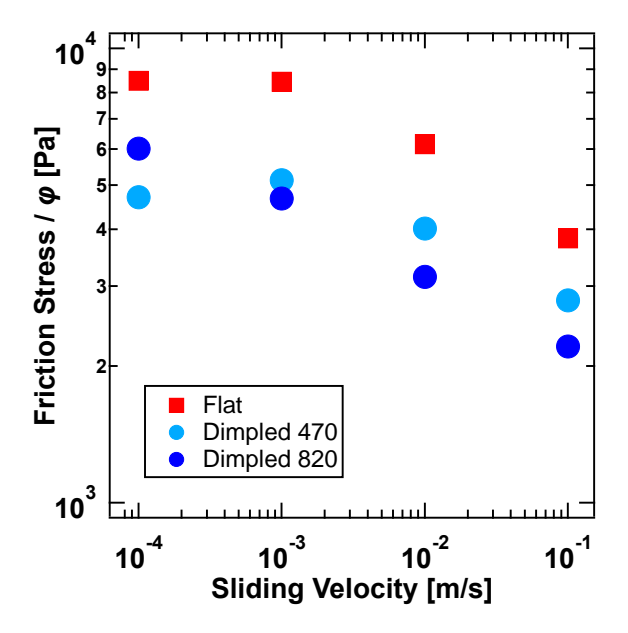


Fig. 2-9 Sliding velocity dependency of friction stress divided by the Torque fraction φ . The contact angle of the counter substrate was $\theta \sim 110^{\circ}$. The normalized value for Dimpled series was lower than that of Flat, indicating micro-lubrication by the water trapped in dimples on the surface of Dimpled series.

Since the viscous resistance $\tau_{\rm vis}$ has small contribution to sliding friction in particularly lower velocity region, the difference of τ/ϕ between Flat and Dimpled mainly depends on the difference of the true contact area where generate the elastic resistance.

In this study, we tried the normalization by two means; one was the Ratio of flat region obtained from the surface observation by an optical microscope (Fig. 2-6), and the other was Torque fraction, which took into consideration the distance between the contact position and the rotational center obtained from *in situ* interface observation under sliding motion (Fig. 2-9). There was a conflict between the two normalizations; the former could normalize the friction stress of Dimpled gel in the low to medium velocity regions, on the other hand, the latter could not normalize it even in the low to medium velocity regions, and the value for Dimpled gel was lower than that of Flat gel in all the velocity.

Although both normalizations took into account the factor of "decreased friction due to reduced gel/glass contact area", they cannot take into account the factor of "increase in friction due to higher

in local contact pressure due to decrease in contact area". Neither can be normalized accurately, as there was no second factor. The effect of reducing the friction was considered to be large when the contact area was reduced since the pressure dependence of friction $(\tau \sim \sigma^{\alpha})$ was small $(\alpha < 1)$, as shown in Fig. 2-5. The first normalization, by "Ratio of flat region," is determined by the surface design as stated earlier and is useful for verifying the effect of simple friction reduction from the surface design. However, it is assumed that the gel surface was in full contact with the substrate, and in particular, the value for Flat gel was assumed to be 1, without taking into account the true contact state at all. Therefore, the normalized values for Dimpled were almost the same with that for Flat in Fig. 2-6, but the result would have been a coincidence and the friction reduction was caused not only by the contact area reduction. In contrast, the second normalization using "Torque fraction" reflects the actual contact state during friction unless there is a thin water layer that cannot be captured by the camera. It does not require the assumption of full contact and is a normalization that can be used regardless of the presence or absence of dimples on the surface. Because it reflects the actual contact state and measures friction in a rotating system, it is thought to allow for more accurate verification in that it takes into account the distance from the center of the contact position. We therefore tried to see if we could actually capture the frictional behavior using in situ observation images, but it did not work very well at now.

To consider the effect of the increase in the contact pressure on the friction of Dimpled gel, we developed a model incorporating the pressure dependence of friction based on the friction of Flat gel. As shown in Fig. 2-5, the friction stress, τ , follows a power-law relationship with contact pressure, σ , which can be expressed as $\tau = k\sigma^{\alpha}$, so we experimentally obtained the coefficient k and the exponent α at each sliding velocity. The inclusion of this pressure dependence allows us to account for the altered load distribution caused by surface structure.

By incorporating the effects, the friction stress for dimpled hydrogels is formulated as Eq. 2-7.

$$\tau_{\text{Dimple}} = k \left(\frac{\sigma_{\text{Flat}}}{\phi} \right)^{\alpha} \phi$$
(Eq. 2-7)

where ϕ represents the Ratio of flat region, and σ_{Flat} denote the normal pressure for Flat sample, respectively. The predictions of the model are shown in Fig. 2-10, where the experimental friction data for Dimpled and Flat are compared with the calculated values in Eq. 2-7.

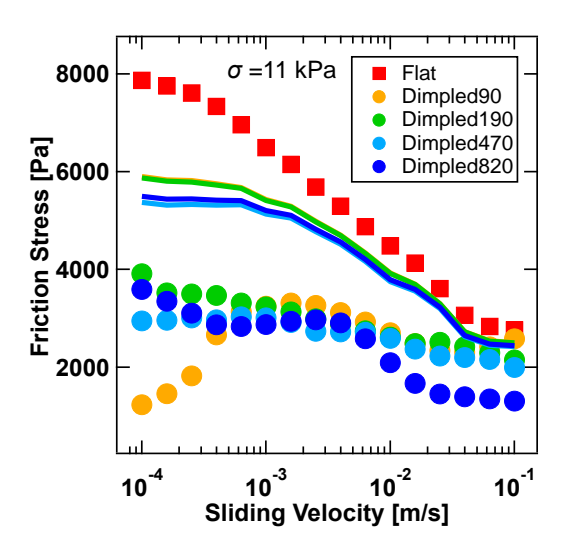


Fig. 2-10 Sliding velocity dependence of friction stress; a comparison of the experimental data (round marker) and the model (line), which considers the reduction in contact area and the increase in contact pressure.

Although the model in Fig. 2-10 successfully captures key trends in the friction behavior of Dimpled hydrogels, there remain discrepancies between the predicted and experimental values. One possible explanation for the lower experimental values than the predicted values may be the presence of unobservable water layer supplied from the surface dimples. The elastic resistance per true contact area $\tau_{\rm ela}$ should be equal for Flat and Dimpled, therefore, the thin lubricating layer that exceeds the observation limit that might occur in Dimpled 820 and Dimpled 470 has a wider in lubrication area than that for Flat in Fig. 2-7. The wider the lubricating layer, the smaller the true contact area, so the elastic resistance is smaller. Flat should also have an unobservable thin lubrication layer partially, but it should be smaller and/or thinner than that of Dimpled. If we could capture this unobservable lubrication layer by camera with higher magnification or shallower depth of field, the normalization and the modeling by Eq. 2-7 would go well.

In the higher velocity region, it gets more complicated because the viscous resistance of the lubricant $\tau_{\rm vis}$ increases in proportion to the velocity, however, since Dimpled is considered to have a wider lubrication layer in the low-velocity region and τ/φ of Dimpled is still lower than that of Flat in higher velocity region in Fig. 2-9, it is reasonable to assume that Dimpled has a wider and/or thicker unobservable lubricating layer even at higher velocity. These results are not direct evidence but suggest the lubrication by the water supplied from the dimples (effect (2)).

To confirm the lubrication due to water in surface dimples (effect (2)) supported by the above results, we observed the interface dynamics of Dimpled series using a high-speed camera in 1000 frames per second and a higher magnification lens with a shallow depth of field. A part of the obtained images is

shown in Fig. 2-11, and the movies are available in the Supporting Information (Videos S1 and S2). The observation system was the same, except for the camera and lens, and the dark part is the area where the gel and glass were not in contact, and a water film existed.

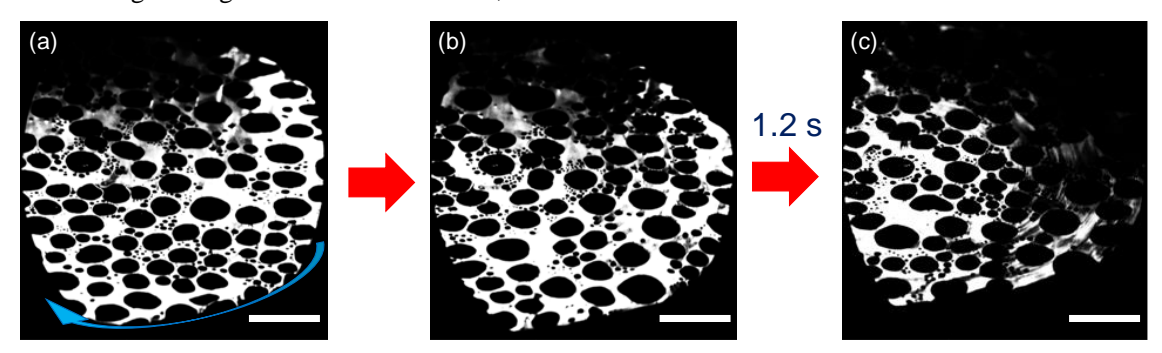


Fig. 2-11 Image of the interface between Dimpled 820 and the glass substrate at sliding velocity (a) $v = 1 \times 10^{-2}$ m/s, and (b) (c) $v = 1 \times 10^{-1}$ m/s. The image, (c) was taken 1.2 seconds later of (b). The contact angle of the counter substrate was $\theta \sim 110^{\circ}$. The white area is where the gel and the glass substrate are in contact and the black area is where the gel and the glass substrate are not in contact and water exists. In (a), the blue arrow indicates the sliding direction, and water was trapped in the dimples at the surface. When sliding velocity was changed from $v = 1 \times 10^{-2}$ m/s, (a), to $v = 1 \times 10^{-1}$ m/s, (b), trapped water started to be provided to the interface, leaving a trajectory of rotational motion, and in (c), more water existed and covered the interface. Scale bar: 2 mm.

At 10^{-2} m/s, no water invasion from the dimples to the flat area could be observed, the dark area showed round shape, which means that water was completely trapped in the dimples. Whereas at 10^{-1} m/s, water invaded the interface of the flat area, leaving a trajectory of rotational motion. Water filled the contact regions between dimples within a few seconds, forming a thin lubricating layer, except for the area near the center of the gel where the rotating velocity was low (Video S2). Therefore, we confirmed that the water in the dimples was supplied to the contact interface, and the lubrication of the flat part was promoted, confirming the effect (2) in high-velocity region. At present, it is not clear that the effect (2) works for the Dimpled series which have smaller dimples on their surface because the observation could not be performed for them due to the low magnification. Besides, to reiterate, it might be possible to observe the micro-lubrication behavior in the low-velocity region if we could use an optical system with higher magnification and shallower depth of field and explain the exact reason why the values of τ/φ for Dimpled were lower than that for Flat, but this is future topics of discussion. However, it can be easily predicted that an unobservable lubrication layer is formed by water invasion from the dimples even under more harsh conditions, such as a lower velocity and a higher load than those of this study. Therefore, a very thin lubrication layer, which could not be observed in this system, is produced, which may contribute to the fact that the τ/φ of Dimpled is lower than that of Flat in a low-velocity region ($<10^{-2}$ m/s).

Though we developed a model incorporating the pressure dependence of friction in Eq. 2-7, the friction stress could not be explained by two factors: the reduction in gel/glass contact area and the increase in the contact pressure. To further analyze the friction behavior of Dimpled hydrogels, we modified a model adding the effect, the reduction in contact area due to water release from dimples, as confirmed by *in situ* observation by high-speed camera in Fig. **2-11**.

The first effect, pressure dependence, is the same with the model in Eq. 2-7. The second effect considers the influence of water released from dimples, as observed in Fig. 2-11, which contributes to a further reduction in the contact area, $\Delta A_{\text{dynamic}}$. This effect is modeled as

$$\Delta A_{\text{dynamic}} = k' V_{\text{dimple}}$$
 (Eq. 2-8)

By incorporating these two effects, the friction stress for dimpled hydrogels is formulated as

$$\tau_{\text{Dimple}} = k \left(\frac{\sigma_{\text{Flat}}}{\phi} \right)^{\alpha} \cdot \left(\phi - \frac{k' V_{\text{dimple}}}{\pi R^2} \right)$$
(Eq. 2-9)

where V_{dimple} means the total volume of all dimples on the hydrogel surface, which was calculated from the relation of diameter and depth obtained from the surface observation by optical and laser microscopes, and the values were 5.3×10^6 , 3.0×10^9 , 3.5×10^{10} , 4.7×10^{10} µm³ for Dimpled 90, 190, 470 and 820, respectively.

We estimated k' based on the high-speed camera observations in Fig. **2-11**, where water release from dimples was analyzed. Based on these observations, we determined that setting k' = 10^3 results in a 10 μ m-thick lubricating layer for Dimpled 820, covering approximately 75% of the interface. This estimation corresponds to approximately 10% of the dimple volume of Dimpled 820 being supplied to the contact interface, which appears to be a reasonable assumption.

The predictions of the model are shown in Fig. 2-12, where the experimental friction data for Dimpled and Flat are compared with the calculated values.

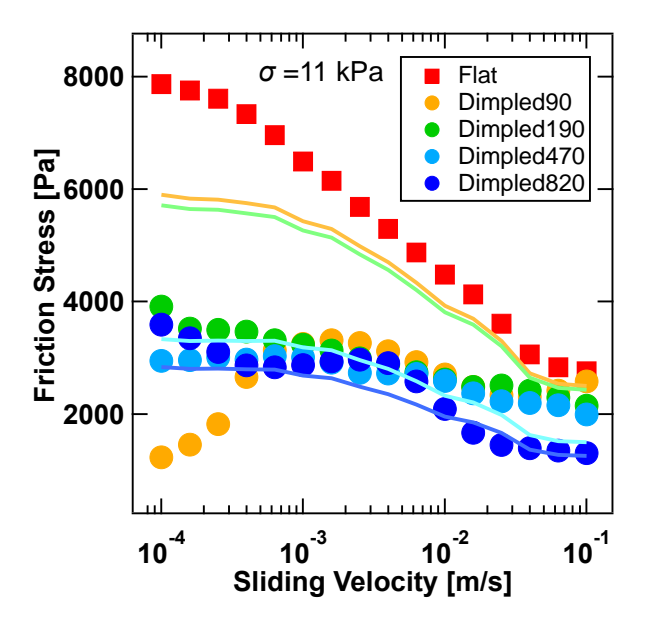


Fig. 2-12 Sliding velocity dependence of friction stress; a comparison of the experimental data (round marker) and the model (line), which takes into account the increase in contact pressure due to the reduction in contact area, and the water supply from dimples.

Although the model in Eq. 2-7 successfully has been captured key trends in the friction behavior of Dimpled hydrogels, the modified model in Eq. 2-9 has better captured, in particular, the friction for Dimpled gel with larger dimples, Dimpled 470 and 820.

There remain discrepancies between the predicted and experimental values. The overestimation of friction for Dimpled gel with smaller dimples suggests that additional effects, which are not explicitly included in the model, play a role in determining the frictional response. One possible explanation is geometric parameters such as dimple perimeter and pattern spacing. Future refinements should consider these effects to improve the accuracy of the model.

The relationship between the average volume of dimples per unit area of Dimpled series and the friction stress is shown in Fig. 2-13. V/A on the horizontal axis was calculated from the optical microscope observation. The total volume of dimples in the entire observed area V was divided by the entire observed area V/A was calculated as the average V/A for each of the four Dimpled series.

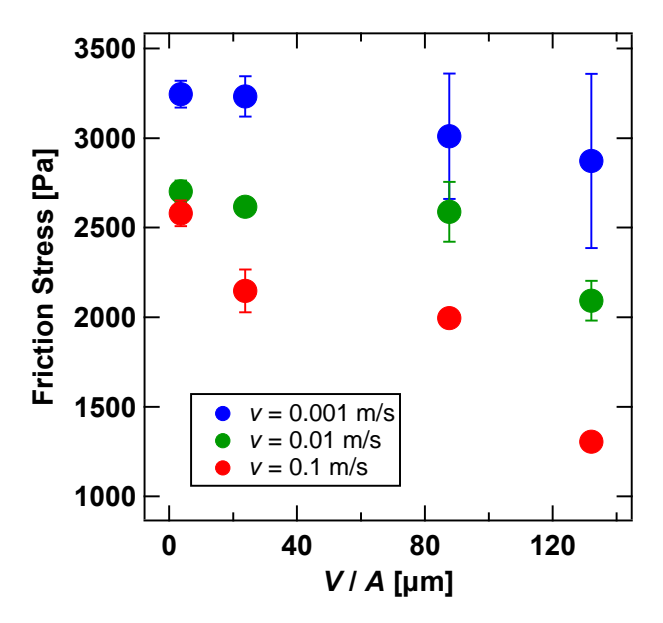


Fig. 2-13 Relationship between friction stress and the mean volume of dimple per unit area on the surface of Dimpled series. The contact angle of the counter substrate was $\theta \sim 110^{\circ}$. The friction stress decreases as the sliding velocity and mean volume of dimple increase.

The friction stress decreased with an increase in the volume of the dimples at higher velocities. Since the dimple volume could be treated as the water volume retained in dimples, lubrication by water invasion from the dimples is more likely to occur at higher velocities with larger dimples. The larger the volume of the dimple per unit area, the less friction, but it is unclear what kind of function can be fitted for their relations. Dimpled 820 with the largest dimple volume showed the lowest friction, but we could not investigate whether gels with even larger dimples would have lower friction. Though we cannot evaluate the contact state at the gel/glass interface with the present system, there are possibilities that the effects of the reduction in the contact area (effect (1)) and microscopic lubrication (effect (2)) have occurred. This is an issue that we should verify in the future.

The effect (3), which shows that water in dimples behaves like a thick lubricating layer and prevents an increase in viscous resistance, is considered to occur reliably because the dimple's shape does not become flat even when a load is applied. However, since a hydrophobic glass substrate was used as the counter substrate, the gel and glass easily formed a contact, and lubrication was relatively difficult³². PVA has relatively strong adhesion to the hydrophobic substrate, and the elastic resistance is so high that the viscous resistance by the water in the dimples is negligible. Therefore, even if the effect (3) occurs, it is not reflected in the friction force.

Next, we discuss the results of friction on the substrate with the contact angle of $\theta \sim 70^{\circ}$ shown in Fig. 2-3 (b). As mentioned in the section of the adhesion test in Chapter 1, this substrate shows a

medium degree of easiness of contact or drainage of water but strongly adsorb with the gel because the surface energy of the substrate is relatively similar to that of the gel. The work of adhesion, $W_{\rm adh}$ was the highest on this substrate compared with the other substrates (Fig. 1-16). Therefore, it is considered that the elastic resistance dominates the friction on this substrate. As shown in adsorption model, the elastic resistance increases with the sliding velocity and shows the maximum value at a certain velocity, then decreases with the velocity.

Dimpled series tended to show lower friction stress compared with Flat within the sliding velocity range of low to medium ($\sim 10^{-2}\,$ m/s), however, their friction stress did not largely decrease and were comparable with Flat at high-velocity region, though this velocity region was considered to the lubrication regime.

For this substrate, the characteristic velocity at which the friction stress reaches its maximum peak appears to be different between flat and dimpled. In Chapter 1, we have already shown that the work of adhesion of the Dimpled gel is smaller than that of the Flat gel. In a previous paper 1,7 describing this characteristic velocity $v_{\rm f}$, it was shown that this velocity varies depending on the lifetime of adsorption $\tau_{\rm b}$, time for a desurbed porymer to be re-adsorbed on the surface $\tau_{\rm f}$, adsorption energy per polymer chain $F_{\rm ads}$, elastic energy due to stretching of the adsorbing chain $F_{\rm el}$, absolute temperature in energy unit T, and radius of the polymer blob of the gel surface $R_{\rm f}$, and is expressed by the following equations.

$$\tau_{\rm b}^{-1} = \tau_{\rm f}^{-1} \exp\left[-\frac{F_{\rm ads} - F_{\rm el}}{T}\right]$$
 (Eq. 2-10)

$$v_{\rm f} \approx R_{\rm f}/\tau_{\rm f}$$
 (Eq. 2-11)

Regardless of the surface geometry, all the gels used here are made of PVA, so if we assume that τ_b , F_{el} , and R_f are the same and that the F_{ads} varies depending on W_{adh} , we can estimate the characteristic velocity v_f , which is lower for smaller W_{adh} . In the case of the Dimpled gel, the local contact pressure increases, which may result in more water being drained from the interface and stronger gel/glass contact, and also in an apparent increase in τ_b . However, even if τ_b increases, v_f still decreases. Therefore, it is considered that the friction behavior of the Dimpled gel cannot be discussed based on the change in the peak position within the framework of the adsorption model which describes the friction of hydrogels from a perspective considering the thermal agitation of molecule. Actually, it was stated that the adsorption model might not be valid for the substrate which shows strong adhesion with gels³². Considering the classical Stribeck curve^{18,71,72}, identifying boundary, mixed, elastohydrodynamic, and hydrodynamic lubrication regimes, which was experimentally derived from

the friction characteristics of plain bearings, the higher contact pressure means the friction property is explained by the boundary lubrication. Therefore, on this adgesive substrate, the friction of PVA gel was high and the macroscopic contact state should affect the friction.

As shown in Fig. 2-14, the friction stress normalized by Ratio of flat region that is the ratio of the flat area except for the dimple area to the whole upper surface of Dimpled series was almost identical in low to medium velocity region ($\sim 4 \times 10^{-3}$ m/s), but could not be normalized, and particularly the values of Dimpled series were higher than that of Flat gel in high-velocity region. Since the contact pressure between the flat part of Dimpled surface and the substrate is higher than that of Flat gel and Dimpled contacts with the substrate strongly, it is considered that Dimpled surface is difficult to make a transition to the lubrication state even in the high-velocity region. Therefore, among the four effects shown in introduction section, the effect of friction reduction due to the reduction in contact area is considered to be cancelled out and the friction stress of Dimpled series was almost the same with that of Flat.

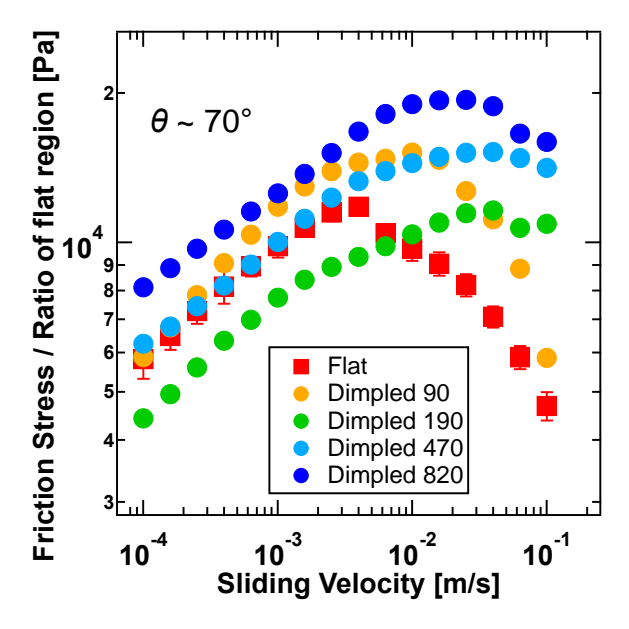


Fig. 2-14 Sliding velocity dependence of friction stress normalized by Ratio of flat region. The contact angle of the substrate is $\theta \sim 70^{\circ}$.

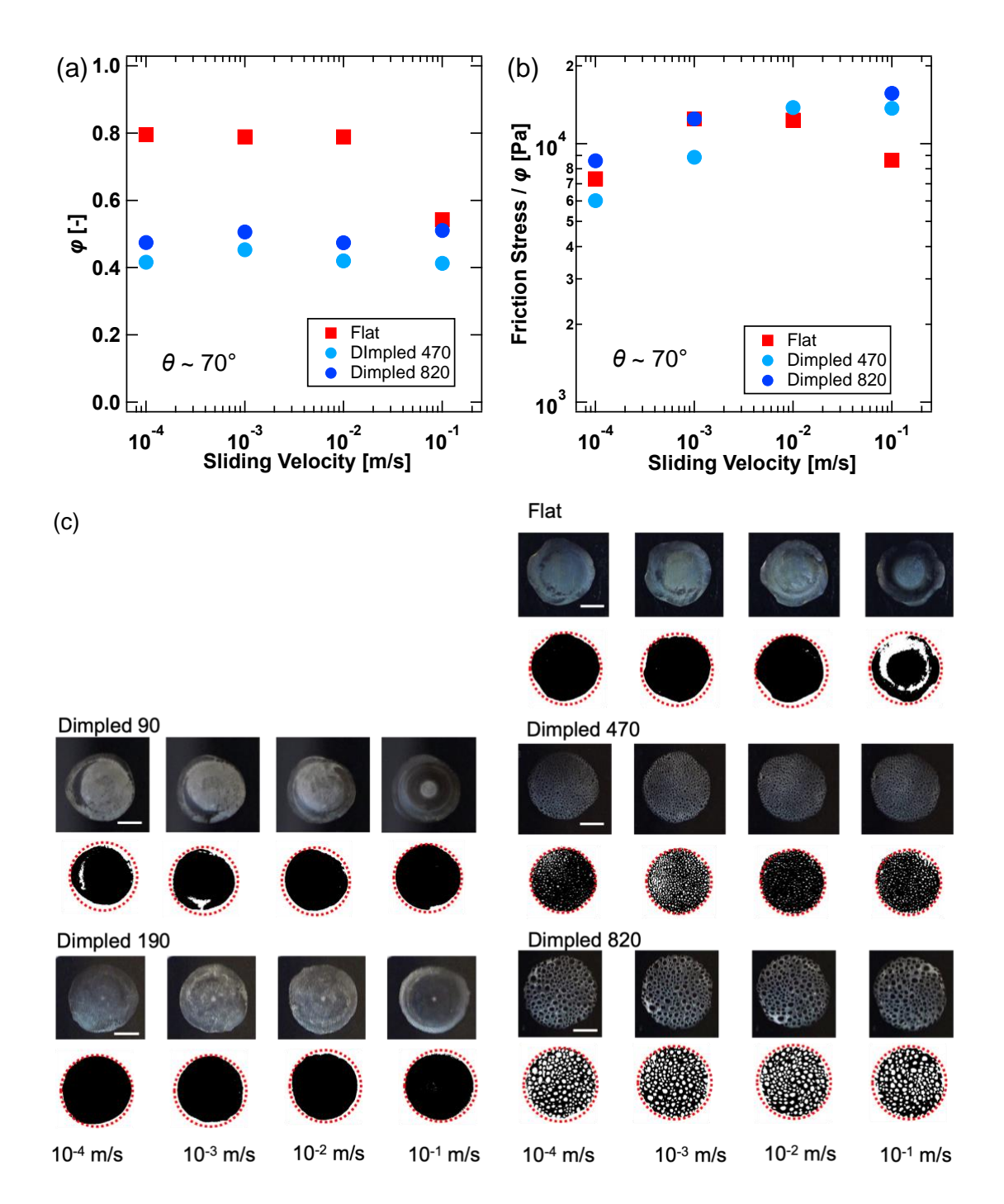


Fig. 2-15 Sliding velocity dependence of (a) Torque fraction φ and (b) friction stress divided by Torque fraction φ . (c) The *in situ* observation images of each gel and their binarized images at certain sliding velocity. The red dashed line means the perimeter of the gel. Scale bar: 5 mm. The contact angle of the counter substrate was ~70°.

As with the case of the substrate with the contact angle of $\theta \sim 110^{\circ}$, Torque fraction φ was analyzed but the small size surface dimples on Dimpled 90 and Dimpled 190 could not be recognized after all,

so the results for Flat gel, Dimpled 470 and Dimpled 820 are displayed in Fig. 2-15. From Fig. 2-15 (a), Torque fraction φ of Flat gel was less than 1 under the sliding condition, therefore it is clear that the whole surface did not contact the substrate and the value massively decreased in the high-velocity region. While on the contrary, Torque fraction of Dimpled series was almost constant even when the velocity changed, and this indicated the stable contact with the substrate. From this result, it can be said that Flat reached the lubrication state at the high-velocity region, but Dimpled was difficult to form a water layer at the gel/glass interface and reach the lubrication state due to high local contact pressure. In Fig. 2-15(b), the friction stress was normalized by the Torque fraction in low to medium velocity region, but the values for Dimpled were higher than those for Flat in high-velocity region. As shown in Chapter 1, this substrate strongly adheres to the gel, so it is considered that the elastic resistance dominates the friction, and the friction stress was apparently normalized by the dynamic contact area in the sliding test for low to medium velocity region, though the effect of the increase in the contact pressure was not considered. Compared with Fig. 2-9, the difference in the values of τ/ϕ between Flat and Dimpled was small in Fig. 2-15(b). This might be because PVA gel contacts this substrate most strongly and stably, so an unobservable water layer was difficult to form, unlike the substrate with the contact angle $\theta \sim 110^{\circ}$, and the real contact state was reflected to the Torque fraction φ . Then, in the high-velocity region where the contribution of the viscous resistance increase, the friction stress for Dimpled was not normalized by Torque fraction because Flat gel reached the lubrication state. The decrease in friction stress of Flat gel was larger than Dimpled gel, and this behavior might correspond to the mixed lubrication regime in Stribeck curve. Because of the higher contact pressure for Dimpled gel than Flat gel, Dimpled gel was difficult to reach the same lubrication state as Flat and still in the boundary lubrication regime. Therefore, the friction stress for Dimpled gel was higher than Flat gel in the high-velocity region.

Finally, we discuss the results on the substrate with the contact angle of $\theta < 10^{\circ}$ shown in Fig. 2-3(a). This substrate is the most hydrophilic among the substrates used in this study, so the contact of the substrate and the gel tends to be hindered by water. Also, as shown in the section of adhesion test, the work of adhesion, W_{adh} , between the substrate and the gel was the smallest among the substrates used in this study, this can make the contribution of the elastic resistance to the friction small and the friction stress low within the sliding velocity region of low to medium, for both Flat and Dimpled gels.

It is expected that the friction stress proportionally increases with the sliding velocity because lubrication is likely to occur on this substrate and the contribution of the elastic resistance is difficult to obtain, also the viscous resistance dominates the friction. Actually, it is confirmed that the friction stress of Flat gel increased with the velocity but that of Dimpled series did not increase in high velocity region that is considered to correspond to the lubrication regime. The velocity dependence of the

friction stress for Flat gel was smaller than that predicted by Newton's law of viscosity, even in the high-velocity region where viscous resistance was considered to be dominant. This might be because the friction measurement was performed in a rotating system, so there was a velocity gradient from the rotational center of the gel to the outer periphery, and the lubricating layer at the interface had an uneven thickness. For Dimpled gel, since water in the dimples was predicted to behave as a thick water layer (effect (3)), the formation of the uniformly thin and wide lubrication layer was hindered and the contribution of the viscous resistance, $\tau_{\rm vis}$, to the friction hardly arose. In addition, the contribution of the elastic resistance, $\tau_{\rm ela}$, though the contribution would be small, to the friction decreases with the sliding velocity in the high-velocity region, so the total friction was considered to decrease.

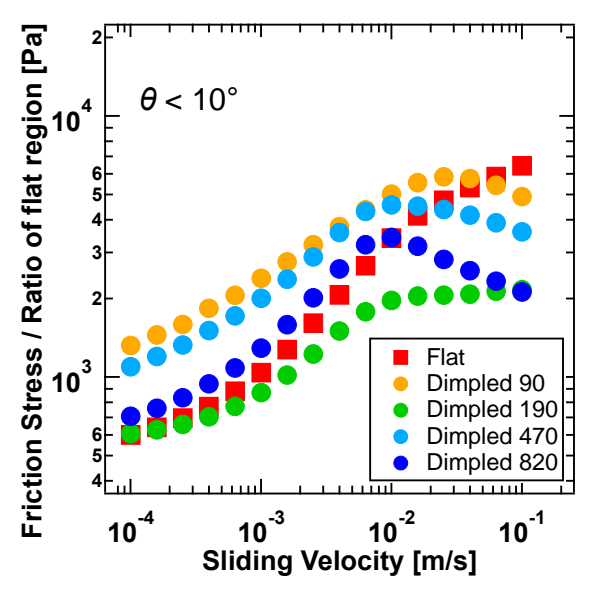


Fig. 2-16 Sliding velocity dependence of friction stress divided by Ratio of flat region. The contact angle of the counter substrate was $<10^{\circ}$.

As presented in Fig. 2-16, although the effect of the reduction in contact area was considered in high-velocity region, the friction for Dimpled series was lower than that of Flat. Therefore, it is clear that the decrease of the friction of Dimpled gels is attributed to the effect except for the contact area and it is expected that there is the lubricating effect by water trapped in dimples. As seen in chapter 1, the work of adhesion for this substrate was lower than other substrates, so it was considered that the interface was easily transferred to the lubricating state. In particular, Dimpled gels, which can retain water on their surface are considered to provide water as a lubricant into the interface in high-velocity region and a thicker lubricating water layer was formed compared with Flat gel, so the friction of Dimpled gels drastically decreased.

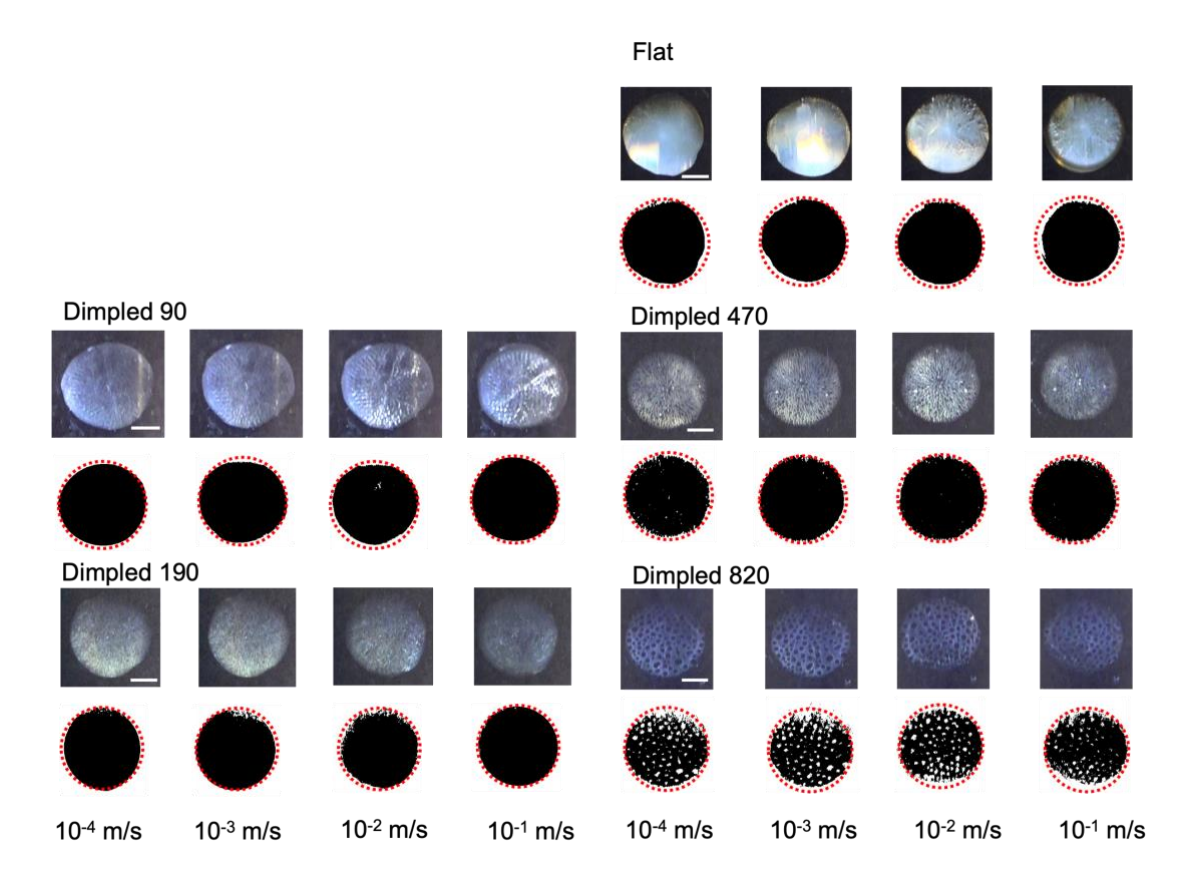


Fig. 2-17 The contact images of the gel and the substrate with the contact angle of $<10^{\circ}$ under sliding at certain velocity. The colored images in upper row were converted to the binarized images in the lower row.

Although the image analysis of that obtained by *in situ* observation was tried even for the test with this substrate with the contact angle of $\theta < 10^{\circ}$ similarly with other substrates with different contact angle (shown in Fig. 2-17), the contrast of the contact area and non-contact area was unclear compared with others, so the analysis was impossible. Intrinsically, the contact region should be seen as white or bright, but the brightness of the area was low and this may be because a thin water layer was existed between the gel and the substrate. In addition, there is a possibility that the difference in the brightness could reflect the contact strength of the gel and the substrate, however, this is not clear at present.

2-4 Conclusion

The sliding friction of PVA gels with hemispherical surface dimples of $100-1000~\mu m$ in diameter against three kinds of glass substrates was measured in water. We evaluated the influence of the surface wettability of the counter substrates used for the friction test of the gels. The friction behavior of gels, both Flat and Dimpled gels, changed depending on the surface wettability of the counter

substrate in the friction test, and especially the behavior of Flat gel was consistent with the previous study³².

In this study, we confirmed that the friction behavior of the gels with surface dimples was also changer depend on the substrate wettability. In particular, there were trends that Dimpled gel, which has numerous dimples on their surface, showed the lower friction stress than Flat gel. The effects of surface dimples on Dimpled gels were different against three kinds of the substrate.

First, on the substrate with the contact angle of $\theta \sim 110^\circ$ (FDTS-glass), in a wide range of sliding velocity from 10^{-4} to 10^{-1} m/s, all the investigated Dimpled series exhibited friction reduction effect, which was basically attributed to the contact area reduction due to the surface dimples denoted as the effect (1). In the high velocity region, Dimpled 820 with the largest dimple exhibited lower friction than the other Dimpled series, and the lubrication effect of the water from the dimples, denoted as the effect (2), was directly observed by the high-speed camera.

Since water in surface dimples behaves like a thick lubricating layer, it was predicted that the viscous resistance is lowered by preventing the formation of a thin lubricating layer. Although the simple estimation showed that the viscous resistance is small, however, this effect, denoted as the effect (3) was not investigated as a friction behavior. This is because the friction originated from the elastic resistance in this system using PVA gel and hydrophobic glass is relatively high.

Next, on the substrate with the contact angle of $\theta \sim 70^\circ$ (HMDS-glass), the work of adhesion between the substrate and the gel was the largest among the substrates used in this study as shown in Chapter 1, so the elastic contribution would be dominant to the friction of gels. Different from the FDTS-glass substrate, the friction stress of Dimpled gel decreased mainly due to the reduction in gel/glass contact area, but the friction reduction effect of Dimpled gels was not obtained on this substrate in high-velocity region. This is considered to be attributed to cancelling out the effect of the reduction in contact area by high elastic resistance due to strong work of adhesion at the gel/glass interface and difficulty in transferring to the lubricating state because of the higher contact pressure than Flat gel.

Finally, regarding on the substrate with the contact angle of $\theta < 10^{\circ}$, this substrate is the most hydrophilic, so it is considered that water between the gel and the substrate is not fully drained and the contribution of the viscous resistance to the friction was large. The friction of Flat increased with the sliding velocity following the Newton's law of viscosity, however, the friction of Dimpled drastically decreased in high velocity region. It is considered to be caused because the contribution of the elastic resistance derived from the elongation of the polymers on the surface of the gel was almost not obtained and also the contribution of the viscous resistance was small because the thin water lubricating layer could not be formed at the interface and also water trapped in surface dimples

behaved like as a thick lubricating layer.

In this study, hemispherical dimples of various sizes were imparted on the surface of gels using the droplet replication method^{29,30} without any special equipment. While dimples in metals are primarily used to enhance lubrication by supplying lubricants^{24,68}, in hydrogels, our study confirmed an additional friction reduction effect due to the decrease in true contact area. This phenomenon arises because the true contact area of the hydrogel does not scale directly with the applied load, resulting in a nonlinear relationship between friction force and load. Due to the effect of surface dimples, the friction of the gel could be lowered while maintaining the bulk properties, such as water content, elastic modulus, and biocompatibility. This method can be combined with other friction-reduction techniques, such as adding a highly viscous polymer to the lubricant⁵⁴, lowering the surface polymer concentration^{73,74}, or introducing graft chains to the surface^{17,19}.

We believe that the results shown in this study are useful for understanding the friction mechanism of biological joints. Since the hydrogel used in this study exhibits key mechanical and lubrication characteristics similar to cartilage, it is reasonable to consider its frictional behavior within the framework of cartilage friction models. Like cartilage, hydrogels are water-swollen, deformable polymer networks that redistribute fluid under load, making them a relevant analog for studying lubrication mechanisms in soft biological tissues.

Additionally, our sliding velocity range (10^{-4} to 10^{-1} m/s) encompasses the range observed in cartilage lubrication (10^{-4} to 10^{-2} m/s)^{61,75}. Although the elastic modulus (100 kPa) of the hydrogel is lower than that of cartilage (1 to 10 MPa), the ratio of applied pressure to elastic modulus (σ/E) is comparable, suggesting similar surface shear deformation behavior.

While traditional cartilage friction models primarily focus on the biphasic nature of cartilage and fluid pressurization effects, they do not explicitly consider the role of surface geometry. In this study, we investigated the effect of surface dimples on hydrogel friction and found that the presence of dimples reduces friction through contact area reduction and water retention mechanisms. These findings suggest that surface topography can play an essential role in soft tissue lubrication and may complement existing cartilage friction models.

To further evaluate the relevance of these findings in biological cartilage lubrication, future studies should employ hydrogel-hydrogel friction systems instead of glass, as compliant contacts more closely mimic the tribological environment of articular cartilage. Additionally, incorporating synovial fluid components, such as hyaluronic acid and lubricin, would allow for a more physiologically relevant comparison with recent cartilage lubrication models. These steps will help establish whether surface dimples contribute to friction reduction in biological joints and improve our understanding of the role of cartilage surface morphology in lubrication.

However, ther remains some issues to consider, so we would like to study on the following as prospects for this research.

In this study, a roughly controlled hemispherical dimple shape was imparted to the gel surface by transferring the shape of a water droplet, and this changed the surface properties such as contact, adhesion, friction, and wear, and a particularly low-friction surface was obtained, but it has not been clarified what parameters of the dimple shape contribute to low friction. If this could be clarified, important knowledge would be gained in the surface design of low-friction gels. Possible parameters include the diameter, depth, perimeter, density, and distribution of the dimple shape. Therefore, in the future study, we would like to create gels using a mold in which these parameters are more controlled and conduct friction tests to understand the role they play.

In addition, by imparting the gel a dimpled shape, we expected that "the water trapped in the dimples would behave as a thick lubricating layer, preventing the formation of a thin and/or wide lubricating layer at the gel/glass interface," but we have not yet been able to verify the authenticity of this effect. We concluded that the decrease in friction of the Dimpled gel compared to the friction of the Flat was due to the reduction in contact area and interfacial lubrication. However, the effect of the dimples on the interfacial lubricating layer has not been clarified. To verify this effect, for example, by observing the interface using an observation system with a higher magnification and a shallower depth of field, or by changing the viscosity of the lubricant, we should be able to obtain more information about the lubricating layer and verify the effect of the dimpled shape.

Chapter 3 Effect of elasticity of hydrogel on the surface property

3-1 Introduction

Hydrogels are already being used as soft contact lenses, cell culture scaffolds, wound dressings, etc.^{51,76,77}, and are expected to be applied to biomaterials such as artificial joint cartilage. In the examples where they are already being used, high mechanical strength of the gel is not required, but knee joints and hip joints are subjected to loads several times the body weight and are subject to repeated friction, so a high elastic modulus on the order of MPa³⁴ and mechanical strength are required. If the elastic modulus of the gel changes, it is thought that the polymer density of the surface and the shear deformation rate will change, and therefore it is predicted that the surface properties will be affected by the elastic modulus.

In this chapter, the influence of the elastic modulus of PVA gel with surface dimples on its adhesion or friction property was investigated. As shown in Chapter 1 and Chapter 2, it was obvious that the dimple structure on the gel surface has influences on adhesion and friction behaviour, and especially it showed a friction reduction effect. The effect of the reduction in the contact area is considered to be maintained even when the elastic modulus of the gel is changed. Particularly in the high velocity region, it was confirmed that water trapped in dimples was provided to the gel/glass interface and the friction of the gel decreased because water contributed as a lubricant. Regarding this effect, because the lower the elastic modulus, the larger the shear deformation, the surface dimple structure easily deforms and water in dimples is expelled into the interface, then it is predicted that the predominant friction reduction effect is achieved.

As methods to change the elastic modulus of the PVA gel, the variation of the solution concentration or the solvent mixture composition^{78,79}, the introduction of the chemical crosslinking point, the preparation of the interpenetrating network (IPN) gel composed of PVA and the other polymer^{16,80}, the repeating Freeze-Thawing (FT) method^{13,81,82} and the dry-anneal method³⁴ are considered.

For performing the measurement of the surface property after the gel preparation, there are some issues when changing the modulus of gels; for example, to maintain the planarity of the gel, not to be disappeared the surface dimple structure of the gel, to be able to obtain the uniform properties in the whole gel, and to be able to control the water content or elastic modulus in a reproducible manner.

The moduli of the gels used in Chapter 1 and Chapter 2 were estimated at about 100 kPa from the

compression test. In our previous study, the elastic modulus of the gel could be raised up to about 200 kPa by using the repeating FT method, however, water froze on the gel surface and the trace was formed, so this method is inadequate to prepare the samples for the investigation of the effects of the surface dimple structure. Also, the elastic modulus was changed by varying the composition of the solvent, but especially in the case where only deionized water or dimethyl Isulfoxide was used, the prepared gel was quite soft and brittle, it was difficult to handle. Therefore, the gel with the low modulus was prepared by changing the solution concentration and that with the high modulus was prepared by applying the dry-anneal method, respectively in this study.

In the dry-anneal method, the polymers in the gel are brought close to each other in the process of drying, and the polymers move flexibly by the annealing treatment to form new physical cross-linking points, thereby increasing the elastic modulus. It has been reported that a gel having the fracture energy and elastic modulus comparable to that of living cartilage was produced by using this method. From the viewpoint of understanding the friction mechanism of living joints, it is desirable to verify the effect of the surface structure using a gel with mechanical properties equivalent to those of living cartilage.

3-2 Materials and Methods

3-2-1 Materials

2-propanol was purchased from Wako Chem. Ind., and was used without any purification. Other chemicals for gel preparation are the same with the ones stated in Chapter 1.

3-2-2 Preparation of Poly(vinyl alcohol) gels with different elasticities

Three kinds of PVA gel with different elastic modulus were prepared in this work.

Two types of PVA solutions with 5 or 10 wt% concentration using DMSO/ $H_2O(= 3:1 \text{ w/w})$ mixed solvent were prepared. The preparation method was the same shown in Chapter 1, section 1-2-3. These solutions were poured into the home-made reaction cell, then were quenched at -40°C for 16 hours for gelation. After producing the gel from the cell, it was soaked in a large amount of deionized water, and the solvent in it was exchanged from the mixed solvent to deionized water.

The dry-anneal method was applied to one of the PVA gel made from the 10 wt% solution so as to

prepare the gel with high elasticity. To prevent the gel from being curved in the drying process, the gel was dried by exchanging the solvent⁸³ as shown in Fig. 3-1. First, the gel was soaked in 60 wt% 2-propanol aqueous solution for 3 days, then 85 wt% 2-propanol aqueous solution for 3 days, 100% 2-propanol for 3 days at last. This process made the gel dehydrated and dried. The dried gel was put onto the glass piece and annealed at 80°C for 3 hours then 120°C for 1 hour. After the treatment, the gel was soaked in a large amount of water again and swelled.

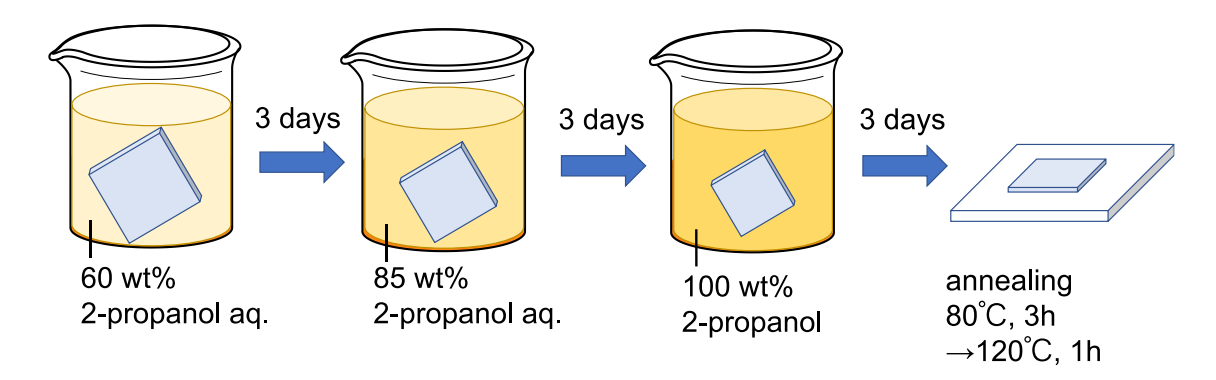


Fig. 3-1 Schematic of the dry-annealing process of the gel.

3-2-3 Measurement of Young's modulus

Strain-controlled rheometer was used to determine the Young's modulus E by measuring the shear modulus G'. The gel cut into 15.70 mm in diameter and 2.70 mm in thickness was set onto the stage of the rheometer after drying it with a laboratory wipe. The jig was contacted to the gel and the test was started soon after the normal load (\sim 3 N) was applied to the gel. The dynamic frequency sweep test mode was conducted. As test conditions, the shear strain was fixed at 1.0% and the frequency was swept from 1 to 100 s⁻¹.

The measured value is displayed in Table 3-1.

3-2-4 Measurement of Swelling ratio

The swelling ratio Q, equilibrium water content (EWC), and equilibrium polymer content (EPC) of the gel was calculated by measuring the wight of the gel before and after drying it absolutely.

After weighting W_{sw} , the weight of the gel in swollen state, the gel was put on the polytetrafluoroethylene-plate and was dried by heating in the oven at 120°C for 2 hours. Then, W_{dry} , the weight of the gel in absolute dry, was weighted. Q, EWC and EPC were calculated by using the

formula as shown below respectively (Eq. 3-1, Eq. 3-2, and Eq. 3-3).

$$Q = \frac{W_{\rm sw}}{W_{\rm dry}} \tag{Eq. 3-1}$$

$$EWC = \frac{W_{sw} - W_{dry}}{W_{sw}}$$
 (Eq. 3-2)

$$EPC = \frac{W_{\text{dry}}}{W_{\text{sw}}} = 1 - EWC$$
 (Eq. 3-3)

The measured values are displayed in Table 3-1. Here, only EPC is shown as a representative value in Table 3-1.

Table 3-1 Preparation of PVA gels and its mechanical properties.

PVA sol. concentration[wt%]	Treatment	Young's Modulus[k Pa]	EPC [%]
5	-	30	10.8
10	-	70	12.2
10	dry-anneal	230	22.1

3-2-5 Friction measurement

The friction of the gels with different elastic modulus was measured in the same way shown in chapter 2, section 2-2-3. The glass substrate with the contact angle of $\theta < 10^{\circ}$ was used as a counter substrate.

3-2-6 Adhesion test

The work of adhesion W_{adh} for the gels with different elasticity was measured in the same way as shown in chapter 1, section 1-2-7.

3-3 Results and Discussion

3-3-1 Friction behavior

The results for the friction measurement of PVA gels with different elasticity are shown below in Fig. 3-2.

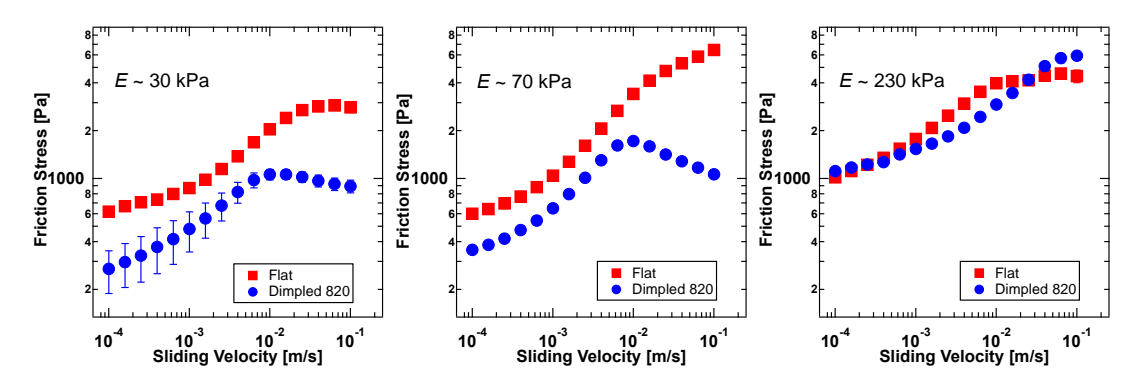


Fig. 3-3 Sliding velocity dependency of friction stress of PVA gels with different Young's moduli.

As shown in Fig. 3-3, in case that the gel which shows relatively low elastic modulus and is soft was used, the friction stress of Dimpled was lower than that of Flat, and in case that the gel which shows relatively high elastic modulus and is hard was used, the difference in the friction stress of Flat and Dimpled was little.

First, the gels with low elastic modulus were featured. To investigate whether the friction stress is normalized by the apparent contact area, the values, the friction stress was divided by the Ratio of flat region, are displayed in Fig. 3-4.

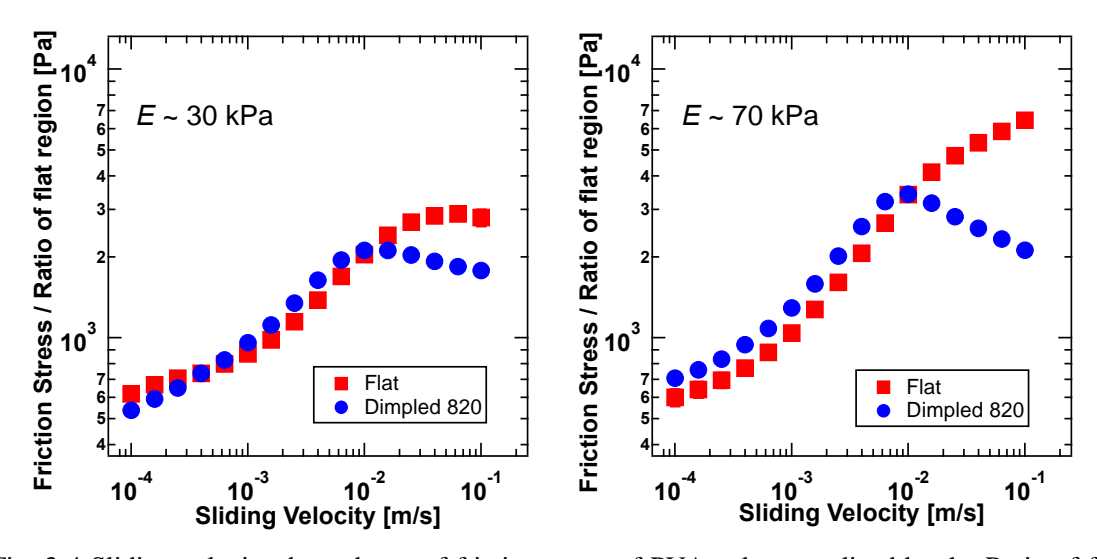


Fig. 3-4 Sliding velocity dependency of friction stress of PVA gels normalized by the Ratio of flat region.

In Fig. 3-4, the friction stress of Flat and Dimpled was almost consistent with each other within the sliding velocity up to about 1×10^{-2} m/s. Therefore, the friction stress of Dimpled decreased

reflecting the macroscopic reduction in contact area. However, the decrease of the friction stress of Dimpled in high velocity region could not be explained even though excluding the effect of the contact area by normalization.

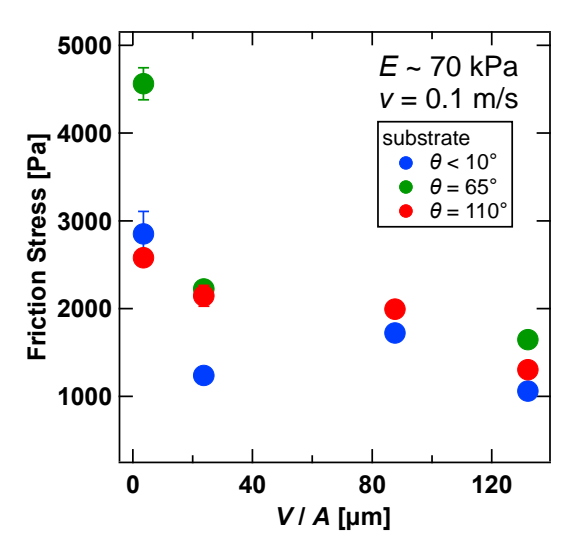


Fig. 3-5 Relation of friction stress and mean volume of dimple per unit area, V/A.

As shown in Fig. 3-5, it is clear that the high-velocity region showed almost the same friction stress for each sample, regardless of the contact angle of the counter substrate. This indicates that the hydrodynamic lubrication determined the friction in this velocity region. In addition, the larger the average volume of the dimple shape per unit area, the lower the friction, suggesting that the water trapped in the dimples was supplied to the interface and behaved as a lubricant. In particular, in the case of the Dimpled used in this study, in interface observation using a high-speed camera, it was confirmed that the water that was trapped in the dimples up to the medium-velocity region came out to the interface when it moved to the high-velocity region (Chapter 2). Therefore, it is predicted that the high-velocity region was also a lubricating region in Fig. 3-4, and it is considered that the lubrication of the interface was promoted by the water trapped in the dimples, which reduced friction.

On the other hand, focusing on the gel with high elasticity, the friction stress of Dimpled did not decrease compared with Flat gel and this trend was not consistent with others. As shown in chapter 1, the local contact pressure of Dimpled gel was higher than that of Flat gel, so the friction reduction effect due to the reduction in contact area by the surface dimples could not be appeared and showed the higher friction stress. In addition, the surface dimple geometry was difficult to deform because of high elasticity, which did not lead water supply to the interface, then lubrication in high-velocity region was not promoted. In this study, the most hydrophilic substrate was used and the same normal load was applied to the gel regardless the elasticity of the gel, it is considered that the gel was difficult to

be sheared compared with the gel with low elasticity. For that, the difference of friction between Flat and Dimpled gel might be clear even in the gel with high elasticity when we use the hydrophobic substrate or apply a higher normal load. These measurements have not been conducted yet, and we would like to clarify in the future.

3-3-2 Adhesion property

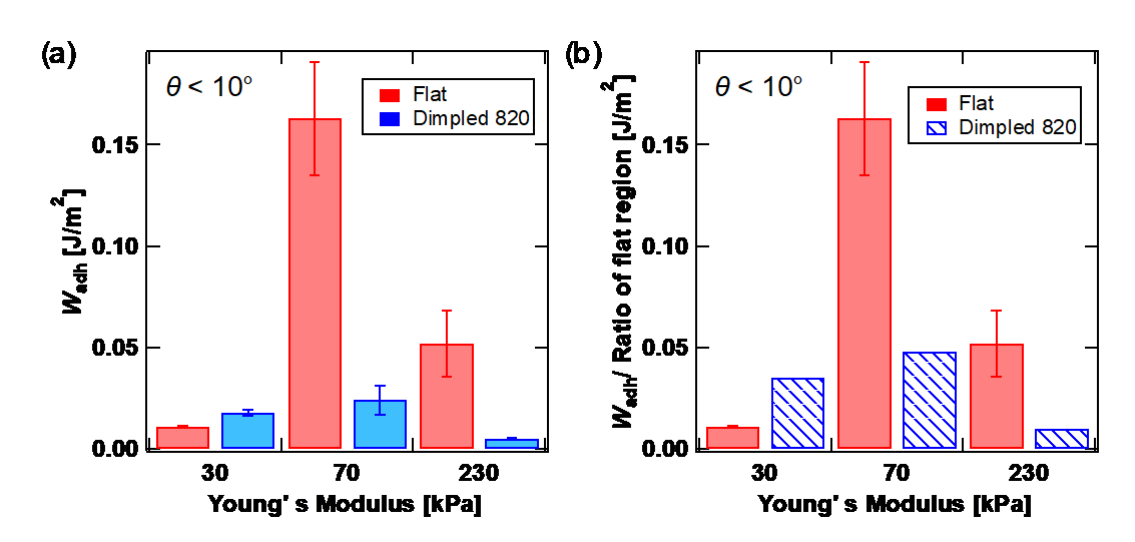


Fig. 3-6 Work of adhesion of PVA gels with different Young's modulus.

In Fig. 3-6, the gel with Young's modulus E = 70 kPa showed the largest $W_{\rm adh}$. Regardless of the elastic moduli of the gels, a prescribed value was loaded to the gels, and the jig was drawn up at a steady rate in this measurement. This might have led the gel with the high modulus (230 kPa) to incomplete contact with the substrate glass when the prescribed load was applied and a part of the gel surface to be not in contact because of the geometrical distortion when the load was removed to 0 N, then to show a low $W_{\rm adh}$. On the other hand, the gel with the low modulus (30 kPa) showed quite low $W_{\rm adh}$. The normal strain due to the compression was the largest among the three samples, so it took a long time to completely peel off from the counter substrate. Water penetrated the interface during that time and weakened the adhesion, and the polymer chains on the gel surface were detached from the substrate due to their thermal motion, so it is considered not to contribute to adhesion.

In addition, the Dimpled showed a low $W_{\rm adh}$ compared to the Flat. One reason for this is considered to be the reduction in the contact area due to the surface dimples, but another factor is thought to exist because the $W_{\rm adh}$ value is still small even when normalized by the Ratio of flat

region. For example, water trapped in the dimples promotes interfacial peeling. For gels with low elasticity, no significant difference was observed between Flat and Dimpled; in fact, when normalized, Dimpled showed a higher value. It is possible that because the gel was soft, the shape of the dimples on the surface was deformed by compression, increasing the contact area. In addition, the deformation of the dimples may have had an effect like a suction cup.

3-4 Conclusions

This study investigated the friction and adhesion properties of three kinds of PVA gels with different elastic moduli.

The elastic modulus could be varied from about 30 to 230 kPa by changing the concentration of PVA solution for gelation and applying the dry-anneal method.

Flat, the gel with the flat surface, and Dimpled 820, the gel with the dimple structure on its surface, were prepared and their surface properties were researched. As a result of the friction measurement, the friction reduction effect of the surface dimples was obvious for especially the gel with low elastic modulus but not for the gel with high modulus.

This might be because the surface of the gel with low elastic modulus easily deforms and the gel/glass interface is lubricated with water trapped in dimples expelled due to the surface deformation under shear motion. Note that, the most hydrophilic glass substrate, which the gel is relatively difficult to contact strongly, was used and the measurement was conducted by applying low normal pressure to the gel compared with the elastic modulus of the gel in this system, so there is a possibility that the shear was inadequate for the surface of the gel with high elastic modulus and the effect of the surface dimples was not obtained. For this reason, we should re-evaluate the friction property using the hydrophobic substrate with a high contact angle to water or applying high normal pressure to the gel in the future study.

Also, the work of adhesion of the gels with different elasticities to the hydrophilic glass substrate were evaluated. The gel with elastic modulus E = 70 kPa showed the highest work of adhesion among the three gel samples with different moduli. Furthermore, the effect of the surface dimple was seen especially in gels with a high elastic modulus, and the $W_{\rm adh}$ of the gel with surface dimple was lower than that of the Flat gel. One possible reason for this is that with low elastic modulus gels, the contact area increased by compression due to their softness, but with high elastic modulus gels, the small contact area was maintained. However, in this test, the same load was applied regardless of the elastic

modulus of the gel, and the jig was pulled up at the same rate, but it is possible that different results would be obtained by uniforming the normal strain of the gel or the time until unloading. Therefore, we would like to conduct another examination, including the measurement conditions, and systematically discuss the effects of the gel's elastic modulus and surface geometry.

Chapter 4 Wear Evaluation of Poly(vinyl alcohol) Hydrogel by UV Spectrometry and Total Organic Carbon Measurement of Lubricant

4-1 Introduction

Hydrogel is a substance that has a three-dimensional polymer network structure swollen with water. It has many features, such as high-water content, wide range of elastic modulus, permeability, and stimuli-responsiveness. Therefore, hydrogels are applicable in biomaterials, and there are many studies on the application of hydrogels as artificial joint cartilages 12,13,16,84,85. Biocompatibility, mechanical properties, and durability are issues and evaluation points that must be considered in order to apply hydrogels as biomaterials 26,27. For artificial cartilage, hydrogels must have the same level of low friction and wear resistance as biological joints.

In the tribological studies of hydrogels, although there are many reports on the friction of gels, there are few reports on the wear of gels. One of the reasons for this is that the evaluation methods used for other solids, such as metals, are difficult to apply to hydrogels. The gel, which is in the equilibrium swollen state, is worn by rubbing interaction, then it reaches a new equilibrium state by swelling when it is stored in water, or drying when it is stored in air. Therefore, it is hard to maintain the worn state of the gel. The measurement of weight change of the sample before and after the test, observation by microscope, and surface roughness meter are used as the evaluation methods for the wear of gels^{35–37}, however, each method cannot avoid the influences of swelling and drying.

As stated earlier, wear is often evaluated by observing its surface morphology; however, this method cannot distinguish whether the wear scars on the gel are generated by releasing the wear particles into the lubricant or by changing its surface shape. The wear particles in the lubricant obviously reflects the loss amount of the materials, and they are the effective target for the wear evaluation particularly in low wear conditions. The term "wear particle" is not precise for materials with networks such as hydrogels. However, in this paper, regardless of the size of the particles released from the gel surface due to wear, even if they are single strand, they will be referred to simply as "wear particles" for the sake of simplicity. The wear amount can be estimated regardless of the size of the wear particles and this will be described in detail in a later section.

To the best of our knowledge, research on the evaluation of gel wear using lubricants has not been reported, and a new method for evaluating the concentration of wear particles in lubricants is required. Herein, we attempt to evaluate the wear of gels using a *lubricant* that may contain wear particles

instead of a worn gel sample. As the evaluation methods for the lubricant, spectrometric oil analysis program (SOAP) method, ferrography and particle counter method are known to detect the metal wear^{86–90}. In addition, spectroanalysis such as UV-vis spectrometry and total organic carbon (TOC) measurement are useful. The advantages of the latter two methods are the following: the relatively short measurement time, recoverability, and the ability to measure with a small amount of lubricant make it possible to detect even a small amount of the gel wear. It has been reported that inflammation seems unlikely to occur with wear particles of PVA gel⁹¹, but with ultra-high molecular weight polyethylene, which is commonly used in artificial articular cartilage, wear particle is the main source of inflammation. In this study, we simply measured the wear of the PVA gel, but it would be beneficial to measure the concentration of worn polymers from the gel in view of the medical application of other gels.

In this study, we evaluated the wear of poly(vinyl alcohol) (PVA) gels. Because PVA gel is biocompatible and has superior mechanical properties, it has been widely studied as a candidate for artificial cartilage^{13,16,92}. PVA is fabricated industrially by saponification of poly(vinyl acetate); however, the saponification process is not perfect, and hence, un-saponified parts remain⁹³ (Scheme 1). It has been reported that the carbonyl group contained in these un-saponified parts has an absorbance band around the wavelength of 280 nm^{94,95}. Therefore, it is possible to detect PVA and quantitatively evaluate its concentration or wear amount. Moreover, TOC measurement may be a key method because the PVA polymer itself is composed of organic carbons. Here, we adopted two methods to evaluate the wear of PVA gels, UV-vis spectrometry and TOC measurement.

$$\begin{bmatrix}
H & H \\
C & C
\end{bmatrix}$$
Base cat.
$$\begin{bmatrix}
H & H \\
C & C
\end{bmatrix}$$

$$\begin{bmatrix}
H & H \\
C & C
\end{bmatrix}$$

$$\begin{bmatrix}
H & H \\
C & C
\end{bmatrix}$$

$$\begin{bmatrix}
H & H \\
C & C
\end{bmatrix}$$

$$\begin{bmatrix}
H & H \\
C & C
\end{bmatrix}$$

$$\begin{bmatrix}
H & H \\
C & C
\end{bmatrix}$$

$$C & C \\
H & OH
\end{bmatrix}$$

$$C & CH_3$$

Scheme 1. Poly(vinyl alcohol) is obtained by saponification of poly(vinyl acetate). Poly(vinyl acetate) remains partially in poly(vinyl alcohol) due to incomplete saponification. Degree of saponification: >98.5 mol%.

We confirmed that the friction property of the PVA gel is drastically changed by its surface geometry ¹⁰. In particular, the gel with hemispherical surface dimples, showed lower friction compared with the gel with a flat surface. The relationship between the friction of the gel and wear, however, is still unclear, and the effects of the gel surface geometry on the wear properties are not well known.

In this work, PVA gels were prepared and sliding tests were performed. Then, we studied whether it was possible to evaluate the wear of gels by evaluating the lubricant that was obtained after the sliding tests using UV-vis spectrometry and TOC measurement. First, the glass substrates with surface roughness were used as a counter substrate for the sliding test of the gel to examine whether these methods could evaluate the wear of gels. The rough substrate is considered to be suitable for the first try because it is predicted that the hard glass surface asperity will cause abrasive wear that cuts the soft gel surface and the wear particle will be surely generated and released into the lubricant.

Then, the hydrophobically treated flat glass was also used as a counter substrate and it is examined these wear evaluation methods are appropriate even in the system that adhesive wear is predicted to predominantly occur. In addition, the relationship between the surface geometry of gels and friction or wear properties was studied using PVA gels that were given hemispherical dimples on their surfaces. Furthermore, in bio-system such as our articular joints, soft tissues which resemble gel slide against the other soft tissue, so the sliding test was conducted in the configuration of gel-on-gel and performed its wear evaluation.

4-2 Materials and Methods

4-2-1 Materials

All the chemicals for the hydrogel and the substrate preparation are the same with what we have already shown in Chapter 1, Section 1-2-1.

4-2-2 Hydrogel preparation

Physically crosslinked PVA hydrogels with hemispherical surface dimples were prepared using the same method mentioned in Chapter 1, Section 1-2-3. PVA gel was prepared by the same conditions regarding concentration, temperature, reaction time and PDMS template for imparting the surface dimples on the gel surface. In this chapter, we used the gels, Flat and Dimpled 820 that the mean dimple size was $820 \pm 80~\mu m$ in diameter and $390 \pm 50~\mu m$ in depth. The mean distance between the dimples was $210 \pm 20~\mu m$ and the area ratio of dimples was approximately 0.50. Comparatively, no surface pattern shape was observed for Flat. Also, the modulus of the gel was $94.0 \pm 1.4~kPa$, and the equilibrium water content was about 86~wt%.

Only in this chapter, we abbreviate Dimpled 820 as Dimpled for simplicity.

4-2-3 Sliding test

Friction and wear measurements were performed using a strain-controlled rheometer (ARES, TA Instruments, Co.). The disc-shaped hydrogel, which was 15.70 mm in diameter and 2.70 mm in thickness, was glued onto the stage of the rheometer using a cyanoacrylate instant adhesive agent (Toa Gosei Co., Ltd.). To prevent the adhesive from seeping into the lubricating solution, the sample gels were washed under running water for at least 5 minutes after gluing and immersed in large volumes of water for at least 10 hours. The normal pressure, σ , was set as an experimental parameter. Prior to the friction and wear measurements, the normal strain was applied and gradually increased until the normal stress reached a prescribed value. Although the normal load changes during the tests, the primary normal stress σ_0 was set to 28 kPa. After 10 minutes of preloading, the test was started in step rate test (SRT) mode. For the first 5 seconds, the stage was rotated with angular velocity $\omega = 0.13$ rad/s, then ω was increased to $\omega = 1.3$ or 5.2 rad/s. The friction force, F, was calculated as F =3T/2r, where T is the friction torque recorded during the measurement and r = 7.85 mm) is the radius of the apparent contact area³³. The data acquisition rate was set to 350 points per measurement time, 600, 1800, 3600, 7200 seconds. The average friction stress, τ , generated at the interface is qualified as the friction force per unit area, $\tau = F/\pi r^2$. Although the sliding velocity varies along the radial direction in the parallel-plate geometry from 0 at the rotational centre to ωr at the perimeter, we adopted the sliding velocity v at the perimeter of the disc-shaped samples, $v = \omega r$, when indicating the sliding velocity as a representative value. When $\omega = 0.13$, 1.3, and 5.2 rad/s, $\nu = 0.001$, 0.01, and 0.04 m/s respectively.

In this study, we conducted three types of friction and wear measurements: (1) Flat gel sliding against glass substrates with different surface roughness (Fig. 4-1(a)), (2) Flat and Dimpled gels sliding against the FDTS-treated flat glass substrate (Fig. 4-1(b)), and (3) gel sliding against gel (Fig. 4-1(c)). A schematic of the measurement system is shown in Fig. 4-1.

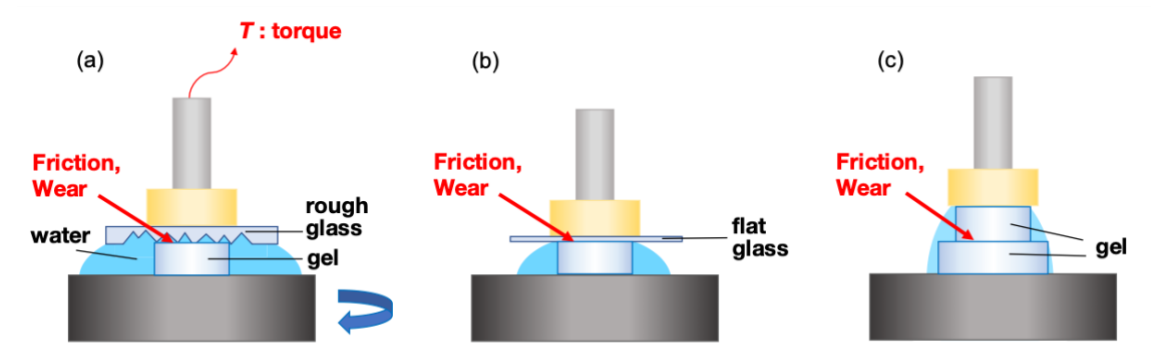


Fig. 4-1 Schematic of the system for the three types of sliding tests. (a) Flat gel sliding against the rough glass substrates. (b) Flat or Dimpled gel sliding against the FDTS-treated flat glass substrate. (c) Gel sliding against gel. All three types of measurements were performed in water.

In measurement (1), Flat gel was slid against five kinds of glasses with different roughness. The substrates were prepared by sandblasting soda glass plates (thickness, t = 3 mm) with different particle sizes (Niki Token. Co. ltd), the ten-point average roughness, R_z values were 53, 31, 18, 12, and 7.9 μ m, respectively. The surface images of the glass substrates are presented in Fig. 4-2. All rough glass substrates were cleaned by soaking in 10 wt% HCl aqueous solution before the measurements.

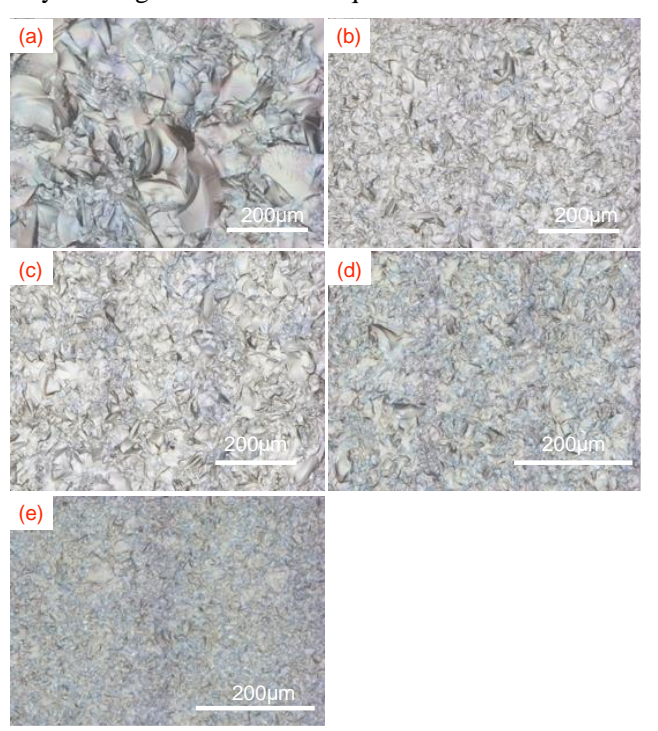


Fig. 4-2 Surface images of the glass substrates with different surface roughness, R_z . The glasses were treated by sandblasting. The R_z values are (a) 53, (b) 31, (c) 18, (d) 12, (e) 7.9 μ m, respectively. Scale bar: 200 μ m.

In measurement (2), two kinds of gels, Flat and Dimpled, were slid against the FDTS-treated glass substrate. The preparation method of the substrate is the same as that mentioned in Chapter 1, section 1-2-4.

Measurement (3) was performed for three configurations: Flat-on-Flat, Dimpled-on-Flat, and Dimpled-on-Dimpled. Both gels were cut into disc shapes, and each sample was glued onto the lower stage or upper jig of the rheometer. The size of the lower gel was 24.80 mm in diameter and 2.70 mm in thickness, and that of the upper gel was the same with the one in measurements (1) and (2).

4-2-4 Wear evaluation

4-2-4-1 Observation by optical microscope

An optical microscope (SZX-12, OLYMPUS) was used for the observation. To avoid the influence of

swelling and drying of the gel, the sample surface was observed in air within approximately 10 minutes after the sliding test.

4-2-4-2 UV spectrometry

After the sliding test, the lubricant (water in this work) was syringed, and the UV spectrum of the lubricant was acquired using a UV-vis spectrometer (V-660 Spectrophotometer, JASCO), and PVA was detected in the lubricant. Deionized water was used as the baseline. Prior to the measurement, the lubricant was heated in a water bath at 80°C for 30 minutes to unlink the crosslinks of the wear particles of the PVA gel, resulting in a uniform linear polymer solution of PVA (Fig. 4-3). This procedure allows the determination of the amount of PVA in the lubricant independent of the size of all wear particles released from the gel surface, regardless of whether they are micrometer-order gel particles or single strands.

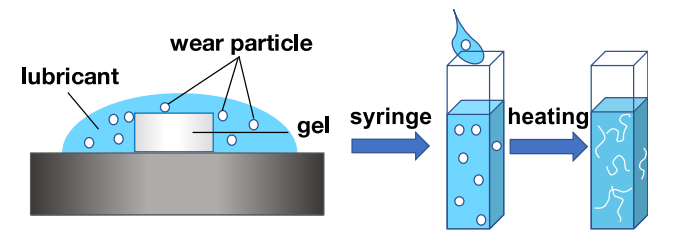


Fig. 4-3 Lubricant that contains the wear particles of the PVA gel was syringed, then heated at 80°C in a water bath to form the homogeneous solution of the linear polymer of PVA by unlinking the crosslinks of the wear particles of the PVA gel.

To prepare a calibration curve, PVA powder was dissolved in deionized water to prepare solutions with concentrations of 0.01, 0.025, 0.05, 0.1, 0.25, 0.5, and 1 wt%. It has been reported that the unsaponified part of the PVA polymer have an absorption band near the wavelength of 280 nm^{94,95}. Actually, the absorption band was confirmed in Fig. 4-4(a) for each PVA aqueous solution with various concentrations. A calibration curve (Fig. 4-4(b)) was prepared using the value of absorbance at the wavelength of 280 nm for each solution shown in Fig. 4-4(a). The linear proportional relation between the absorbance and the PVA concentration was confirmed.

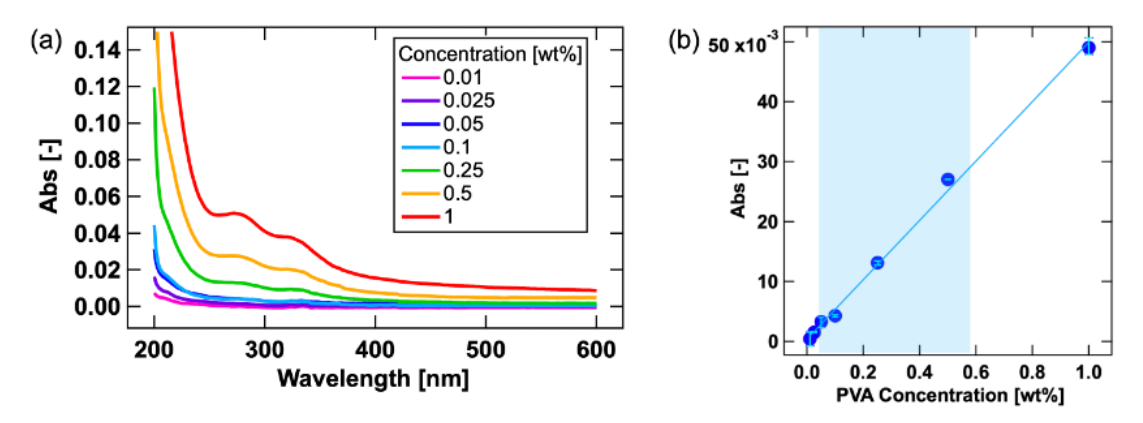


Fig. 4-4 UV spectrometry results. (a) UV spectra of the PVA aqueous solutions with different PVA concentrations. (b) Calibration curve of the PVA concentration and UV absorbance obtained from UV spectra at a wavelength of 280 nm. The range with the coloured background approximately indicates the concentration used for the measurement. Error bars indicate maximum and minimum values of 3 tests.

The amount of linear polymer of PVA contained in the lubricant was defined as the wear amount. In addition, the specific wear rate was calculated by dividing the wear amount by the sliding distance.

4-2-4-3 TOC measurement

The amount of TOC contained in the lubricant was quantitatively evaluated as non-purgeable organic carbon (NPOC) using a total organic carbon meter (TOC-V CSH, Shimadzu Corp.). Because the detection sensitivity is very high compared with UV spectrometry, the TOC of solutions of 0.0001, 0.0005, and 0.001 wt% prepared by dissolving PVA powder in deionized water was measured. In addition, the TOC of deionized water was also measured. Though the TOC of deionized water showed a negative value close to zero, due to the calibration of the equipment, but this time, the calibration curve in the low concentration region was prepared by adopting that value (Fig. 4-5).

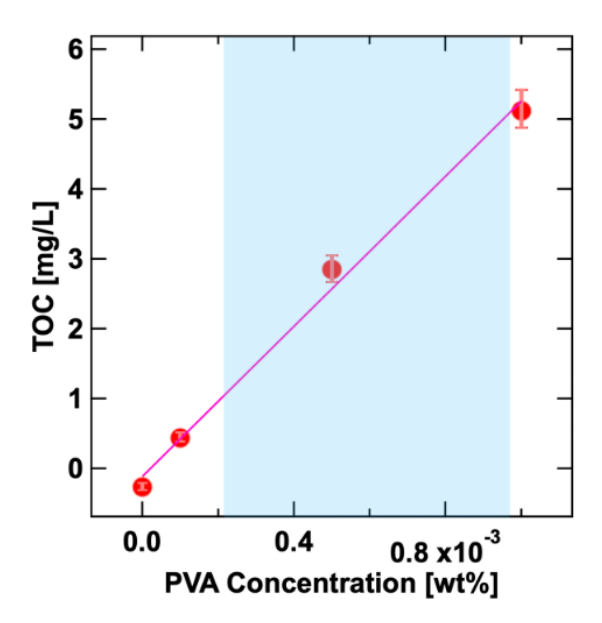


Fig. 4-5 Calibration curve of the PVA concentration and the TOC obtained from the TOC measurement. The range with the coloured background approximately indicates the concentration used for the measurement. Error bars indicate maximum and minimum values of 3 tests.

After acquiring the UV spectrum, the solution was used as the measurement sample for TOC. The lubricant samples were diluted as needed for TOC measurement. The calculation of the wear amount and specific wear rate is the same as that described in the UV spectrometry section.

Note that for a more exact measurement of the wear amount, wear particles that remain on the gel surface and have not been released into the lubricant should be included in the wear amount. After sampling the lubricant solution, the surface was further washed with water, and this was sampled to measure the TOC, which was found to be less than 1% of the previous solution. It is possible that wear particles are still present on the surface after washing, however, no method has been found to measure this.

In addition, the lubricant was also measured under the same conditions except that the gel was not slid, i.e., the gel was simply placed in water without sliding, however, PVA was not detected in TOC measurement, therefore PVA that dissolves from the gel into the lubricant during the measurement time can be negligible.

The wear amount lost from the gel surface can be divided into two categories: (1) wear particles released into the lubricant, and (2) worn polymers (gels and/or linear polymers) transferred to the gel or the substrate. Of these, only (1) is quantified in this work. Therefore, if the transfer of (2) is very large, the wear amount measurement does not match the actual wear situation, and it would be difficult to use the method in this work. In the observation of wear scars, in addition to the above two factors, "deformation of the gel without release of wear particles" will be added.

4-3 Results and Discussion

4-3-1 UV spectra and TOC

The UV-vis spectra of the three types of PVA solutions are presented in Fig. 4-6. One was prepared by dissolving the PVA polymer powder in water. The second was prepared by heating the PVA gel in water. The last was prepared by heating the lubricant, which is considered to contain the wear particles of the PVA gels. All the aqueous solutions had absorbance bands around 280 nm, and the shapes of the spectra were similar. Therefore, it can be said that quantitative evaluation of PVA concentration in the lubricant is possible using the calibration curve, which is obtained from the absorbance of PVA solutions prepared from PVA *powder*.

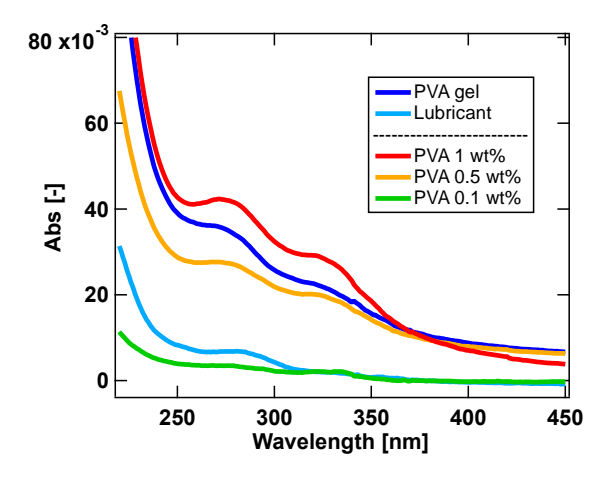


Fig. 4-6 Representative examples of UV-vis spectra of PVA aqueous solutions obtained by dissolving the predefined amount of PVA polymer powder, PVA hydrogel, and by heating the lubricant that contains wear particles of the PVA gel.

It is possible to distinguish the contaminants that have absorbance at a different wavelength from PVA, if the solution is contaminated. In addition, TOC measurements were performed for the solution prepared by heating the PVA gel in water, similar to UV spectrometry, and a peak of carbon was detected (data not shown). The PVA concentration calculated by using the calibration curve was almost consistent with the predicted value from the weight of PVA gel considering the polymer fraction of the gel. Therefore, the PVA concentration in the lubricant can also be quantitated using the calibration curve for TOC. Wear scars reflect the result of complex wear derived from surface deformation, the transfer of wear particles to the counter surface, and the loss of gel as wear particles to the lubricant. On the contrary, the concentration of wear particles in the lubricant can only reflect the loss of gel, making it possible to analyse wear by combining the results of the optical observation of wear scars.

Hereafter, the results of each measurement system for evaluating friction, wear scars, and wear particle concentration in the lubricant are discussed.

4-3-2 Wear of PVA gels

4-3-2-1 Gel vs. rough glass

Wear measurement of hydrogels should be conducted in water for the stability because the gels easily change their volume due to drying. However, when lubrication occurs, the viscous resistance of lubricant also donates to the friction force, and wear is reduced because the contact of gel/substrate is hindered. That makes it difficult to understand the relationship between friction and wear and to judge whether this evaluation method is appropriate. Therefore, we first performed the sliding test in the gel vs rough glass system, in which the gel and the counter substrate are expected to surely form contact due to very fast drainage.

To our best knowledge, the equation for wear of gels has not been developed, we use the wear model of rubber and polymer. From the classical wear model developed by Archard, Schallamach and Tabor, the abrasive wear of the gels was assumed to be described by the friction force F (Eq. 4-1), or the normal load N for more simple expression (Eq. 4-2)⁹⁶⁻⁹⁸.

$$W = kFl (Eq. 4-1)$$

$$W = k'Nl (Eq. 4-2)$$

These are based on the premise that the real contact area A_r is proportional to the normal load N. In the classical wear model, the wear amount W is proportional to the friction force F or normal load N, and the sliding distance l, as in Eq. 4-1 and Eq. 4-2, regardless of the material. If it is described by Ratner's wear model for polymer materials⁹⁹, $k = k_2/Hs\varepsilon$, and $k' = k_2\mu/Hs\varepsilon$. H is the hardness, s is the tensile strength, ε is the breaking elongation, μ is the friction coefficient, and k_2 is the constant. For soft matters such as rubber and gels, the real contact area quickly approaches the apparent contact area 100 . When the gel is in contact with the bottom surface of the rough glass substrate, Eq. 4-1 is expected to describe the result well rather than Eq. 4-2 because the real contact area A_r is not proportional to the load N anymore.

In Fig. 4-7(a), the relationship between friction stress and sliding time, which was measured under the condition that Flat, the gel with a flat surface, slid against the glass substrate with surface roughness, R_z = 53 μ m, is presented. The friction stress tended to decrease with time, which perfectly follows the decrease in normal force (Fig. 4-7(b)).

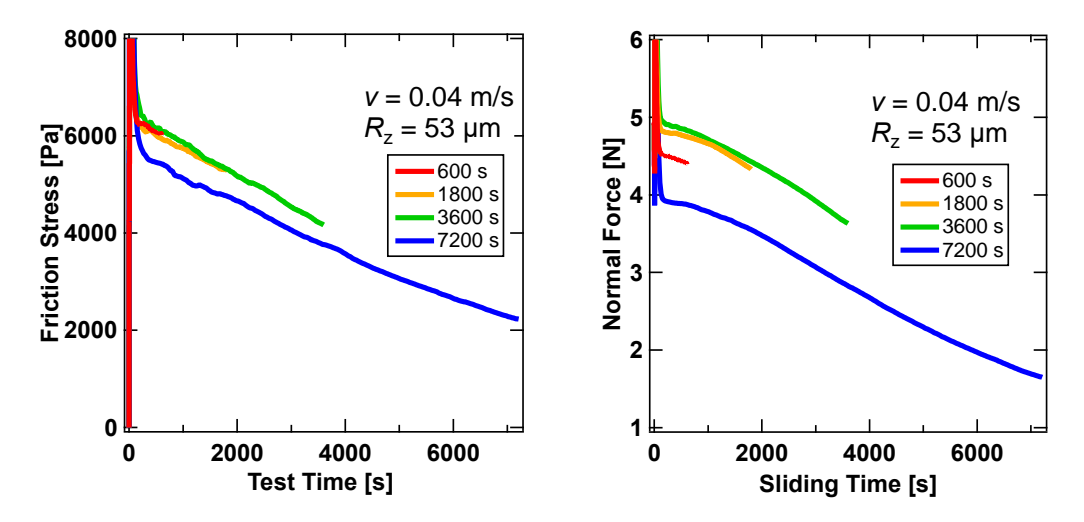


Fig. 4-7 Representative examples of the relationship between the sliding time and (a) friction stress and (b) normal force for test where Flat was slid against the glass substrate with surface roughness, R_z = 53 μ m for 600, 1800, 3600, and 7200 seconds.

Also, the decrease in normal force depends on the volume change caused by the wear loss of gels and not the stress relaxation due to the solvent flow in the gel (Fig. 4-8).

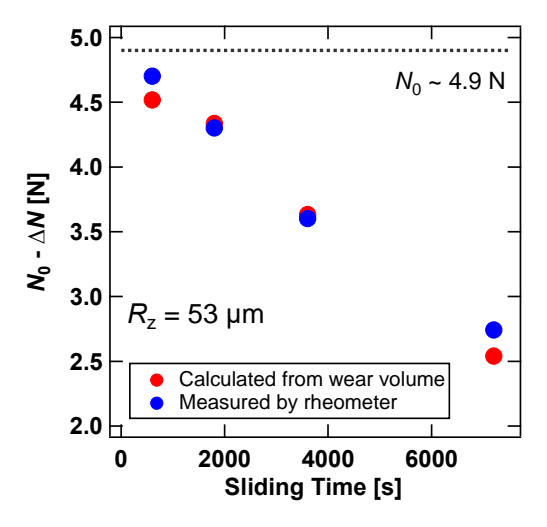


Fig. 4-8 Relation of the sliding time and the normal force at the end of the sliding test that Flat gel slid against the rough glass substrate. The dashed line indicates the primary normal force, $N_0 \sim 4.9 \text{ N}$.

Fig. 4-8 shows the normal force calculated from the loss volume of the gel estimated from the TOC and the actual normal force at the end of the sliding test measured by the rheometer. The two results are in pretty good agreement, indicating that the decrease in normal force is dominated by volume change due to wear, not stress relaxation due to water flow.

When the normal force at the end of the sliding test indicated the vertical axis in Fig. 4-8 described as $N_0 - \Delta N$, and ΔN calculated from wear volume is,

$$\Delta N = E^* \frac{\Delta t_{\text{test}} - \Delta t_{\text{wear}}}{t_0} A = E^* \frac{\Delta t_{\text{test}} - \frac{\Delta V_{\text{wear}}}{A}}{t_0} A$$
 (Eq. 4-3)

$$\Delta V_{\text{wear}} = \frac{W_{\text{TOC}} d}{\text{EPC}}$$
 (Eq. 4-4)

where E^* is apparent Young's modulus, Δt_{test} is the displacement for the sliding test, Δt_{wear} is the change of thickness due to wear, t_0 is the thickness of gel, ΔV_{wear} is the volume change of gel due to wear, A is the surface area of gel sample, W_{TOC} is the wear amount evaluated by TOC, d is the density of gel, and EPC is the polymer fraction of gel, respectively. The density d was set to 1 for simplicity, and the polymer fraction EPC was 0.14.

The results of the wear amount measured by UV spectrometry and TOC are shown in Fig. 4-9. In Fig. 4-9(a), the *wear amount* on the left axis means the amount of *linear polymer* of PVA released into the lubricant as wear particles. The *loss of PVA gel*, wear amount divided by the polymer fraction (~14%) in PVA gel, is also shown on the right axis and it refers to the weight of PVA *gel*. If the polymer fraction of the gel is known, it can be described in both formats, but we discuss wear behavior hereafter using the value of wear amount.

Since the UV spectrometry only measures 1.5 mol% of PVA, which is the un-saponified fraction (Degree of Saponification: min. 98.5 mol%), and is easily affected by the contamination, TOC is expected to be more reliable. An approximate line estimated by the least squares method was drawn for the PVA concentration obtained from the UV spectrometry, and the modified values, denoted as "modified-UV" in Fig. 4-9, were calculated by setting the intercept to 0. The modified values were similar to those obtained from the TOC measurements. In UV spectrometry, the absorbance at 280 nm was considered to be affected by contamination, such as the adhesive agent or others. The contaminant had the absorbance at the wavelength of 280 nm and molar absorptivity was relatively higher than PVA.

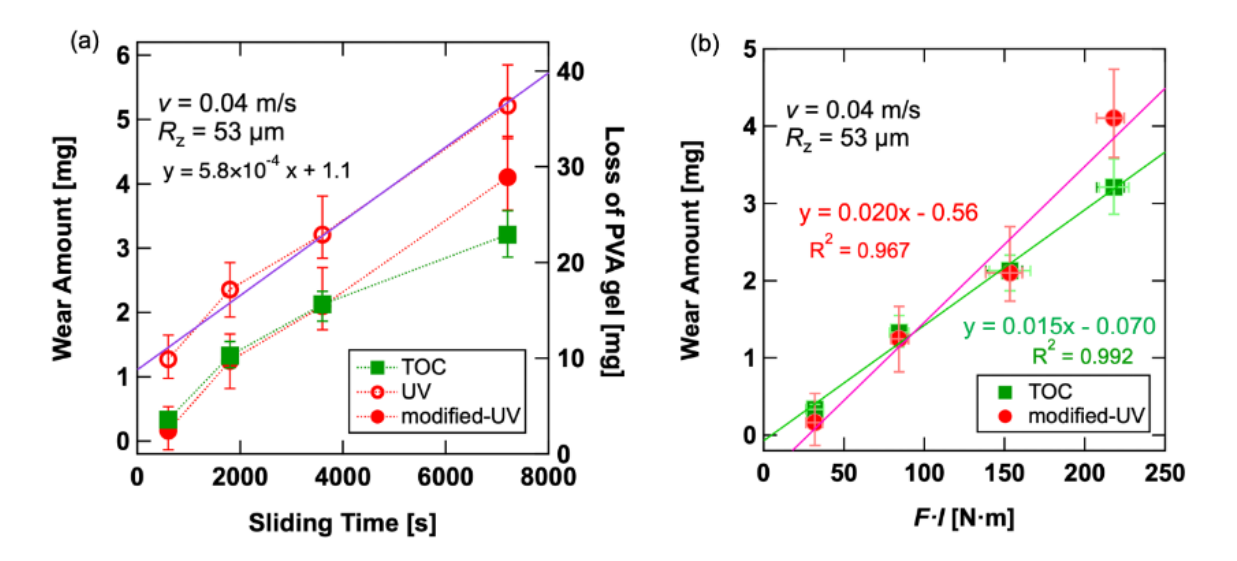


Fig. 4-9 Results of wear amount evaluated by two methods, UV spectrometry and TOC. (a) Sliding time dependence of wear amount and loss of PVA gel. Wear amount on the left axis indicates the weight of PVA polymer contained in the lubricant. Loss of PVA gel on the right axis was calculated by considering the polymer fraction in PVA gel. (b) Relation of wear amount and the product of friction force and the sliding distance. Straight-line fitting is performed and the coefficient of determination R^2 values are shown. Error bars indicate maximum and minimum values of 3 tests.

It was confirmed that the wear amount increased with the sliding time in both UV and TOC. Especially in TOC, the wear amount changes more moderately as the sliding time is longer. The wear amount was approximately 400-1100 times the volume derived from the surface roughness of the glass; hence, it can be said that abrasive wear occurred when the gel was ground by the rough glass. In this measurement, the indentation depth of the gel was more than approximately $300 \, \mu m$; hence, the gel was compressed sufficiently compared with the surface roughness of the glass substrate.

In the microscopic image of the sample surface taken after the wear measurement (Fig. 4-10), it was confirmed that there were obviously more severe annular wear scars with longer test time. This corresponds to the wear amount obtained from the UV spectrum and the TOC measurement. Because rotational sliding friction and wear tests were performed in this work, annular wear scars were generated concentrically from the center of rotation. The non-uniformity of the wear marks in the radial direction suggests that the wear is velocity dependent, but this has not yet been investigated in detail.

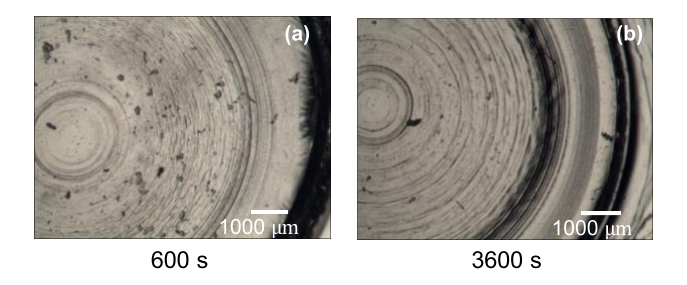


Fig. 4-10 Surface images of the PVA gels after sliding tests, where they were slid against the glass substrate with surface roughness, $R_z = 53 \mu m$. The sliding time were (a) 600 and (b) 3600 seconds, respectively.

To examine the relation of wear amount and friction or normal load in detail, the plot in which the wear amount is on the vertical axis and the product of friction force F and sliding distance l, calculated as $F \cdot l = \sum_i f_i(t_i) \cdot \Delta t \cdot v$, is on the horizontal axis is presented in Fig. 4-9(b). The $f_i(t_i)$ is the friction force at the sliding time $t = t_i$, Δt is the data acquisition time, and v is the sliding velocity. In the system where the gel slid against the rough glass, the result was consistent with the classical wear model in which the wear amount is proportional to the product of friction and sliding distance (Eq. 4-1). The fact that the results of Flat on rough glass fit well with Eq. 4-1 means that the friction and wear behavior of this system is as follows:

- 1. The asperity of the glass substrate makes firm contact with the gel, also the gel is in contact with almost the entire glass surface until it reaches the bottom of the asperity because the gel is sufficiently compressed. Then, the contact area of the gel and the glass substrate with the asperity becomes smaller as the load decreases with the volume loss of gels due to wear.
- 2. Friction is dominated by the resistance of gel/glass, and the viscous resistance of lubricant is small because the system is not lubricated, due to the firm contact of gels and glass asperity.
- 3. Wear particles are easily released into the lubricant, and the rate of transfer to the glass or the gel itself is small.

Also, the results of the wear amount follow Eq. 4-2 well, and the plot is presented in Fig. 4-11.

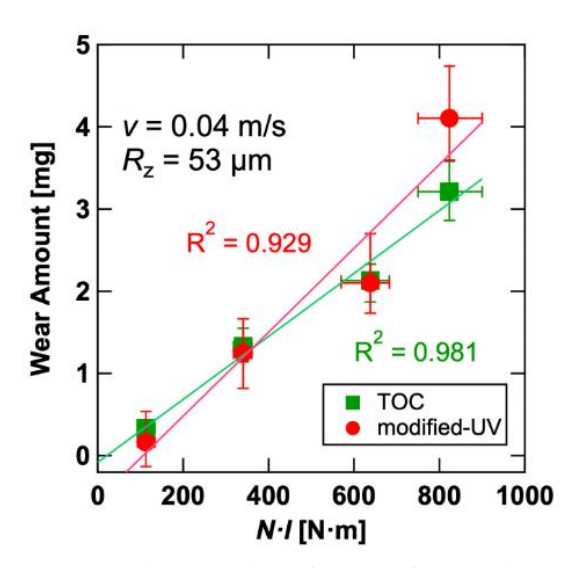


Fig. 4-11 Relation of wear amount and the product of normal force and the sliding distance for the test Flat slid against the glass substrate with surface roughness, $R_z = 53 \mu m$. Straight-line fitting is performed and the coefficient of determination R^2 values are shown. Error bars indicate maximum and minimum values of 3 tests.

The product of normal force N and sliding distance l, calculated as $\sum_i n_i(t_i) \cdot \Delta t \cdot v$, is on the horizontal axis, where the $n_i(t_i)$ is the normal force at the sliding time $t = t_i$. The measured wear amount is approximately consistent with Eq. 4-2, which is derived from the classical wear model.

We would like to claim that the results are consistent with the classical wear model because this method accurately measures the wear particles in the lubricant. In particular, the TOC indicated a remarkable linearity in Fig. 4-9(b), suggesting that the wear amount can be accurately quantified. In addition, the linear approximation equation for TOC with a small intercept suggests that the effect of contamination on TOC in this measurement system is very small.

The relationship between the surface roughness of the substrate and the specific wear rate is shown in Fig. 4-12. The specific wear rate is defined as the value at which the weight of the PVA (polymer) contained in the lubricant is divided by the total sliding distance. As shown in Fig. 4-12(a), the specific wear rate increased as the surface roughness of the substrate increased, and the rate of change gradually decreased. It is known that the wear rate is proportional to the surface roughness, and this trend is observed for metals⁸⁹, polyethylene¹⁰¹, and rubber in lubricant¹⁰⁰. The results shown in Fig. 4-12(a) depend on the fact that the volume that can be ground is large because the contact area between the gel and the glass is large as the surface roughness of the substrate increases. The larger the surface roughness, the easier it is for the contact area to change with stress relaxation. Therefore, the specific wear rate changes moderately as the surface roughness gets larger.

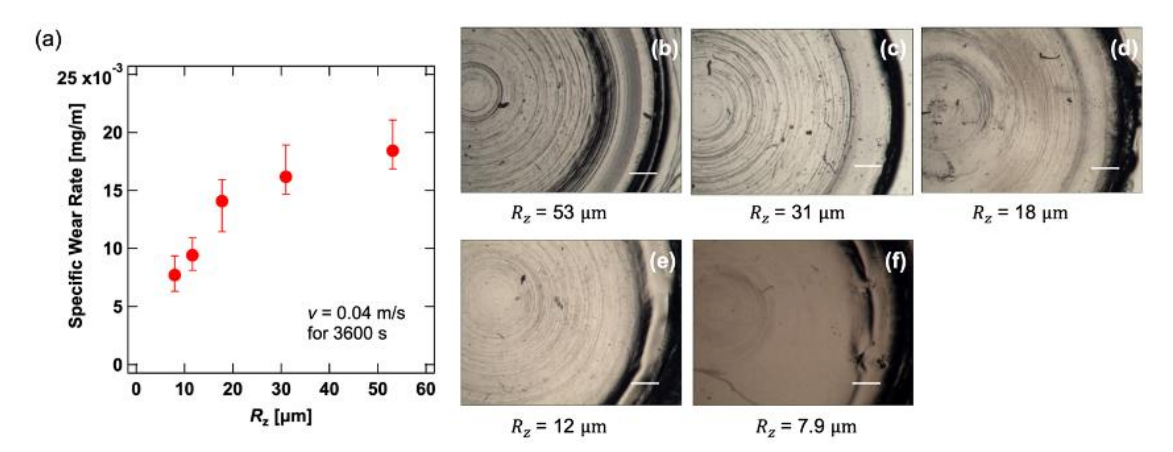


Fig. 4-12 Results of the sliding tests slid against the glass substrate with various surface roughness. (a) Surface roughness, R_z , dependence of specific wear rate. Error bars indicate maximum and minimum values of 3 tests. (b–f) Surface images of the PVA gels after the wear tests. Each gel slid against the glass substrate with different surface roughness, R_z , shown under each image. Scale bar: 1 mm.

The microscopic images taken after the tests (Fig. 4-12(b)-(f)) also show that the sample slid against the substrate with a larger surface roughness was more severely worn. However, the friction stress did not show a clear correlation between the size of the surface roughness on the substrate and the specific wear rate (Fig. 4-13).

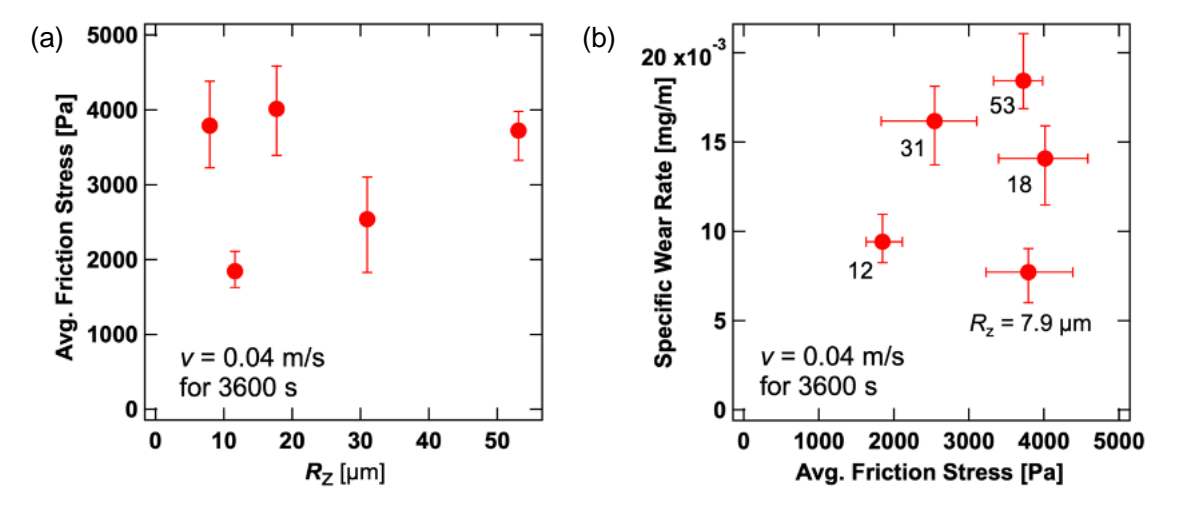


Fig. 4-13 Wear results for the tests Flat slid against the glass substrate with various surface roughness, R_z . (a) Relation of average friction stress and the surface roughness R_z of the substrate. (b) Relation of specific wear rate and average friction stress. The number in the figure means the R_z value of the substrate used in each measurement. Error bars indicate maximum and minimum values of 3 tests.

4-3-2-2 Gel vs. flat hydrophobic glass

Next, the results for the hydrophobically treated glass substrate with a flat surface used as the counter substrate of the gel will be described. The schematics of the system are shown in Fig. 4-14. In this system, two kinds of gels, Flat and Dimpled, were used. It is predicted that mostly adhesive wear occurs because the substrate with a flat surface was used, unlike the case the rough substrate was used.

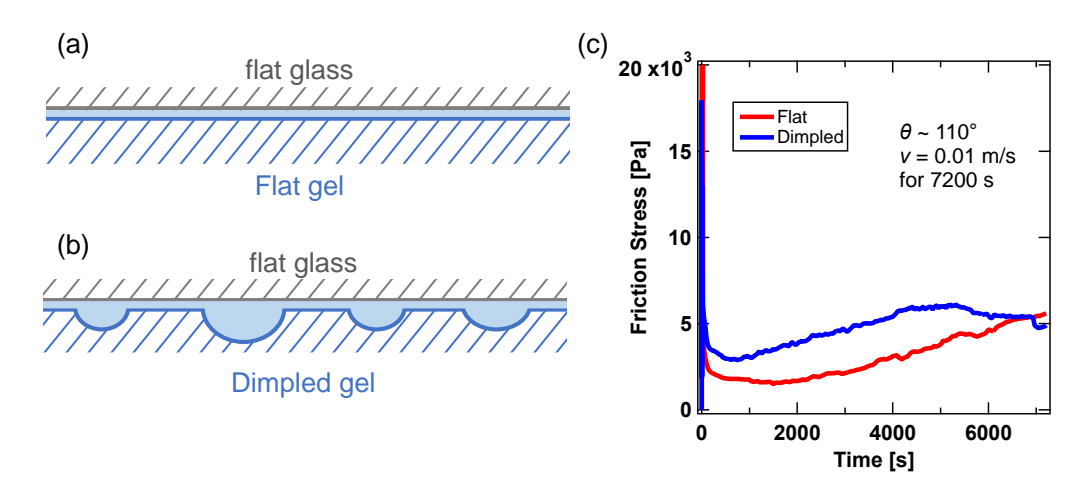


Fig. 4-14 Illustrations of gel/glass interfaces and the result of the sliding test. Schematic of (a) Flat gel/flat glass and (b) Dimpled gel/flat glass. (c) Representative examples of sliding time variation of friction stress. Gels, Flat and Dimpled, slid against FDTS-treated flat glass for 7200 seconds.

For almost all the measurement time, the friction stress of Flat was slightly lower than Dimpled (Fig. 4-14(c)). Also, for a very short time at the beginning of the movement, Dimpled shows higher friction, and its effect on wear is unclear but expected to be small. The graphs for the ratio of the friction stress of Flat to that of Dimpled over the entire measurement time and at the very beginning of the measurement are shown in Fig. 4-15.

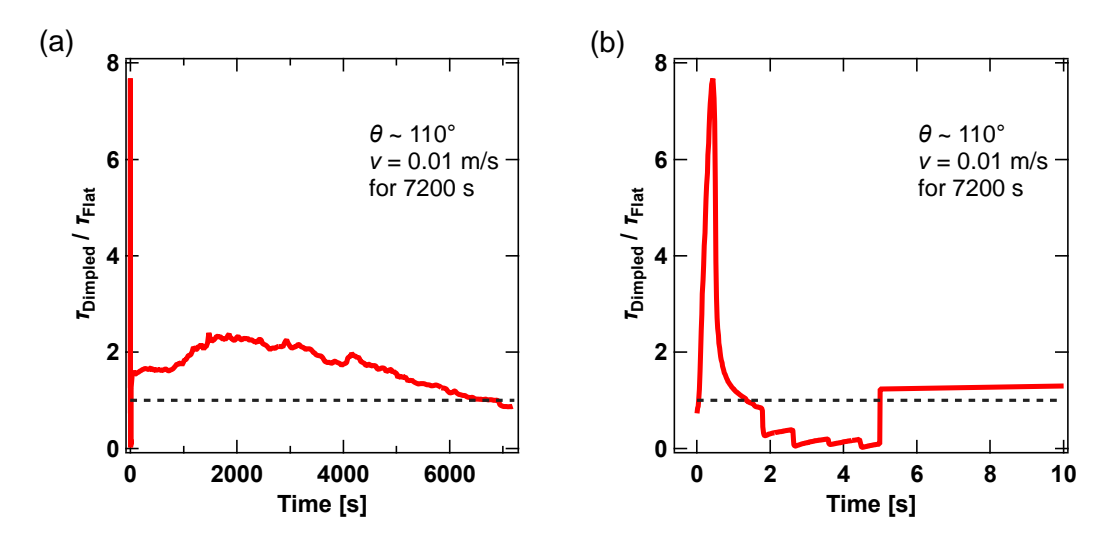


Fig. 4-15 Representative examples of sliding time variation of friction stress. Gels, Flat and Dimpled, slid against FDTS-treated flat glass for 7200 seconds. The vertical axis indicates the relative value of friction stress between Flat and Dimpled. The horizontal axis shows (a) all of the measurement time and (b) the initial measurement time of 10 seconds.

The graph shown in Fig. 4-14(c) has been modified to Fig. 4-15(a) to make the difference between Flat and Dimpled clearer and Fig. 4-15(b) to show the time of first movement.

The stage initially moves at v = 0.001 m/s, reaching v = 0.01 m/s after 5 seconds. Dimpled shows significantly higher friction force than Flat at the very beginning, but then does lower friction for about 3 seconds after that.

Dimpled is expected to exhibit lower friction than Flat due to the smaller contact area by the difference in surface geometry, but the measurement results indicate that Flat has lower friction. The reasons for this are considered as follows. When Flat contacts the FDTS-treated hydrophobic substrate, both wetting and dewetting domains are formed by lodging the lubricant water between the gel and the glass substrate³². For Dimpled, it is difficult for a water film to exist between the gel and the glass substrate due to higher pressure at the flat region than that of Flat, this makes firm contact with gel and glass, and the water inside the dimples may be relatively difficult to contribute to lubrication under 28 kPa of normal pressure; hence, it can be said that the effect of lubrication in the high-velocity region is small. These effects are considered to be responsible for the slightly lower friction of Flat compared to Dimpled under the present condition, however, detailed friction mechanism of Dimpled gel needs to be systematically measured under various conditions, which is reported in Chapter 2.

The specific wear rate measured in the tests with Flat and Dimpled sliding against the FDTS-treated glass substrate are displayed in Fig. 4-16. The results of the gel sliding against the other gel are also shown, but they are described later. The specific wear rates adopted in Fig. 4-16 are the values

calculated from the TOC.

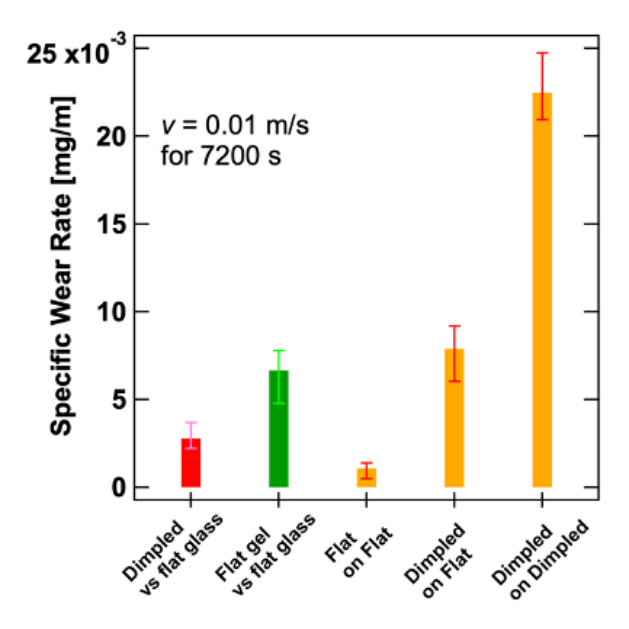


Fig. 4-16 Specific wear rate for the test with different conditions; gels sliding against the FDTS-treated flat and gel sliding against the other gel in the gel-on-gel configuration. Error bars indicate maximum and minimum values of 3 tests.

Although friction stress of Flat was slightly lower than that of Dimpled (Fig. 4-14(c)), the specific wear rate of Flat was higher than that of Dimpled. Since the friction stress does not correspond to the wear amount, it can be seen that the classic wear model cannot be applied to systems with different geometries, Dimpled and Flat. Wear reduction of Dimpled is predicted considering its surface geometry because the contact area of Dimpled is smaller than that of Flat. However, the real contact area under sliding cannot be easily compared because there are both wetting and dewetting domains for Flat, as mentioned earlier. The contact area or normal pressure may define the wear of the gels, but there is no evidence that the difference in the wear amount of Flat and Dimpled is attributed to these parameters.

Annular wear scars were observed concentrically for Flat, but almost no wear scars were observed for Dimpled (Fig. 4-17). From the friction behavior, the microscopic images and the wear evaluation using the lubricant, we predict that the effect of determining the degree of wear is not the contact area or friction, but the ability of the dimples to trap the wear particles into them, as in the case of surface textured metals^{24,68}. The small wear particles generated by the sliding motion are expected to be taken into the dimples, which suppresses further wear of the surface due to the wear particles¹⁰².

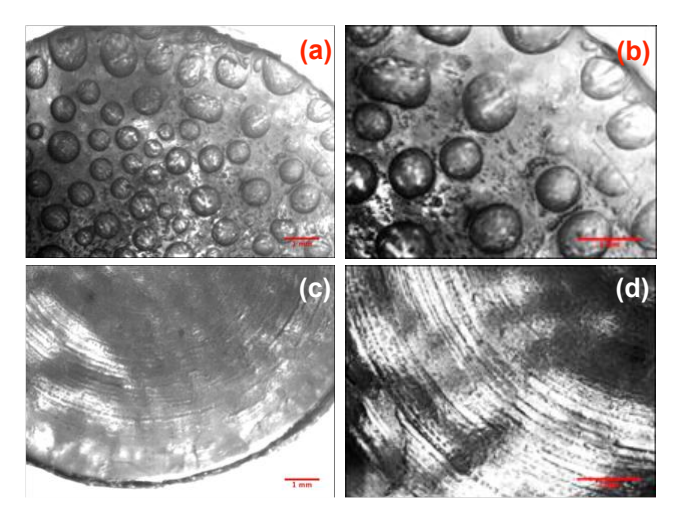


Fig. 4-17 Surface images of the PVA gels after the sliding tests. The test was performed using FDTS-treated flat glasses and lasted 7200 seconds. (a–b) Images of Dimpled surfaces. (c–d) Images of Flat surfaces. Images in the right column were taken in higher magnification than those in the left column. Scale bar: 1 mm.

4-3-2-3 Gel-on-gel

Finally, the results on friction and wear when a gel slides against the other gel are discussed. The sliding tests were conducted under three configurations: Flat-on-Flat, Dimpled-on-Flat, and Dimpled-on-Dimpled, using two types of gels, Flat and Dimpled, which had different surface geometries (Fig. 4-20(a)). The sliding velocity dependency of the friction stress is shown in Fig. 4-18. We evaluated friction and wear of the gels at the sliding velocity of 0.01 m/s for 7200 seconds, in this work.

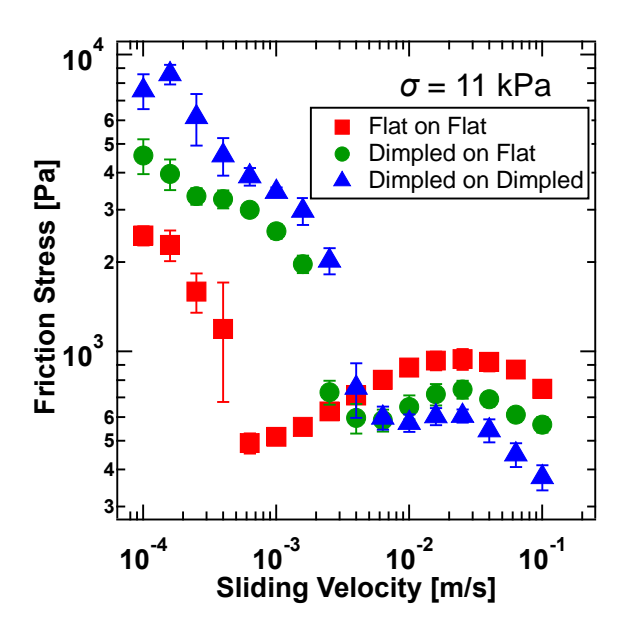


Fig. 4-18 Sliding velocity dependency of friction stress of three types of gel-on-gel configurations, Flat-on-Flat, Dimpled-on-Flat, and Dimpled-on-Dimpled.

We explain the friction of gel-on-gel by dividing the velocity into two regions, the low to medium velocity region ($< 3 \times 10^{-3} \text{ m/s}$) and medium to high velocity region ($> 3 \times 10^{-3} \text{ m/s}$). First, in the relatively low velocity region, Dimpled showed higher friction than Flat. In this region, it is considered that the gels on the upper and lower surfaces are sliding in a state of firm contact because hydrodynamic lubrication at the whole interface is hard to occur. In addition, normal strain at the test was 11, 14, and 13% for Flat-on-Flat, Dimpled-on-Flat, and Dimpled-on-Dimpled, respectively, so it is expected that Dimpled more strongly contacts the opposite gel compared with Flat. Since the gel is soft and can be easily deformed, it is predicted that the gel on the opposite surface was deformed so as to enter to the dimples of Dimpled, and the gel slid while receiving the deformation resistance, resulting in high friction. Next, the lubrication state was probably reached in the relatively high velocity region. Since Dimpled can be expected to have the effect that the water trapped in the dimples exudes to the interface and contributes as a lubricant, it is considered that Dimpled-on-Dimpled showed the lowest friction.

As in the case of *Gel versus flat hydrophobic glass*, the very beginning friction behavior and relative friction stress are shown in Fig. **4-19**.

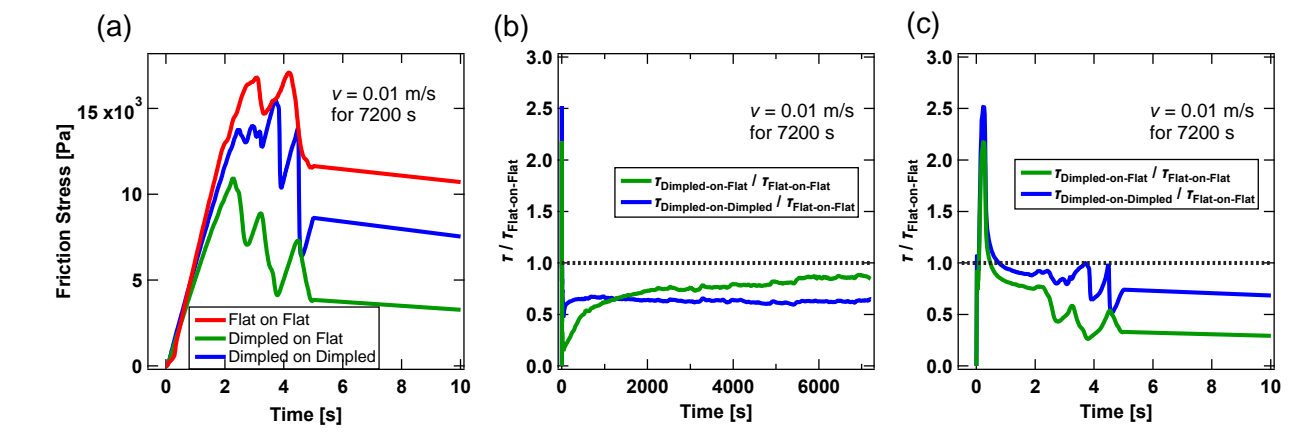


Fig. 4-19 Representative examples of sliding time variation of friction stress for the tests of gel-on-gel configurations. The vertical axis indicates (a) the friction stress, and (b, c) relative value of friction stress with the friction stress of Flat-on-Flat as the denominator. The horizontal axis indicates (a, c) the initial measurement time of 10seconds, and (b) all of the measurement time.

The similar graph as in Fig. **4-15** was applied to the Gel-on-Gel configuration (Fig. 4-20(a)) in Fig. **4-19**. As in the Gel-on-Glass system, Dimpled shows higher friction only for a very short time after the beginning of the sliding motion. As in Fig. **4-15**, the friction stress in this 5 seconds accounts for a very small proportion of the total friction stress.

Fig. 4-20(b) displays the sliding time dependence of the friction stress, and Fig. 4-16 shows the specific wear rate. For these measurement conditions, both the upper and lower gels were worn, as shown in Fig. 4-20(c)–(h); therefore, the specific wear rate shown in Fig. 4-16 is the sum of the wear of PVA released from both gels. Comparing the sliding friction, the friction stress was higher in the order of Flat-on-Flat, Dimpled-on-Flat, and Dimpled-on-Dimpled. However, the wear was larger in the reverse order, that is, Dimpled-on-Dimpled, Dimpled-on-Flat, and Flat-on-Flat. In addition, the optical microscope images revealed that there were more severe wear scars on the surface of Flat, but there were few wear scars on the surface of Dimpled.

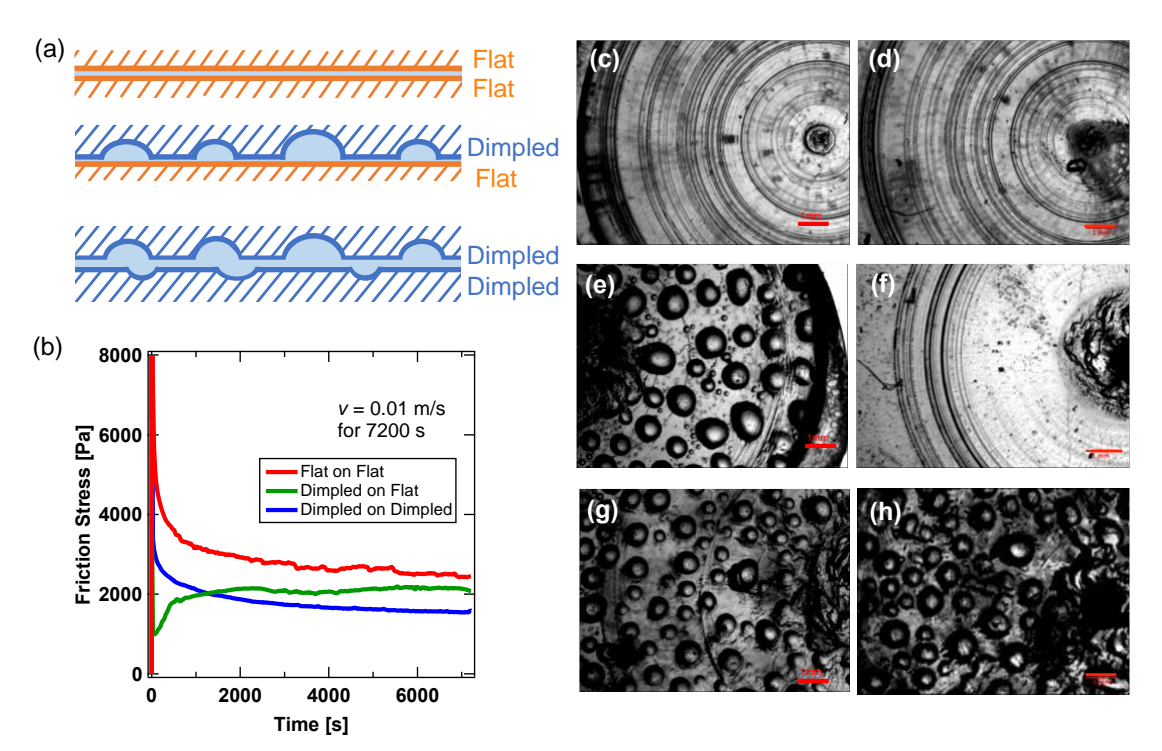


Fig. 4-20 Illustration and results for the sliding test performed in gel-on-gel configurations. (a) Schematic of three types of gel-on-gel configurations. (b) Representing examples of sliding time dependence of friction stress for the tests of three types of gel-on-gel configurations. (c—h) Optical microscope surface images of the PVA gels taken after the sliding tests. The tests were performed for the configurations of Flat-on-Flat (c, d), Dimpled-on-Flat (e, f), and Dimpled-on-Dimpled (g, h). The images in the left column show the upper gels and the images in the right column show the lower gels. Scale bar: 1 mm.

The results for Flat-on-Flat shown in Fig. 4-16 and Fig. 4-20 were counter-intuitive, showing higher friction and more severe wear scars than Dimpled-on-Flat and Dimpled-on-Dimpled, but the wear amount derived from PVA released from the gel surface in the lubricant (wear particles) was very low. Friction for the configuration of gel-on-gel will be explained as below. The most influential effect for the higher friction of Flat-on-Flat compared with Dimpled-on-Flat or Dimpled-on-Dimpled is predicted to be the high contact ratio because the contact ratio is reduced for the latter two configurations due to the surface dimples of Dimpled. From the presence of wear scars, it is clear that friction occurs in the condition that the gel is in contact with each other, and the difference in contact area affects the friction. Since they are sliding in a relatively high velocity region, partial lubrication is also expected to occur, and the viscous resistance due to lubrication is also predicted to be higher in Flat-on-Flat than in Dimpled-on-Flat or Dimpled-on-Dimpled, because the water in surface dimples of Dimpled behaves like a thick lubricating layer, and the viscous resistance does not increase, considering Newton's law of viscosity.

Regarding the wear, the wear amount of Flat-on-Flat was the smallest among all the combinations, including Flat vs. flat glass, although the friction was highest in gel-on-gel configuration and severe wear scars were generated. This result indicates that, unlike the case of abrasive wear, most of the wear particles are not released into the lubricant, but deform the surface and/or transfer to the upper and lower gels as they grow larger (Fig. 4-21(a)). This effect is expected to occur because the gel is flat and soft on both sides, making it easy to contact with each other firmly, and there is no pathway for the particles to be released into the lubricant.

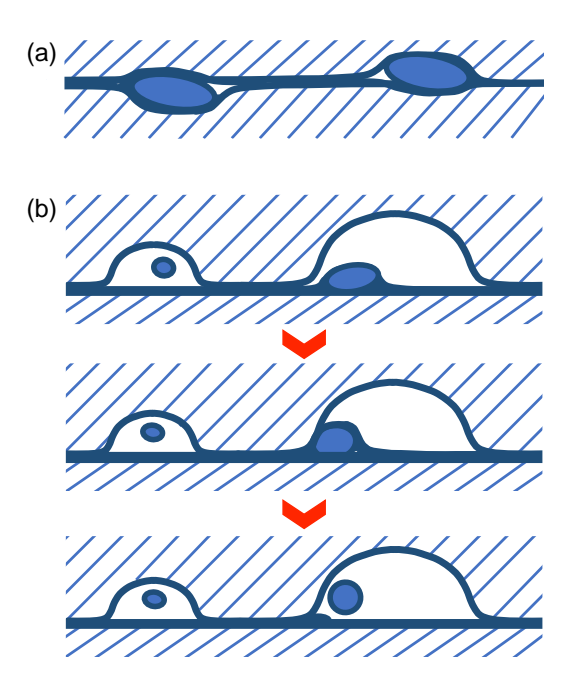


Fig. 4-21 Schematic of (a) Flat/Flat and (b) Dimpled/Flat interfaces. (a) Most of the wear particles are not released into the lubricant and deform the gel surfaces. (b) Generated wear particles are scraped by the dimples on the counter surface.

Comparatively, Dimpled increased the wear amount when the counter substrate was gels, and the wear amount was the highest for Dimpled-on-Dimpled. One of the reasons for this result is that the gel is soft and easily deformed, the surface of the gel on one side probably enters the dimples of the gel on the opposite side, and wear is likely to occur at the edges of the dimples. Furthermore, the more effective and plausible reason is as follows: when wear particles are generated on the surface, they are considered to be scraped by the dimple's edges, and they are moved from the gel surface to the lubricant (Fig. 4-21(b)). Scraping with dimples' edges is expected to release the generated small particles into the lubricant much more efficiently than the case of Flat, therefore, the evaluated wear amount in the lubricant increased. We also predict that the observed wear scars were reduced because

the wear particles are less likely to grow large on the gel surface. In particular, the configuration of Dimpled-on-Dimpled has the largest number of dimples compared with other configurations, therefore, it is considered to have the largest wear amount and the minimum wear scars due to the scraping effect. The meaning of "scrape" in this paper is that the dimples on Dimpled merely take the wear particles into them and make the counter surface planar; not that the dimples generate new wear scars on the counter surface. In the case of Dimpled sliding against a flat glass substrate, fewer wear scars were observed and the wear amount was small compared with the case of Flat gel sliding against the flat glass substrate. In this system, scraping of the counter gel does not occur, and thus the result is appropriate.

Fig. 4-22 shows the similar plot of wear amount versus the product of the friction force and the sliding distance as shown in Fig. 4-9(b). Unlike the case of abrasive wear using rough glass, this figure shows that it is impossible to predict the concentration of wear particles released into the lubricant from the friction force when the gel has surface dimples or when the gel slides against the gel. Moreover, we have already shown that these results are not predictable from the observed severity of wear scars. In contrast to the classical model, which assumes simple adhesive or abrasive wear, the effects of trapping and scraping of wear particles by surface dimples have a much larger effect on the particle concentration than the magnitude of sliding friction between gel and substrate. Also, one possibility is that the results suggest that the wear amount is inversely proportional to the frictional energy, *Fl*, but further investigation is needed to clarify this.

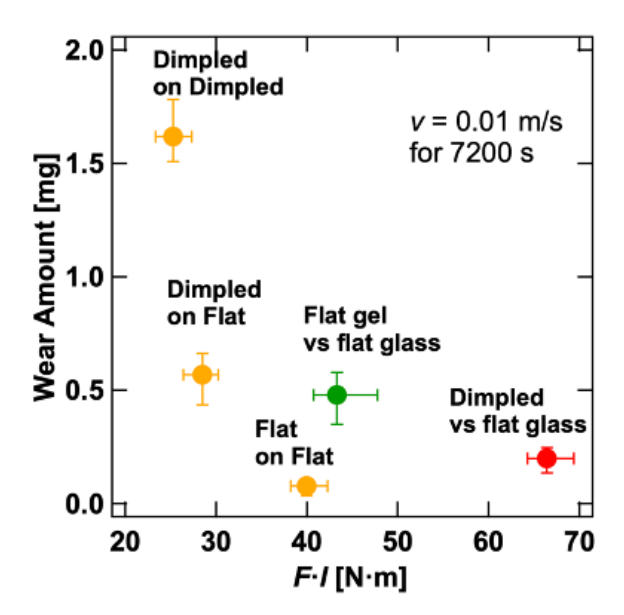


Fig. 4-22 Relation of wear amount and the product of the friction force and the sliding distance. Error bars indicate maximum and minimum values of 3 tests.

4-4 Conclusion

In this work, the wear of poly(vinyl alcohol) (PVA) gels could be evaluated quantitatively using two methods, UV spectrometry and total organic carbon (TOC) measurement, with a polymer solution derived from the lubricant containing the wear particles of the worn gels after the sliding test. For UV spectrometry, the range limitation of the detectable concentration is higher than that of the TOC measurement, but it has the advantage that the sample can be recovered and measured quickly. It would be able to perform more precise measurements for PVA gels prepared using PVA polymers with a lower degree of saponification. TOC measurement is also able to evaluate the wear with a lower measurable concentration limit than UV spectrometry, down to approximately 2×10^{-4} wt%. Although sample solutions cannot be recovered, TOC is useful to measure the very low wear of gels.

The results of the wear amount measurements using PVA gels with dimpled surface (Dimpled) and gels with flat surface (Flat) indicated that the wear amount was smaller for Dimpled when a flat glass was used as the friction substrate, and that the wear amount was larger for Dimpled in the configuration of gel-on-gel.

The traditional methods used for wear analysis, such as observation by optical microscope, can only evaluate the degree of deformation on the worn gel surface. It is possible to evaluate the wear amount quantitatively by measuring the lubricant, so we can distinguish the wear mode, which means that the surface is deformed by wear or the surface is damaged by releasing wear particles.

UV spectrometry can be used to detect the wear particles of the gel composed of not only PVA but also other polymers that have any specific absorbance within the measuring wavelength range, such as polymers with aryl groups in their backbone. In addition, as TOC measurement is a method to quantify the amount of carbon in the solution, almost all the polymers composed of organic carbon can be detected as with PVA. However, in any measurement when the wear particles of the gel are not homogeneously dispersed, the measurement accuracy may decrease. Therefore, just as the measurements in this work, crosslinks of the gels made of other polymers may also need to be unlinked. For instance, the addition of an acid or base that does not contain organic carbon or UV irradiation can be considered. It may be easy for gels with reversible cross-linking points, such as cross-linking by Schiff bases.

In this study, we could confirm the usefulness of the wear evaluation methods using UV spectrometry or total organic carbon measurement in the lubricant which contains wear particles. However, the relationship between friction and wear has still been unclear. When considering the application of gel

to products, reducing wear leads to a longer life of the product. Therefore, it is necessary to achieve low wear and adjust the surface friction required for the use of the product. Therefore, we would like to utilize these methods to repeatedly perform friction tests and wear evaluations and conduct a systematic investigation. In addition, among the few wear evaluations conducted in this study, high wear was shown due to the edge part of the dimple. Therefore, if a smoother dimple shape can be given to the edge shape, it may be possible to reduce wear, so we would like to verify the effect of this edge shape as well.

Conclusions

The surface geometry affects the surface properties of solid materials like metal, but there were few studies that systematically investigated the influence of the surface geometry of gels. For example, our living cartilage, which is in the hydrogel state, has hemispherical surface dimples, but their role and the friction mechanism of joints that show quite low friction are still unclear. In this study, we prepared the hydrogel with some dimples on the surface, and then investigated the tribological properties, such as friction, adhesion, and wear. Using the method that changes the surface shape by water droplets, applied to the Polydimethylsiloxane (PDMS)^{29,30}, we could prepare some kinds of Poly(vinyl alcohol) (PVA) hydrogels with various sizes of hemispherical dimples on their surface. Then, we evaluated the effects of the surface shape on the tribological properties of gels against the glass substrate. As the summary of this study, we state the conclusions as below.

In Chapter 1, we prepared PVA gel with hemispherical dimples on the surface (Dimpled gel) and evaluated the contact state or adhesion property against the glass substrate, combining the *in situ* observation of the interface³¹. The diameter and the depth of the surface dimples were distributed but in similar shapes.

For this surface geometry, two effects were confirmed: (i) the dimple shapes were maintained under compression, so the contact area between the gel and the glass was reduced, and (ii) the water in dimples did almost not sustain the load compared with the other flat contact region and the local contact pressure of Dimpled gel was higher than that of the gel with flat surface (Flat gel).

In the adhesion tests of PVA gels against the glass substrates, the work of adhesion of the gel against the substrate with the contact angle of $\theta \sim 70^{\circ}$, which has similar surface energy to the gel and is considered to make the most stable contact, was the highest. The work of adhesion for Dimpled tended to be lower than that for Flat on any substrates with different wettability. This may be attributed to the small contact area of Dimpled and the glass, and also the promotion of the detaching by invasion of water trapped in dimples to the interface.

In Chapter 2, how the wettability of the counter substrate for the friction measurement influenced the friction behavior of gels with surface dimples (Dimpled) was investigated. As a result of friction measurement, the friction behavior of Flat gel was consistent with the previous study³², and we confirmed that the behavior of Dimpled gel was also varied with the surface wettability of the counter glass substrate. Especially on the substrate with the contact angle to water $\theta \sim 110^{\circ}$, the friction stress of Dimpled tended to be lower than that of Flat in a wide range of sliding velocities.

As predicted from the surface shape of the gels, the contact area at the gel/glass interface was reduced and lubrication occurred by the water trapped in dimples supplied to the interface, so the friction stress of Dimpled have decreased. The latter effect was confirmed by in situ observation using a high-speed camera, where water invaded the interface of the flat area on Dimpled gel, leaving a trajectory of rotational motion, which was the same motion as sliding. Though the surface of Dimpled gel with relatively small dimples was also observed in situ, the pattern shape was too small to recognise and analyse. It might be possible to observe the micro-lubrication behavior in the low-velocity region if we could use an optical system with higher magnification and shallower depth of field and explain the exact reason why Dimpled with small dimples showed lower friction stress, but this is the future topic of discussion. Besides, we showed that Dimpled gel had the smaller friction stress than Flat gel, but it has not been clear what parameters of the dimple shape contribute to low friction. If this could be clarified, important knowledge would be gained in the surface design of low-friction and low-wear gels. Possible parameters include the diameter, depth, perimeter, density, and distribution of the dimple shape. Therefore, in the future study, we would like to create gels using a mold in which these parameters are more controlled, and conduct similar friction and wear tests to understand the role they play.

In Chapter 3, we investigated how the elastic moduli of gels with surface dimples affect their friction behavior. We could prepare PVA gels with different elastic moduli by changing the PVA polymer concentration for the solution for gelation or applying the dry-anneal method³⁴. Regarding the friction behavior, the influence of the surface dimple clearly appeared for the gel with lower modulus, that the friction stress was decreased. This might be because the surface was easy to deform under the shear motion, and the water trapped in dimples was supplied as a lubricant to the interface. On the contrary, the influence of the surface dimples on the work of adhesion did not appear well. However, it may need to change the measurement condition depending on the moduli of the gel, we would like to conduct another examination and systematically discuss the effects of the elastic moduli and the surface geometry.

In Chapter 4, we reported the wear evaluation of PVA gels. The traditional methods used for wear analysis, such as observation by optical microscope, were the qualitative evaluation, which can only evaluate the degree of deformation on the worn gel surface^{35–37}. However, in this study, we quantitatively evaluated the wear particles of the worn gel in lubricants by the measurements of the UV spectrum and the total organic carbon (TOC). Combining the TOC measurement, which has a comparatively low measurement limit, and the UV spectrum measurement, which has a comparatively high measurement limit, we could evaluate low to high degrees of wear.

The results of the wear amount measurements using PVA gels with dimpled surface (Dimpled) and gels with flat surface (Flat) indicated that the wear amount was smaller for Dimpled when a flat glass was used as the friction substrate, and that the wear amount was larger for Dimpled in the configuration of gel-on-gel, where gel slid against the other gel.

The sample gel itself can be influenced by swelling or drying after the wear test, so it is difficult to maintain and evaluate the worn state, but the methods we conducted could eliminate those influences because the lubricant was used. In addition, the measurement can be conducted for a relatively short time and repeatedly, so it can be said that these methods are superior to wear evaluations, which use the sample gel.

In this study, we investigated the influence of the surface hemispherical dimples on the tribological properties of PVA gels. Friction and wear of gels against the glass substrate were lower than the gel with a flat surface. Hereafter, it is expected the applications of hydrogels in various cases, such as the bio- or medical field. Therefore, it is very valuable to understand the relationship between the surface geometry of gels and the tribological properties.

However, in this study, we only investigated the four kinds of PVA gels with different sizes of surface dimples. In future studies, we would like to study whether the smaller or larger dimples, than we have used, have similar effects on the tribological properties. Then, the relationship between friction and wear is not clear. When considering the application of gel to products, reducing wear leads to a longer life of the product. Therefore, it is necessary to achieve low wear and adjust the surface friction required for the use of the product. In this study, we showed that UV spectrometry and total organic carbon measurement of lubricant are effective for quantitative wear evaluation of PVA gel. However, it cannot be said that sufficient friction and wear measurements have been conducted. Therefore, we would like to utilize these methods to perform friction tests and wear evaluations and conduct a systematic investigation. In addition, among the few wear evaluations conducted in this study, high wear was shown due to the edge part of the dimple. Therefore, if a smoother dimple shape can be given to the edge shape, it may be possible to reduce wear, so we would like to verify the effect of this edge shape as well.

Besides, though we selected physically crosslinked PVA gel as a common and durable hydrogel which can withstand some tribological tests, it is unclear whether similar results are obtained or whether the same theoretical concept could be applied in various tribological measurements, especially in the wear testing method, for gel composed from the other chemicals, so we would

also like to confirm the generality for the tribological properties of gels with surface dimples.

References

- (1) Schallamach, A. A Theory of Dynamic Rubber Friction. *Wear* **1963**, *6* (5), 375–382. https://doi.org/10.1016/0043-1648(63)90206-0.
- (2) A.R.Savkoor. ON THE FRICTION OF RUBBER. Wear 1965, 8, 222–237.
- (3) Ludema, K. C.; Tabor, D. The Friction and Visco-Elastic Properties of Polymeric Solids. *Wear* **1966**, *9*, 329–348. https://doi.org/10.1016/0043-1648(66)90018-4.
- (4) Leonov, A. I. On the Theory of the Adhesive Friction of Elastomers. **1986**, *108*, 105–138.
- (5) Persson, B. N. J.; Volokitin, A. I. Theory of Rubber Friction: Nonstationary Sliding. *Phys. Rev. B Condens. Matter Mater. Phys.* **2002**, *65* (13), 1–11. https://doi.org/10.1103/PhysRevB.65.134106.
- (6) Persson, B. N. J. Theory of Rubber Friction and Contact Mechanics. J. Chem. Phys. 2001, 115 (8), 3840–3861. https://doi.org/10.1063/1.1388626.
- (7) Gong, J. P. Friction and Lubrication of Hydrogels-Its Richness and Complexity. *Soft Matter* **2006**, 2 (7), 544. https://doi.org/10.1039/b603209p.
- (8) Kakugo, A.; Gong, J.; Osada, Y. Friction and Lubrication of Hydrogel. *Biophys. Biopgisicology Japanese* **2007**, *47* (4), 253–258. https://doi.org/10.2142/biophys.47.253.
- (9) Nguyen, Q. T.; Wong, B. L.; Chun, J.; Yoon, Y. C.; Talke, F. E.; Sah, R. L. Macroscopic Assessment of Cartilage Shear: Effects of Counter-Surface Roughness, Synovial Fluid Lubricant, and Compression Offset. *J. Biomech.* 2010, 43 (9), 1787–1793. https://doi.org/10.1016/j.jbiomech.2010.02.014.
- (10) Yashima, S.; Takase, N.; Kurokawa, T.; Gong, J. P. Friction of Hydrogels with Controlled Surface Roughness on Solid Flat Substrates. Soft Matter 2014, 10 (18). https://doi.org/10.1039/C3SM52883A.
- (11) Tominaga, T.; Kurokawa, T.; Furukawa, H.; Osada, Y.; Gong, J. P. Friction of a Soft Hydrogel on Rough Solid Substrates. *Soft Matter* **2008**, *4* (8), 1645–1652. https://doi.org/10.1039/b802568a.
- (12) Arakaki, K.; Kitamura, N.; Fujiki, H.; Kurokawa, T.; Iwamoto, M.; Ueno, M.; Kanaya, F.; Osada, Y.; Gong, J. P.; Yasuda, K. Artificial Cartilage Made from a Novel Double-Network Hydrogel: In Vivo Effects on the Normal Cartilage and Ex Vivo Evaluation of the Friction Property. *J. Biomed. Mater. Res. Part A* 2010, 93 (3), 1160–1168. https://doi.org/10.1002/jbm.a.32613.
- Murakami, T.; Yarimitsu, S.; Nakashima, K.; Yamaguchi, T.; Sawae, Y.; Sakai, N.; Suzuki, A. Superior Lubricity in Articular Cartilage and Artificial Hydrogel Cartilage. *Proc. Inst. Mech. Eng. Part J-Journal Eng. Tribol.* 2014, 228 (10), 1099–1111. https://doi.org/10.1177/1350650114530273.
- (14) Bodugoz-Senturk, H.; Macias, C. E.; Kung, J. H.; Muratoglu, O. K. Poly(Vinyl Alcohol)—Acrylamide Hydrogels as Load-Bearing Cartilage Substitute. *Biomaterials* **2009**, *30* (4), 589–596. https://doi.org/10.1016/J.BIOMATERIALS.2008.10.010.
- (15) Arakaki, K.; Kitamura, N.; Fujiki, H.; Kurokawa, T.; Iwamoto, M.; Ueno, M.; Kanaya, F.; Osada,

- Y.; Gong, J. P.; Yasuda, K. Artificial Cartilage Made from a Novel Double-Network Hydrogel: In Vivo Effects on the Normal Cartilage and Ex Vivo Evaluation of the Friction Property. **2009**. https://doi.org/10.1002/jbm.a.32613.
- (16) Ling, D.; Bodugoz-senturk, H.; Nanda, S.; Braithwaite, G. Quantifying the Lubricity of Mechanically Tough Polyvinyl Alcohol Hydrogels for Cartilage Repair. 2015, 229 (12), 845–852. https://doi.org/10.1177/0954411915599016.
- (17) Pitenis, A. A.; Urue, J. M.; Nixon, R. M.; Krick, B. A.; Dunn, A. C.; Angelini, T. E.; Sawyer, W.
 G. Lubricity from Entangled Polymer Networks on Hydrogels. 2016, 138 (October), 1–4. https://doi.org/10.1115/1.4032889.
- (18) Kavehpour, H. P.; McKinley, G. H. Tribo-Rheometry: From Gap-Dependent Rheology to Tribology. *Tribol. Lett.* **2004**, *17* (2), 327–335. https://doi.org/10.1023/B:TRIL.0000032471.06795.ea.
- (19) Li, A.; Benetti, E. M.; Tranchida, D.; Clasohm, J. N.; Schönherr, H.; Spencer, N. D. Surface-Grafted, Covalently Cross-Linked Hydrogel Brushes with Tunable Interfacial and Bulk Properties. *Macromolecules* 2011, 44 (13), 5344–5351. https://doi.org/10.1021/ma2006443.
- (20) Lawless, B. M.; Sadeghi, H.; Temple, D. K.; Dhaliwal, H.; Espino, D. M.; Hukins, D. W. L. Viscoelasticity of Articular Cartilage: Analysing the Effect of Induced Stress and the Restraint of Bone in a Dynamic Environment. *J. Mech. Behav. Biomed. Mater.* 2017, 75 (May), 293–301. https://doi.org/10.1016/j.jmbbm.2017.07.040.
- (21) Persson, B. N. J.; Scaraggi, M. Some Comments on Hydrogel and Cartilage Contact Mechanics and Friction. *Tribol. Lett.* **2018**, *66* (1), 1–6. https://doi.org/10.1007/s11249-017-0973-y.
- (22) Cha, W.-I.; Hyon, S.-H.; Oka, M.; Ikada, Y. Mechanical and Wear Properties of Poly(Vinyl Alcohol) Hydrogels. *Macromol. Symp.* **1996**, *109* (1), 115–126. https://doi.org/10.1002/masy.19961090111.
- (23) Takahashi, K.; Berengueres, J. O. L.; Obata, K. J.; Saito, S. Geckos' Foot Hair Structure and Their Ability to Hang from Rough Surfaces and Move Quickly. *Int. J. Adhes. Adhes.* **2006**, *26* (8), 639–643. https://doi.org/10.1016/j.ijadhadh.2005.12.002.
- (24) Segu, D. Z.; Wang, L.-L.; Hwang, P.; Kang, S.-W. Experimental Characterization of Friction and Wear Behavior of Textured Titanium Alloy (Ti-6Al-4V) for Enhanced Tribological Performance. *Mater. Res. Express* **2021**, *8* (8), 085008. https://doi.org/10.1088/2053-1591/ac1ae6.
- (25) Putignano, C.; Parente, G.; Profito, F. J.; Gaudiuso, C.; Ancona, A.; Carbone, G. Laser Microtextured Surfaces for Friction Reduction: Does the Pattern Matter? *Materials (Basel)*. 2020, 13 (21), 1–21. https://doi.org/10.3390/ma13214915.
- (26) Ikada, Y. Surface Modification of Polymers for Medical Applications. *Biomaterials* **1994**, *15* (10), 725–736. https://doi.org/10.1016/0142-9612(94)90025-6.
- (27) Teo, A. J. T.; Mishra, A.; Park, I.; Kim, Y. J.; Park, W. T.; Yoon, Y. J. Polymeric Biomaterials for

- Medical Implants and Devices. *ACS Biomater. Sci. Eng.* **2016**, 2 (4), 454–472. https://doi.org/10.1021/acsbiomaterials.5b00429.
- (28) Alexandre, N.; Ribeiro, J.; Gärtner, A.; Pereira, T.; Amorim, I.; Fragoso, J.; Lopes, A.; Fernandes, J.; Costa, E.; Santos-Silva, A.; Rodrigues, M.; Santos, J. D.; Maurício, A. C.; Luís, A. L. Biocompatibility and Hemocompatibility of Polyvinyl Alcohol Hydrogel Used for Vascular Grafting In Vitro and in Vivo Studies. *J. Biomed. Mater. Res. Part A* 2014, 102 (12), 4262–4275. https://doi.org/10.1002/jbm.a.35098.
- Yashima, S.; Romero, V.; Wandersman, E.; Frétigny, C.; Chaudhury, M. K.; Chateauminois, A.; Prevost, A. M. Normal Contact and Friction of Rubber with Model Randomly Rough Surfaces. *Soft Matter* 2015, 11 (5), 871–881. https://doi.org/10.1039/c4sm02346c.
- Biswas, S.; Chakrabarti, A.; Chateauminois, A.; Wandersman, E.; Prevost, A. M.; Chaudhury, M.
 K. Soft Lithography Using Nectar Droplets. *Langmuir* 2015, 31 (48), 13155–13164. https://doi.org/10.1021/acs.langmuir.5b03829.
- (31) Yamamoto, T.; Kurokawa, T.; Ahmed, J.; Kamita, G.; Yashima, S.; Furukawa, Y.; Ota, Y.; Furukawa, H.; Gong, J. P. In Situ Observation of a Hydrogel-Glass Interface during Sliding Friction. *Soft Matter* **2014**, *10*, 5589–5596. https://doi.org/10.1039/c4sm00338a.
- (32) Tominaga, T.; Takedomi, N.; Biederman, H.; Furukawa, H.; Osada, Y.; Gong, J. P. Effect of Substrate Adhesion and Hydrophobicity on Hydrogel Friction. *Soft Matter* 2008, 4 (5), 1033. https://doi.org/10.1039/b716465c.
- (33) Ahmed, J.; Yamamoto, T.; Guo, H.; Kurokawa, T.; Nonoyama, T.; Nakajima, T.; Gong, J. P. Friction of Zwitterionic Hydrogel by Dynamic Polymer Adsorption. *Macromolecules* **2015**, *48* (15), 5394–5401. https://doi.org/10.1021/acs.macromol.5b00602.
- (34) Li, J.; Suo, Z.; Vlassak, J. J. Stiff, Strong, and Tough Hydrogels with Good Chemical Stability. *J. Mater. Chem. B* **2014**, 2 (39), 6708–6713. https://doi.org/10.1039/c4tb01194e.
- (35) Nakashima, K.; Murakami, T.; Sawae, Y. Evaluation of Wear Property of PVA Hydrogel as Artifical Cartilage and Effect of Protein Film on Wear–Resistant Property. *Trans. JSME. C. (in Japanese)* **2004**, 70 (697), 218–225.
- (36) Bonyadi, S. Z.; Dunn, A. C. Compositional Dependence of Polyacrylamide Hydrogel Abrasive Wear Resistance. *ACS Appl. Polym. Mater.* **2020**, 2 (12), 5444–5451. https://doi.org/10.1021/acsapm.0c00769.
- (37) Suciu, A. N.; Iwatsubo, T.; Matsuda, M.; Nishino, T. A Study upon Durability of the Artificial Knee Joint with PVA Hydrogel Cartilage. *JSME International Journal, Series C: Mechanical Systems, Machine Elements and Manufacturing*. 2004, pp 199–208. https://doi.org/10.1299/jsmec.47.199.
- (38) Rao, P.; Sun, T. L.; Chen, L.; Takahashi, R.; Shinohara, G.; Guo, H.; King, D. R.; Kurokawa, T.; Gong, J. P. Tough Hydrogels with Fast, Strong, and Reversible Underwater Adhesion Based on a

- Multiscale Design. Adv. Mater. 2018, 30 (32), 1-8. https://doi.org/10.1002/adma.201801884.
- (39) Fowkes, F. M. Attractive Forces at Interfaces. *Ind. Eng. Chem.* **1964**, *56* (12), 40–52. https://doi.org/10.1021/ie50660a008.
- (40) 三刀基郷. 接着の基礎. 溶接学会誌 2012, 81 (6), 23-27.
- (41) 堤和男. 固体の付着と表面自由エネルギー. 日本複合材料学会誌 1976, 2 (3), 9-15.
- (42) Trieu, H.; Qutubuddin, S. Poly(Vinyl Alcohol) Hydrogels: 2. Effects of Processing Parameters on Structure and Properties. *Polymer (Guildf)*. **1995**, *36* (13), 2531–2539. https://doi.org/10.1016/0032-3861(95)91198-G.
- (43) Hyon, S. H.; Cha, W. I.; Ikada, Y. Preparation of Transparent Poly(Vinyl Alcohol) Hydrogel. *Polym. Bull.* **1989**, 22 (2), 119–122. https://doi.org/10.1007/BF00255200.
- (44) Rasband, W. S. Image J.
- (45) Hui, C. Y.; Lin, Y. Y.; Chuang, F. U. C.; Shull, K. R.; Lin, W. C. A Contact Mechanics Method for Characterizing the Elastic Properties and Permeability of Gels. *J. Polym. Sci. Part B Polym. Phys.* **2006**, *44* (2), 359–370. https://doi.org/10.1002/polb.20613.
- (46) Persson, B. N. J. Sliding Friction-Physical Principles And Applications. Springer 1998, 14 (6).
- (47) Hsieh, S. S.; Li, S. Y.; Hsieh, Y. C. Velocity Measurements in DI Water Flow Microchannels with Hydrophilic and Hydrophobic Surfaces. *Appl. Therm. Eng.* **2017**, *127*, 901–905. https://doi.org/10.1016/j.applthermaleng.2017.08.101.
- (48) Huang, D. M.; Sendner, C.; Horinek, D.; Netz, R. R.; Bocquet, L. Water Slippage versus Contact Angle: A Quasiuniversal Relationship. *Phys. Rev. Lett.* **2008**, *101* (22), 1–4. https://doi.org/10.1103/PhysRevLett.101.226101.
- (49) Vinogradova, O. I. Drainage of a Thin Liquid Film Confined between Hydrophobic Surfaces. Langmuir 1995, 11 (6), 2213–2220. https://doi.org/10.1021/la00006a059.
- (50) Caliari, S. R.; Burdick, J. A. A Practical Guide to Hydrogels for Cell Culture. *Nat. Methods* **2016**, *13* (5), 405–414. https://doi.org/10.1038/nmeth.3839.
- (51) Gull, N.; Khan, S. M.; Islam, A.; Butt, M. T. Z. Hydrogels Used for Biomedical Applications. *Bio Monomers Green Polym. Compos. Mater.* **2019**, *54*, 175–199. https://doi.org/10.1002/9781119301714.ch9.
- (52) Gong, J.; Go, K.; Osada, Y. Friction of Gels. 4. Friction on Charged Gels. *J. Phys. Chem. B* **1999**, *103* (29), 6007–6014. https://doi.org/10.1021/jp990256.
- (53) Tsukeshiba, H.; Huang, M.; Na, Y. H.; Kurokawa, T.; Kuwabara, R.; Tanaka, Y.; Furukawa, H.; Osada, Y.; Gong, J. P. Effect of Polymer Entanglement on the Toughening of Double Network Hydrogels. *J. Phys. Chem. B* **2005**, *109* (34), 16304–16309. https://doi.org/10.1021/jp052419n.
- (54) Nakano, Y.; Kurokawa, T.; Du, M.; Liu, J.; Tominaga, T.; Osada, Y.; Gong, J. P. Effect of Hyaluronan Solution on Dynamic Friction of PVA Gel Sliding on Weakly Adhesive Glass Substrate. *Macromolecules* 2011, 44 (22), 8908–8915. https://doi.org/10.1021/ma201522q.

- (55) Kamada, K.; Furukawa, H.; Kurokawa, T.; Tada, T.; Tominaga, T.; Nakano, Y.; Gong, J. P. Surfactant-Induced Friction Reduction for Hydrogels in the Boundary Lubrication Regime. *J. Phys. Condens. Matter* 2011, 23 (28). https://doi.org/10.1088/0953-8984/23/28/284107.
- (56) Lin, W.; Kluzek, M.; Iuster, N.; Shimoni, E.; Kampf, N.; Goldberg, R.; Klein, J. Cartilage-Inspired, Lipid-Based Boundary-Lubricated Hydrogels. *Science* (80-.). 2020, 338 (October), 335–338.
- (57) Farias, B. V.; Hsiao, L. C.; Khan, S. A. Rheological and Tribological Behavior of Gels and Emulsions Containing Polymer and Phospholipid. *ACS Appl. Polym. Mater.* **2020**, 2 (4), 1623–1633. https://doi.org/10.1021/acsapm.0c00053.
- (58) V.C. Mow; S. C. Kuei; W. M. Lai; C. G. Armstrong. Biphasic Creep and Stress Relaxation of Articular Cartilage in Compression: Theory and Experiments. J. Biomech Eng. 1980, 102 (1), 73– 84. https://doi.org/10.1115/1.3138202.
- (59) Walker, P. S.; Dowson, D.; Longfield, M. D.; Wright, V. "Boosted Lubrication" in Synovial Joints by Fluid Entrapment and Enrichment. *Ann. Rheum. Dis.* **1968**, 27 (6), 512–520. https://doi.org/10.1136/ard.27.6.512.
- (60) McCutchen, C. W. The Frictional Properties of Animal Joints. *Wear* **1962**, *5* (1), 1–17. https://doi.org/10.1016/0043-1648(62)90176-X.
- (61) Caligaris, M.; Ateshian, G. A. Effects of Sustained Interstitial Fluid Pressurization under Migrating Contact Area, and Boundary Lubrication by Synovial Fluid, on Cartilage Friction. *Osteoarthr*. Cartil. 2008, 16 (10), 1220–1227. https://doi.org/10.1016/j.joca.2008.02.020.
- (62) Ateshian, G. A.; Lai, W. M.; Zhu, W. B.; Mow, V. C. An Asymptotic Solution for the Contact of Two Biphasic Cartilage Layers. *J. Biomech.* 1994, 27 (11), 1347–1360. https://doi.org/10.1016/0021-9290(94)90044-2.
- (63) Schmidt, T. A.; Gastelum, N. S.; Nguyen, Q. T.; Schumacher, B. L.; Sah, R. L. Boundary Lubrication of Articular Cartilage: Role of Synovial Fluid Constituents. *Arthritis Rheum.* 2007, 56 (3), 882–891. https://doi.org/10.1002/art.22446.
- (64) Lin, W.; Liu, Z.; Kampf, N.; Klein, J. The Role of Hyaluronic Acid in Cartilage Boundary Lubrication. *Cells* **2020**, *9* (7), 1–14. https://doi.org/10.3390/cells9071606.
- (65) Ito, H.; Kaneda, K.; Yuhta, T.; Nishimura, I.; Yasuda, K.; Matsuno, T. Reduction of Polyethylene Wear by Concave Dimples on the Frictional Surface in Artificial Hip Joints. *J. Arthroplasty* 2000, 15 (3), 332–338. https://doi.org/10.1016/S0883-5403(00)90670-3.
- (66) Wakuda, M.; Yamauchi, Y.; Kanzaki, S.; Yasuda, Y. Effect of Surface Texturing on Friction Reduction between Ceramic and Steel Materials under Lubricated Sliding Contact. Wear 2003, 254 (3–4), 356–363. https://doi.org/10.1016/S0043-1648(03)00004-8.
- (67) Yu, H.; Deng, H.; Huang, W.; Wang, X. The Effect of Dimple Shapes on Friction of Parallel Surfaces. *Proc. Inst. Mech. Eng. Part J J. Eng. Tribol.* 2011, 225 (8), 693–703. https://doi.org/10.1177/1350650111406045.

- (68) Niu, Y.; Pang, X.; Yue, S.; Shangguan, B.; Zhang, Y. The Friction and Wear Behavior of Laser Textured Surfaces in Non-Conformal Contact under Starved Lubrication. Wear 2021, 476 (January), 203723. https://doi.org/10.1016/j.wear.2021.203723.
- (69) Rudge, R. E. D.; Scholten, E.; Dijksman, J. A. Natural and Induced Surface Roughness Determine Frictional Regimes in Hydrogel Pairs. *Tribol. Int.* 2020, 141 (April 2019), 105903. https://doi.org/10.1016/j.triboint.2019.105903.
- (70) Ahmed, J.; Guo, H.; Yamamoto, T.; Kurokawa, T.; Takahata, M.; Nakajima, T.; Gong, J. P. Sliding Friction of Zwitterionic Hydrogel and Its Electrostatic Origin. *Macromolecules* **2014**, *47* (9), 3101–3107. https://doi.org/10.1021/ma500382y.
- (71) Stribeck, R. Kugellager Für Beliebige Belastungen. Zeitschrift des Vereines Dtsch. Ingenieure **1902**, 46, 1341–1348.
- (72) Xiaobin, Lu M.M., Khonsari E.R.M., G. The Stribeck Curve: Experimental Results and Theoretical Prediction. *J. Tribol.* **2006**, *128* (4), 789–794.
- (73) Simič, R.; Yetkin, M.; Zhang, K.; Spencer, N. D. Importance of Hydration and Surface Structure for Friction of Acrylamide Hydrogels. *Tribol. Lett.* **2020**, 68 (2), 1–12. https://doi.org/10.1007/s11249-020-01304-x.
- (74) Jian Ping Gong; Kurokawa, T.; Narita, T.; Kagata, G.; Osada, Y.; Nishimura, G.; Kinjo, M. Synthesis of Hydrogels with Extremely Low Surface Friction [4]. J. Am. Chem. Soc. 2001, 123 (23), 5582–5583. https://doi.org/10.1021/ja003794q.
- (75) Anderst, W. J.; Tashman, S. The Association between Velocity of the Center of Closest Proximity on Subchondral Bones and Osteoarthritis Progression. *J. Orthop. Res.* **2009**, *27* (1), 71–77. https://doi.org/10.1002/jor.20702.
- (76) Taguchi, T. Assembly of Cells and Vesicles for Organ Engineering. *Sci. Technol. Adv. Mater.* **2011**, *12* (6). https://doi.org/10.1088/1468-6996/12/6/064703.
- (77) Liao, I. C.; Moutos, F. T.; Estes, B. T.; Zhao, X.; Guilak, F. Composite Three-Dimensional Woven Scaffolds with Interpenetrating Network Hydrogels to Create Functional Synthetic Articular Cartilage. *Adv. Funct. Mater.* **2013**, *23* (47), 5833–5839. https://doi.org/10.1002/adfm.201300483.
- (78) Matsuoka, T. 弾性表面波法によるポリビニルアルコールゲルの弾性挙動に対する溶媒組成の影響に関する研究. **2010**.
- (79) Takahashi, N.; Kanaya, T.; Koji, N.; Keisuke, K. Effects of Cononsolvency on Gelation of Poly(Vinyl Alcohol) in Mixed Solvents of Dimethyl Sulfoxide and Water. *Polymer (Guildf)*. 2003, 44 (15). https://doi.org/10.1016/S0032-3861(03)00390-2.
- (80) Haque, A.; Kurokawa, T.; Ping, J. Super Tough Double Network Hydrogels and Their Application as Biomaterials. *Polymer (Guildf)*. **2012**, *53* (9), 1805–1822. https://doi.org/10.1016/j.polymer.2012.03.013.
- (81) Nakashima, K.; Murakami, T.; Sawae, Y. 人工軟骨候補材料ポリビニルアルコールハイドロ

- ゲルの摩耗評価及び耐摩耗性向上に寄与する蛋白質の影響. *日本機械学会論文集(C編)* **2004**, 70 (697), 218–225.
- (82) Masri, C.; Chagnon, G.; Favier, D. Influence of Processing Parameters on the Macroscopic Mechanical Behavior of PVA Hydrogels. *Mater. Sci. Eng. C* 2017, 75, 769–776. https://doi.org/10.1016/j.msec.2017.02.045.
- (83) Noguerda, A. E. United States Patent [191. **1998**.
- (84) Means, A. K.; Shrode, C. S.; Whitney, L. V.; Ehrhardt, D. A.; Grunlan, M. A. Double Network Hydrogels That Mimic the Modulus, Strength, and Lubricity of Cartilage. *Biomacromolecules* 2019, 20 (5), 2034–2042. https://doi.org/10.1021/acs.biomac.9b00237.
- (85) Li, F.; Wang, A.; Wang, C. Analysis of Friction between Articular Cartilage and Polyvinyl Alcohol Hydrogel Artificial Cartilage. *J. Mater. Sci. Mater. Med.* **2016**, 27 (5), 1–8. https://doi.org/10.1007/s10856-016-5700-y.
- (86) Centers, P. W.; Price, F. D. Real Time Simultaneous In-Line Wear and Lubricant Condition Monitoring. *Wear* **1988**, *123* (3), 303–312. https://doi.org/10.1016/0043-1648(88)90146-9.
- (87) Atkinson, R. B.; Ellis, S. G. Ferrography. *J. Franklin Inst.* **1951**, 252 (5), 373–381. https://doi.org/10.1016/0016-0032(51)90453-X.
- (88) Thomas, R.; Hasme, K.; Wassmuth, A. Integrated Analysis of In-Service Lubricants for Particle Size and Count and Metal Content in a Single Sample Run. Spectrosc. (Santa Monica) 2020, 35 (3).
- (89) Hisakado, T. The Influence of Surface Roughness on Abrasive Wear. *Wear* **1977**, *41* (1), 179–190. https://doi.org/10.1016/0043-1648(77)90200-9.
- (90) Haiden, C.; Wopelka, T.; Jech, M.; Keplinger, F.; Vellekoop, M. J. A Microfluidic Chip and Dark-Field Imaging System for Size Measurement of Metal Wear Particles in Oil. *IEEE Sens. J.* 2016, 16 (5), 1182–1189. https://doi.org/10.1109/JSEN.2015.2501355.
- (91) Omata, S.; Sawae, Y.; Murakami, T. Effect of Poly(Vinyl Alcohol) (PVA) Wear Particles Generated in Water Lubricant on Immune Response of Macrophage. *Biosurface and Biotribology* **2015**, *I* (1), 71–79. https://doi.org/10.1016/j.bsbt.2015.02.003.
- (92) Nakashima, K.; Sawae, Y.; Murakami, T. Study on Wear Reduction Mechanisms of Artificial Cartilage by Synergistic Protein Boundary Film Formation. *JSME Int. Journal, Ser. C Mech. Syst. Mach. Elem. Manuf.* **2006**, *48* (4), 555–561. https://doi.org/10.1299/jsmec.48.555.
- (93) BLAIKIE, K. G.; CROZIER, R. N. Polymerization of Vinyl Acetate. *Ind. Eng. Chem.* 1936, 28 (10), 1155–1159. https://doi.org/10.1246/nikkashi1948.75.437.
- (94) HAAS, H. C.; HUSEK, H.; TAYLOR, L. D. On the Ultraviolet Absorption Spectrum of Polyvinyl Alcohol. *J. Polym. Sci. Part A* **1963**, *1*, 1215–1226. https://doi.org/10.1085/jgp.17.6.797.
- (95) Ferguson, L. N. Ultraviolet Spectroscopic Studies. **1971**, 639 (V), 1971–1975.
- (96) Archard, J. F. Contact and Rubbing of Flat Surfaces. J. Appl. Phys. 1953, 24 (8), 981–988.

- https://doi.org/10.1063/1.1721448.
- (97) Schallamach, A. Friction and Abrasion of Rubber. *Wear* **1958**, *I* (5), 384–417. https://doi.org/10.1016/0043-1648(58)90113-3.
- (98) Tabor, D. . G. C. G. and S. E. E. Friction between Tyre and Road. *Engineering* **1958**, *186*, 838–842.
- (99) S. B. Ratner; I. I. Farverova; O. V. Radyukevich; E. G. Lue'e. Connection between Wear-Resistance of Plastics and Other Mechanical Properties. *Abrasion Rubber, MacLaren Sons Ltd.* 1967, 145–154.
- (100) Feng, D.; Shen, M. xue; Peng, X. dong; Meng, X. kai. Surface Roughness Effect on the Friction and Wear Behaviour of Acrylonitrile–Butadiene Rubber (NBR) Under Oil Lubrication. *Tribol. Lett.*2017, 65 (1), 1–14. https://doi.org/10.1007/s11249-016-0793-5.
- (101) Saikko, V.; Calonius, O.; Kernen, J. Effect of Counterface Roughness on the Wear of Conventional and Crosslinked Ultrahigh Molecular Weight Polyethylene Studied with a Multi-Directional Motion Pin-on-Disk Device. *J. Biomed. Mater. Res.* **2001**, *57* (4), 506–512. https://doi.org/10.1002/1097-4636(20011215)57:4<506::AID-JBM1196>3.0.CO;2-H.
- (102) Putignano, C.; Scarati, D.; Gaudiuso, C.; Di Mundo, R.; Ancona, A.; Carbone, G. Soft Matter Laser Micro-Texturing for Friction Reduction: An Experimental Investigation. *Tribol. Int.* 2019, 136 (December 2018), 82–86. https://doi.org/10.1016/j.triboint.2019.03.001.

Acknowledgement

This work was supported by JSPS KAKENHI Grant Number 18K14285 and 22K14170. We thank Prof. Antoine Chateauminois and Prof. Manoj Chaudhury for teaching us the droplet replication method for surface patterning. The TOC measurement was performed using a TOC-V CSH at the Center for Environment and Safety, Kyushu University, and we also thank Prof. Yoshio Ito and Prof. Tomofumi Miyamoto for their assistance.